12-2017

Multifunctional Polymeric Micelles for Drug Resistant Breast Cancer: Self-Assembling Poly(Lactide-Co-Glycolide)-Graft-Polyethylenimine

Graham MacKenzie Temples
Clemson University, gtemple@g.clemson.edu

MULTIFUNCTIONAL POLYMERIC MICELLES FOR DRUG RESISTANT BREAST CANCER: SELF-ASSEMBLING POLY(LACTIDE-CO-GLYCOLIDE)-GRAFT-POLYETHYLENIMINE

A Dissertation
Presented to
the Graduate School of
Clemson University

In Partial Fulfillment
of the Requirements for the Degree
Doctor of Philosophy
Bioengineering

---

by
Graham Temples
December 2017

Accepted by:
Dr. Jeoung Soo Lee, Committee Chair
Frank Alexis, Ph.D.
Wen Chen, Ph.D.
Wendy Cornett, M.D.
Matt Gevaert, Ph.D.

ABSTRACT

Breast cancer is the most common malignancy and the leading cause of cancer death in women. Systemic breast cancer therapies include 1) hormone therapy, 2) immunotherapy, and 3) chemotherapy. Chemotherapy is commonly used in combination with immunotherapy, achieving synergistic activity by multiple mechanisms specific to the type of breast cancer. However, the efficacy of anticancer drugs has been limited by their toxic side effects in normal cells and drug resistance acquired by cancer cells. Therefore, the development of a novel treatment strategy for the selective delivery of therapeutic agents to breast cancer cells is crucial to improve the therapeutic index and efficacy/toxicity balance. The objective of this project is to develop multi-functional polymeric nanotherapeutics for breast cancer therapy that specifically target malignant cells and provide combinatorial delivery of an anticancer drug and therapeutic nucleic acid designed to reduce the expression of proteins responsible for drug resistance. These multi-functional polymeric nanotherapeutics will consist of three functional components 1) folate (FA) as a targeting moiety to deliver these nanotherapeutics to FA receptor alpha-positive breast cancer cells (FA receptor is over-expressed in 32% of breast cancers), 2) small interfering RNA (siRNA) designed against multidrug resistant protein (ABCB1), a gene responsible for drug resistance in cancer cells, and 3) the chemotherapeutic, Doxorubicin (DOX). The efficacy of these targeted multifunctional nanotherapeutics will be evaluated in FA-receptor alpha positive (FA+) drug resistant breast cancer cells.

To achieve this goal, FA-functionalized polymeric micelle nanoparticles, folate-polyethylenimine-graft-poly (lactide-co-glycolide) (FA-PgP) were designed as a targeted drug and nucleic acid delivery carrier. We synthesized and characterized FA-PgP and demonstrated that the FA-PgP polymeric micelle is a promising carrier for plasmid DNA capable of transfecting breast cancer (MCF-7, MDA-MB-435 Wild Type, and MDA-MB-435 DOX resistant) cells in media containing 10% serum. We also demonstrated that FA-PgP exhibited selectivity by comparing transfection efficiencies in folate receptor alpha positive (MCF-7, MDA-MB-435 Wild Type, and MDA-MB-435 DOX resistant) and negative breast cancer cell lines (MDA-MB-468) *in vitro* and demonstrated that PgP can deliver pGFP (plasmid encoding green fluorescence protein) and pbGal (plasmid encoding beta- galactosidase gene) as reporter genes efficiently in an athymic Nu/Nu mouse drug resistant breast tumor model. Finally, Doxorubicin loaded FA-PgP was able to induce increased or similar cytotoxicity compared its free drug counterpart in MCF-7 and MDA-MB-435 DOX resistant lines and over a LD50 response in MDA-MB-468 and MDA-MB-435 Wild Type cells. Furthermore, FA-PgP exhibited FA+ related selectivity in all breast cancer cell lines tested. Future work includes utilizing therapeutic siRNAs targeting ABCB1 with FA-PgP to overcome drug resistance in breast cancers.

ACKNOWLEDGMENTS

Thanks to Dr. Angela Alexander-Bryant for her help with everything, especially the data and manuscript drafting. Thanks to Dr. So-Jung Gwak, Breanne Hourigan, Justin Nice, Christian Macks, and Erica Beal for all their in-lab work and support

TABLE OF CONTENTS

Table of Contents (Continued)

Page

LIST OF TABLES

LIST OF FIGURES

List of Figures (Continued)

Figure Page

List of Figures (Continued)

List of Figures (Continued)

List of Figures (Continued)

Figure Page

List of Figures (Continued)

Figure Page

CHAPTER I

INTRODUCTION

What is Cancer?

Breast cancer remains a leading cause of death worldwide. [1] It accounts for 22.9% of cancer occurrences and 14% of all cancer related deaths in females internationally. [2] A tumor is the result of the accumulation in cellular genetic defects resulting the unchecked proliferation of cells. [3] The presence of a variety of biological barriers hinders effective therapeutic delivery and contributes to unintended side effects. Tumor populations are often heterogeneous, resulting in the development of drug resistance sub-populations during treatment; ultimately resulting in the failure of the clinical intervention.[4]

Tumor genetics and heterogeneity

Cancer is a cell population that has accumulated a variety of genetic alterations and has lost the ability to be fully regulated by the host. Tumor progression is multistage and involves a variety of genetic factors and mutations that can ultimately result in the tumor's migration into the blood stream and the subsequent deposition and growth of secondary tumors (metastasis) [5]. Metastasized cancers are late stage and often terminal. Tumor cells that have gained the ability to form new anchorage sites and undergo virulent proliferation belong to a classification of cell types termed cancer stem cells (CSC's). Late stage tumors possess heterogeneous populations of cells, which can be then further subdivided into either into stem cell-like populations, or non-stem cell like populations. [5] CSC's often possess a resistance to both chemo and radiotherapies exacerbating

eradication.[6] Therapeutic success requires the elimination of all tumorigenic populations within the host to ensure no nucleation points in the body exist to break remission. Originating from host's native tissue, cancer is able to evade detection by the immune system due to its intrinsic similarities. Given enough time, this mass will continue to collect genetic mutations, and eventually metastasize through the bloodstream or lymph system, and proliferate throughout the body.[3] There often are common motifs between each type of cancer but ultimately each case is uniquely dependent on the host and its history; necessitating customizable treatment options to ensure therapeutic success.

Current Treatments

While radiation and surgery remain excellent short-term options, often-residual cell populations remain post treatment, which subsequently proliferate and result in tumor recurrence. Often these treatments are done in concert to maximize effectiveness.[7]

Surgical removal

Typically, breast cancer is removed surgically with either a mastectomy (full breast removal) or with a lumpectomy (partial breast removal). The removal of the effected and surrounding tissues is meant to ensure the removal of tumor cells to halt proliferation via physical extraction. Partial breast removal is usually accompanied by a radiation regimen, which destroys the components essential to cellular division.[7]

Radiation can be applied immediately after the surgical removal or in daily doses over the course of five weeks following lumpectomy. In the 5-week course treatment, radiation is applied every day across the entire breast with a booster dose being applied at the end of

the course. While excessive damage is avoided to the best of the medical staff's ability, this method aims to irradiate all cancerous cells, often at the cost local healthy tissue damage.[7]

Chemotherapies

Chemotherapy is the introduction of chemical agents that are designed to slow the rapid growth of cancer. This type of treatment has contributed a 24% decrease in breast cancer related deaths between the years 1990 and 2000. [8] However, the nonspecific nature of chemotherapy often has detrimental effects upon the patient, often resulting in nausea, weight loss, loss of hair and loss of energy; making it a less-than-ideal treatment compared to a targeted therapy with a similar anti-tumorigenic efficacy.[8]

Chemotherapeutics are systemic treatments, which aim to halt tumor growth and cancer colonization throughout the body. Current drugs include: vinblastine, vincristine, daunorubicin, docetaxel, doxorubicin, and paclitaxel, of which many exhibit solubility problems in aqueous environments. [9]

The mechanisms of these drugs vary and their delivery is untargeted, often inadvertently effecting healthy populations of rapidly proliferating cells across the entire body. Encapsulation of chemotherapeutics within a drug delivery vehicle (DDV) can assist in increasing drug solubility and mitigating systemic toxicity. Economic considerations of DDVs generally require at least 10% loading by weight and sterilization via 0.22-micron filtration is preferred. [10]

Unfortunately, chemotherapeutic intervention is often insufficient and can result in the development of drug resistant tumors via colonial microevolution. [11]

Drug Resistance and its Challenges

Development of Multiple Drug Resistance in cancer

Cells have the native ability to remove broad classes of hydrophobic drugs via P-glycoprotein (P-gp) pumps. [12] The P-glycoprotein is a 170 kD protein in the ABC cassette binding protein family, which contains nine other members that have been linked to chemoresistance. [9] Encoded by the multidrug resistance gene (ABCB1), this protein functions in the broad removal of toxins from the lipid bilayer. [4] Once chemotherapy has begun, cells with low levels of P-gp begin die; leaving a greater proportion of resources for the surviving populations to utilize in proliferation. [9] This process selects for, and yields populations of cells with overexpressed levels of P-gp pumps. Overtime, these populations proliferate and result in a mass of cells that possess elevated quantities of ABC products and are unresponsive to chemotherapeutic treatment. [4] There are additional factors that contribute to drug resistant phenotypes: multidrug resistant protein (MRP) upregulation, p53 downregulation and BCL-2 alteration have all been cited to desensitize cancer to chemotherapeutic treatment through a variety of mechanisms. Minimization of P-gp levels or restoration of endogenous MRP, P53, BCL-2 gene activity could contribute towards the elimination of drug resistant phenotypes. [3,13]

Gene Therapy

Gene therapy is the alteration in the production or activation of a specific protein to change levels to desired quantities. This process often entails the excision and replacement of a malfunctioning gene with the correct version of DNA, placement of translatable copies of DNA within proximity of nuclear machinery, or interference with protein production. To accomplish any of these goals, a DDV must traffic the correct sequence to the intended cellular target. This can be accomplished in many different ways but can be divided generally into viral and non-viral modalities.[14]

Viral vectors

Viral insertions capitalize on the intrinsically efficient DNA insertion methods that are native to viruses. The replacement DNA is loaded into a viral capsule and released into the body to perform gene excision and substitution, a process termed transduction. Viruses have a limitation to the size of their genetic construct, Adeno-associated virus capacities can be as small as 5.2 kB, limiting their flexibility to deliver more complex sequences. [15] A major drawback to this approach is the result of the non-specific nature of attack virus's use in their lifecycle, which could result in unintended gene replacements in healthy cells. Furthermore, viruses can induce an immune response due to their morphological similarities with their natural counterparts, which could ultimately result in the therapy becoming less effective with time or induce anaphylactic shock adding a potential life threatening allergic response. Despite its shortcomings, this type of approach is still heavily pursued as a treatment option because of the more permanent methodology of gene replacement relative to non-viral vectors.[14]

Non-Viral vectors

Non-viral methods include the use of either DNA or siRNA to either increase or decrease production of a desired protein. DNA is introduced into the cell via endocytic processes and can encounter the nucleus where it is transcribed into mRNA and eventually the protein of interest. siRNAs can be introduced in a similar manner but need only to migrate to the cytosol to induce the destruction of mRNA.

siRNA

siRNA are short RNA segments that can be introduced into the cell environment, where they then interfere with the production of proteins, through a process termed knockdown. siRNA molecules function by harnessing one of the cell's endogenous mRNA control pathways, the RNA-induced silencing complex (RISC). [16,17] This protein complex forms from the uptake and incorporation of siRNA into the protein components of the RISC and forms a sequence specific nuclease that finds and cleaves complementary sequences of mRNA. This complex reduces the levels of mRNA transcript available within the cell; resulting in a reduction of protein translated. Naked siRNA delivery often results in unacceptable efficiency and/or off target effects, resulting in inadequate protein reduction or reduction of non-target proteins respectively. Complexation with a positively charged polymer segments within a targeted DDV has been shown to increase efficacy and specificity of knockdown treatments.[16,17]

The cleaved messengers can no longer pass on their message to a ribosome, and reduce the oncogene's expression within the cell. [14] This method can be exploited to halt

proliferation of cancer cells entirely or enough to allow for other methods to eliminate all traces of the cancer from the body. Much like viral based methodologies there are inherent problems with the treatment's efficaciousness and specificity. The cellular uptake of DNA is often low. [18] Absorption rates are hindered because of the negative charge of the nucleic acids electrostatically repelling the negative charges contained within the cell membrane. In the DNA's case, the relatively larger size of DNA further inhibits uptake. The body also contains DNase/RNase, enzymes that destroy nucleic acids, further exacerbating delivery issues of nucleic acids. [18]

The utilization of nanoparticles as vessels to house either DNA or siRNA for delivery is a promising venture. Nanoparticles are simply any small particles between the sizes of 1-100 nanometers. [19] The particle itself can be made from a variety of materials ranging anywhere from lipids to polymers. The ideal vessel has protective properties for the fragile DNA and even more fragile siRNA. The vessel must be biodegradable and non-toxic, to not poison or harm the cell or body during travel or delivery. The vessel must be conducive to cellular uptake via endocytosis. Nanoparticles that are marked for use with DNA must also perform condensation of nucleic chains into a manageable size for intracellular import. [18] The loading of nucleic acids into nanoparticles has exhibited marked improvements in delivery effectiveness over their naked counterparts.

In a review of polymeric micelle delivery systems by Jhaveri and Torchillin, eight criterion were identified as necessary for a drug delivery vehicles' success in delivering genetic therapeutics, the vector must: 1) not exhibit toxic or immunogenic qualities to

evade acute patient reactions, 2) compact nucleic agents, 3) shield itself and its cargo from nuclease activity, 4) elude recognition from the immune system, 5) be over 50 nm but under 500nm to evade renal clearance and reticuloendothelial system recognition respectively, 6) avoid aggregation with serum proteins and uptake by unintended cellular targets, 7) traverse the blood supply to target tissue and undergo endocytosis to the correct subcellular compartment for 8) adequate release of therapeutic in cell cytosol to induce therapeutic response. [20-22] While originally contextualized to siRNA delivery, it is obvious that such characteristics are necessary for success of any multifunctional drug delivery system regardless of the mechanism of action.[22]

Polymeric Micelles

Polymeric micelles are a subcategory of nanoparticle-based DDV's that have the potential to fulfill all requirements of a successful multifunctional vector. Micellization is thought to be a byproduct of the hydrophobic effect, a phenomena that is resultant of the free energy associated with the total rotational and translational activities between each individual molecule. [23] Self-assembly into ordered aggregates is a result of the relatively increased amount of energy required for water molecules to form a clathrate-like change around the lipophilic moiety compared to the energy required to form aggregates with hydrophobic chains sequestered in a central reservoir. At a certain concentration of micelle (CMC) above a certain temperature (Krafft temperature or critical micelle temperature [CMT]), unimer aggregation occurs. The long-range order is determined by the relative size between hydrophilic and hydrophobic domains in solution or the Hydrophilic Lipophilic Balance (HLB). HLB is defined by the hydrophilic molecular

weight relative to the molecular weight of the whole molecule multiplied by 20. HLB's range from 0-20, with values below 10 representing hydrophobic dominant substances with larger numbers representing hydrophilic dominant substances.

The importance in hydrogen bonding, specifically with amphiphiles in water, help illustrate micelle dynamics are ultimately limited by aggregate energetic properties associated with the hydrophilic/hydrophobic domain size.[24] As a result of the same thermodynamic principles, long range order progresses from micelles, with lipid tails being sequestered in spheres with no long range order, to micelle-cubic, a similar aggregate structure whose interactions induce a long range order of randomly distributed aggregates. This balance also has an effect on the morphology of the individual micelle, as proportion of hydrophobic block increases in a particular system, polymeric micelles will follow a progression through different morphologies: star-like, intermediate, and crew-cut micelles. In star-like micelles, the size of hydrophilic blocks greatly exceed hydrophobic blocks, aggregation will be sterically hindered by the hydrodynamic volume of the hydrophilic moiety. If HLB is similar, packing limitations are still limited by increased hydrophilic volume, as hydrophobic block length increases beyond this point micelles will be limited by the flexibility between associated hydrophobic chains.[25]

As concentrations of amphiphile continues to increases and/or as the hydrophobic portion relatively increases, hydrophobic forces begin to dominate and form cylindrical tubes arranged along a hexagonal lattice, with continued increases these tubes will form an

intermediate tube network on their way to a lamellar conformation before finally dropping out of solution beyond the cloud point.

Many polymeric micelle systems have been shown to evolve in two discreet steps and relaxations. [26] First is the phase transition from aligned surface unimers nucleating and forming the lowest energy aggregates, a process that continues until an individual chain insertion would increase the overall free energy of the system. A second slower process involves individual unimer condensation and expulsion or whole micelle merger and fission. [24] The speed and liquidity of unimer exchanges between micelles and free chains are retarded by increasing hydrophobic block length or number, such an effect may slow kinetic exchange to such a degree that, the micelle population may not exhibit any observable changes over course of the experiment. In such conditions, polymers are considered kinetically frozen during experimental timeframes. [25]

Overtime, these systems evolve to the greatest amount of entropy but the transition timescale and final conformation of aggregates is dependent on synthetic composition, initial formation conditions, temperature, pH, protein and salt contents. [25] Micelle populations can be described by size distribution curves that characterize the minimum and maximum size of aggregates. [27] Polymer composition is an important factor in micelle dynamics, increasing hydrophobic block length and number has been shown to decrease kinetic exchange. [26] If experiments are contingent upon reaction kinetics in any way, experimental timescale may also introduce inadvertent complications in determining underlying factors in DDV performance.

Morphological characteristics of polymeric DDV's have been shown to have a profound impact on performance and are intimately tied to concentration and alteration of microenvironment. Applying traditional drug analytical methodologies, such as dose-response curves, may overlook multiple confounding variables because of morphological differences that are resultant of variation of dose. Increasing polymer concentration may have an effect on morphology of aggregates, which may result in effects that run countercurrent to perceived effect of the elevated dose. In other words, investigations of polymeric system behavior requires coupled experiments that isolate the differences in form as a result of dose in order to accurately determine the dominating factors in DDV performance. This same concept also applies to the formation of nucleic acid and polymeric aggregates or polyplexes.

Formation of polyplex

Limitations of polyplex size follow the same dynamics previously describe that limit polymeric micelle size. Polyplex formation with siRNA has also been show to take part in a two-step process that is reminiscent of micellization. Primary polyplexes first associate in a semi ordered fashion before aggregating into larger polyplexes. Complexation with DNA tended to be a more multilayered and sophisticated process, as longer DNA requires extensive folding for effective condensation.[28] Polyplex compositions are often described as a comparison of the average number of nitrogens per mole of polymer to the average number of phosphates per mole nucleic acid, or N/P ratio.

General Hurdles Regarding DDV

Pathway to tumor

Angiogenesis is a hallmark of advanced cancers. [21] Tumors can no longer receive adequate nutrition via diffusion after growing 1-2 mm^3 and require access to a blood supply. [29] Tumors recruit nearby vasculature to supply them with the required elements for survival. As the vessel is often recruited in a primitive way, the native intracellular junctions are poorly developed. [21,30] This architecture leads to passive size-dependent absorption of nanoparticles, via a process termed the Enhanced Permeation Retention (EPR) effect. [31] DDV's will passively diffuse as a result of the pressure differential between blood vessels and the tumor's interstitial environment, leading to enhanced delivery at target site relative to healthy tissues. Inadequate lymph drainage in tumor peripheries further encourages the nanoparticle retention [1,32]

Blood Circulation

Therapeutic agents must maintain stability in the blood stream in order to reach the target. The agent must be able to circulate in the blood for a least a short period of time without removal by endogenous macrophages, suffering chemical degradation, forming complexes with native blood borne proteins, or inciting non-specific immunogenic reactions. In order to contend with circulation time issues, surface modifications have been formulated that assist in the evasion of immunogenic or reticuloendothelial detection and removal. Polymers such as Polyethylene Glycol (PEG) resist the binding of blood-borne proteins (e.g. opsonin) associated with macrophage removal via formation of a hydration shell around the complex. [32,33]

Tumor Site Deposition

Site deposition does not necessarily result in effective therapeutic administration. The dense cellular and matrix packing on the interior of tumors is a physical barrier that can exacerbate internal passive diffusion as a result of the elevated tumor interstitial pressure relative to nearby healthy tissues. [32]

Cellular Uptake

The DDV must reach the correct intracellular target. This first requires the traversal of the cell membrane. Generally, cell membrane charge is negative due to the lacing of surface with proteins. Negatively charged genetic components are electrostatically repulsed from the membrane; positively charged systems are attracted to the membrane but can become electrostatically bound to membrane proteins and may require active trafficking to progress further into the cell. [34] Some free drugs (e.g.: Doxorubicin) can cross tumor cell membranes via simple diffusion, while others may require interaction with cellular proteins to facilitate uptake.[35]

Given enough time, free drugs can initially cross tumor cell membranes. Often, tumors develop drug resistances (e.g. up regulating P-glycoprotein pump expression) [32]. Macropinocytosis of extracellular fluid containing free drug or DDVs is another potential route of non-specific accumulation. In addition to simple diffusion, there are a variety of protein-mediated endocytosis': clathrin-mediated, caveolae-dependent, and clathrin/caveolae independent endocytosis'. Each pathway is characterized by a unique

set of proteins, trafficking modality, and vesicle size. Pathway determination is often associated with DDV size. [36]

There has been a lot focus on the utilization of active transport to facilitate the uptake of delivery particles. Cancers can over-express receptors that are sensitive to specific molecules. Folate, biotin, galactose, and hyaluronan are examples of targeting moieties that have been identified as potential candidates for assisting uptake of DDV molecules in cancerous tissues. [37] There is an established body of work exhibiting the efficacy of utilizing active transport as a means of overcoming drug resistant cancers. [13] There are also more generalized means of uptake involving the protein complexes Clathrin and Caveolin. Clathrin complexes form when certain receptors, such as transferrin or low-density lipoprotein receptors, are bound. This activates a cascade in which a protein coat forms and pulls in part of the membrane forming a vesicle that fuses with early endosomes and ultimately follows the lysosomal degradation pathway.

Caveolae-initiated complexes play a more sophisticated role in the cell as they involve some signaling functionalities as well as transport duties. Caveolin-1 acts as the catalyst for the formation of the caveolae vesicle, which uniquely fuses with either a multivesicular body or a cavesome, both of which have neutral pH (however, fusion with the endosome occasionally still occurs). [38] This neutral pH state is important to many DDV's as reduced lysosomal pH often results in the degradation of some drug and nucleic acid based therapies. A number of Caveolin focused nanoparticles have been created including a polymeric cross-linked poly(ethylene oxide)-b-poly(methacrylic acid)

micelle as well as the construction of Aminopeptidase P (APP) monoclonal antibodies to target the APP rich caveolae.[38] Caveolae- mediated endocytosis functionality is important as it has the possibility of evading the endosome-lysosome pathway, a common site of genetic component deterioration.

Prepared complexes exist across a range of sizes and charges that variably alter over time. This variation may have a critical impact on cellular uptake distributions.[36] Furthermore, due to the heterogeneity of trafficking mechanisms across cells it is very likely that optimal parameters are cell specific and caution must be taken in the generalization of results.[39]

Intracellular Pitfalls

Therapeutics encapsulated within the DDV complex must be taken up by cell and escape destructive processing pathways. Failure to bypass the late endosome will result in degradation via peroxidase, lysozyme and low pH.[16] Utilization of polymers with primary and secondary amines such as branched polyethylenimine (PEI) can promote early endosome escape via the "proton sponge" effect.[40] The protonation of primary and secondary amines as pH drops in the endosome provides a buffering effect that results in the influx of protons, counter-ions, and water. This influx of molecules causes swelling of the endosome and results in the rupture and release of contents into the cytosol.[41]

This mechanism is still contentious and an alternative hypothesis has been proposed that suggests that PEI facilitates escape via membrane interactions into the cytosol.[42] Once in the cytosol, it is unclear as to whether the positive charge of a protonated PEI promotes

attraction between its cargo and the proteins in the intracellular space including the nucleus (providing potentially increased nuclear localization) and at which point or by what means the genetic cargo is released from the complex. It is clear however, that PEI is trafficked to the nucleus and in some cases provides adequate co-localization of plasmid within the nuclear machinery to ultimately result in protein expression.[43]

Size and surface charge have a direct implication on reticuloendothelial system elimination rates, intracellular uptake and processing, as well as interfacial qualities such as the ability to bind and protect nucleic acids. [33,44] Additionally, polymer based delivery systems with insufficient electrostatic repulsion of units, induced by either great negative or positive charge, tend to aggregate and floc out of solution, rending them ineffective.[45]

It is obvious that incorporated drug within DDV's would have to undergo a similar evasion of degradation to reach their respective intracellular target. Additionally, incorporation of chemotherapeutics into DDV requires dissolution of complex to release free drug or the drug must diffuse out of the micelle core. Further DDV thermodynamic stability may be imbued with the addition of a hydrophobic drug (e.g. DOX), which may affect transgene expression levels. [46]

Need for Increased Specificity

Unfortunately, no single drug has been universally applicable to all cancers. Therefore, targeted therapies were designed to further mediate specific delivery and promote cell internalization in a cancer-specific fashion, as a way to decrease unintended effects on healthy cell populations. The addition of a targeting ligand has been long sought as an

answer to specificity problems. However, because of the similar genetic profile cancer shares with its host, the existence of a cancer-exclusive moiety has yet to be discovered. Fortunately, there are a plethora of overexpressed moieties and transporters that are associated with common cancer types, of which many can easily be conjugated to polymeric micelles.

Ultimate goal of any chemical based interventions is to accumulate enough of agent in target population to induce the desired effect with minimal damage to the host's healthy cell populations.

Receptor Targeting

Because of their selective up regulation in some cancers and relative absence in normal tissue; surface proteins such as Human Epidermal Factor-2 (HER-2), prolactin, and folate receptors have been utilized as a means of actively transporting DDV's into cells. [47]

HER-2

Human epidermal growth factor number 2-receptor tyrosine kinase (HER2/Neu, Her2 or ErbB-2) is a growth receptor that simulates rapid proliferation via inhibition of PI3K/Akt apoptotic pathway. [48] This anti-apoptotic pathway is in excess within cells over expressing Her2, increasing levels of proliferation; resulting in tumors with bigger sizes and higher growth and metastatic rates. The more aggressive nature of the Her2 positive tumor is correlated with reduced survival rates. [8] Many treatments focus on the inhibition of this pathway in an effort to quell tumor aggression via competitive inhibition. [49] Her2

overexpression provides an advantage in selectivity but does not address subsequent intracellular uptake and processing barriers faced by DDV's.

The Her2 receptor is considered over expressed in 25-30% of breast cancers of all types, with an increased rate of expression found in malignant tumors. [50] The Her2 protein receptor is the activator of the "survival" pathway because of its assistance in regulating cell proliferation via apoptotic inhibition. [48] The research undertaken because of the high rates of mortality related to this subsection of cancer has resulted in the FDA approved Trastuzumab (name brand Herceptin).

Herceptin is a humanized monoclonal recombinant antibody that selectively binds to the extracellular side of Her2. This drug has had considerable levels of clinical success exhibiting increased levels of disease free survival. [51] In one study, the addition of Herceptin to chemotherapy resulted in a 33% decrease in mortality after 3 years. [8] The side effects of Herceptin are much less pronounced relative to more traditional therapies, most likely the result of higher levels of specificity as well as the non-lethal mechanism of the drug upon the cell. [52] This reduction of side effects makes Herceptin and drugs like it an improvement over traditional treatments of cancer.

In another system, a nanoparticle was utilized to co-deliver Herceptin and Paclitaxel, a mitotic spindle inhibitor. A poly {(*N*-methyldietheneamine sebacate)-*co*-[(cholesteryl oxocarbonylamido ethyl) methyl bis(ethylene) ammonium bromide] sebacate} nanoparticle was loaded with both drugs. The complex was found to have high levels of anticancer effects, greater than each treatment alone. The ability to co-deliver drugs is

another advantage associated with the use of nanoparticles. Drugs delivered at the same time can work more synergistically than can drugs applied at different times, improving treatment effectiveness.[53]

Herceptin was also conjugated to dextran iron oxide nanoparticles. The vehicle was designed to mark Her2 positive tumors and create greater contrast to their surroundings in magnetic resonance imaging (MRI). When applied to mice with Her2 positive tumors, there was a 45% enhancement drop of the imaging, indicating a high accumulation nanoparticles in the vicinity of the tumor site.[54] This significant increase in enhancement still occurred despite the endogenous low-level presence of the Her2 receptor in normal cells. The presence of Her2 is found to be around 100 times more prevalent in Her2 positive tumors when compared to Her2 negative tumors.[52] The two orders in magnitude difference in the exhibition of Her2 receptors can be capitalized upon in antibody-targeted gene therapy.

Prolactin Receptor Overexpression

The prolactin receptor is a protein that is found in more than half of breast cancer incidences and has been found to be frequently over-expressed in late stage cancers. Over-expression, again, is correlated with an overall reduction in host survivability partially due to increased incidence of metastasis. The activation of the prolactin receptor can lead to further activation of Jak2/Stat5 and Jak1/Stat3 signal cascades, which will ultimately lead to increased amounts of cellular growth, division, and survival.[55] In addition to this main pathway, prolactin receptor activation also leads to activity in the

Ras/Raf/MAP kinase pathway as well as protein kinase C activation, which further promotes cell longevity.[56]

There have been a number of prolactin analogues developed in order to exploit the therapeutic possibilities involving the antagonization of the prolactin receptor. Noticeable success has been found in the G129R protein. [56] This protein replaces the glycine at position 129 in prolactin with an arginine and provides for competitive inhibition of the prolactin receptor; ultimately resulting in an apoptotic-inducing down regulation of BCL-2 and upregulation of TGF-B.[57]

While still in the beginning stages of research, use of prolactin as a stem-cell conversion agent is currently underway. Prolactin natively regulates formation and proliferation of mature breast tissue, indicative of stem cell activity; which suggests potential for other stem cell interactions. [58] There has been suggestion that prolactin antagonism alters stem cell population proportions via alteration of the Stat5 pathway in prostate cancer. This increases the promise that a prolactin antagonist could alter stem populations in other prolactin-expressing cancer types. [59] Furthermore, the creators of the G129R protein have filed for a patent that indicates reduced stem cell population proportions as a result of the administration prolactin in breast cancer. [60] Despite current gaps in prolactin-antagonist-related breast cancer stem cell conversion research there is good foundation to utilize the complex as part of a novel multifunctional drug delivery system.

Folate

Some cancers possess unregulated extracellular receptors that are relatively absent in normal tissue; folate receptor alpha is an exemplar protein and has been frequently utilized as a means of selectively transporting DDV's into cells. [47] Folate is an essential cofactor to DNA replication and is needed in large quantities by rapidly dividing cancer masses. Elevated levels of folate receptor (up to 100x expression) are correlated with aggressive cancers in the brain (75% of cases), ovaries (90%), lung (37%) and breast (32%).[61,62] Breast cancers positive for folate receptor alpha overexpression (FA+) are associated with grim outcomes. [63] Furthermore, triple negative breast cancers, or cancers without elevated levels of estrogen, progesterone, or HER-2, represent a cohort of breast cancers that lack defined targeted therapeutic approach and have been also noted to have (FA+) in over 80% of cases. [64-66]

Cell line	Tissue Type	Estrogen Receptor	Progesterone Receptor	Human Epidermal Factor-2	Folate Receptor Alpha
MCF-7	Luminal-like adenocarcinoma	+	+	-	+
MDA-MB-468	Basal-like adenocarcinoma	-	-	-	-
MDA-MB-435 Wild Type	Ductile Carcinoma (post-EMT)	-	-	-	+
MDA-MB-435 Doxorubicin resistant variant	Ductile Carcinoma (post-EMT)	-	-	-	+

Figure 1.1: Descriptions of cell lines. Estrogen receptor, Progesterone receptor, Human Epidermal Factor-2 absences together represent cell lines that are triple negative breast cancers. [67-70]

Fortunately, both alpha and beta folate receptors (~38 kDa) exhibit limited distribution in normal tissues. [61] This level of upregulation and relative tissue specificity compounded with the great binding affinity of folate (Kd = 10^{-10} M), makes folate an attractive ligand to add targeting functionality to DDV's. [67] There is little difference in the mechanism by which free folate and folate-conjugated particles are trafficked. Free folate (and folate conjugated particles) initiates active transport into cell and is moved along the endosomal pathway; thus allowing DDV's containing branched PEI to escape endosomal degradation via the proton sponge effect. [47,67]

Need for a Multifunctional DDV

Over the pasts few decades three subsequent generations of non-viral delivery vectors have been engineered to address the shortcomings of previous technologies and incorporate lessons learned from a continuously evolving understanding of the delivery challenges associated with drug resistant breast cancer. [71] Initially relying solely on passive diffusion via the EPR effect, it became clear that further modification would be required to sufficiently increase intracellular accumulation. [72] This addition of active targeting via antibody or small molecule ligands improved the specificity of DDVs, but still left much to be desired in therapeutic efficacy. [73] It is currently recognized that a multifunctional drug delivery system that interacts with the target in a combinatorial way, i.e. co-delivery of a variety of genetic therapeutics and conventional pharmacological agents is necessary to address the complexities of breast cancer treatment in an effective manner. [1, 13]

CHAPTER TWO

RESEARCH OBJECTIVES

Project Rationale

Despite the recognition that simplicity often yields the most commercially viable product, increasingly complex molecules have been pursued in an effort to address the multidimensional challenge of breast cancer. [81] These products, while successfully increasing their therapeutic viability, fail to recognize the clinical realities related to dosing, administration and product storage. [82,83] It has been recognized that drug loaded (PLGA)-b-PEI/pDNA lyophilizable systems can be easily reconstituted for use and possess extended shelf life over their contemporaries.[5,6] However, previously investigated iterations utilizing two 36kD PLGA blocks exhibit transfection efficiencies that leave much to be desired despite a high degree of drug loading.[5,6] Low levels of transfection lead to this investigation of the utilization of smaller PLGA blocks in a similar capacity, in an effort to find a balance between drug loading and nucleic acid delivery capabilities. PLGA weights were chosen to investigate the effect of HLB on transfection efficacy and drug loading in the context of a multifunctional drug delivery vehicle.

Proposed is a unique combination of the amphiphilic copolymer, poly (lactic-co-glycolic) acid-g-polyethylenimine) (PgP) micelle delivery system as a flexible platform technology. PgP theoretically has potential advantages as a delivery system: 1) it should maintain some degree of morphological regularity as a result of associated thermodynamic forces, potentially limiting primary amine exposure via steric hindrance

reducing DDV toxicity 2) its hydrophobic core can serve as a reservoir for hydrophobic anticancer drugs 3) its positively charged PEI hydrophilic shell could be used for complexation with negatively charged nucleic acids (therapeutic plasmid DNA or siRNA) which may further reduce primary amine exposure and DDV toxicity, and 4) targeting moieties can be easily conjugated on the surface of micelle. [84,85] All components have ideal chemistries for controlled synthesis with each other and combination with targeting antibodies or other small molecules.

Doxorubicin (DOX) is a commonly used chemotherapeutic drug that functions via Topoisomerase II inhibition, intercalating DNA and impeding proper translation. DOX is often associated with unwanted cardiotoxicity. [95,96] DOX exhibits poor aqueous solubility. [97] Doxil, a PEGalayed liposomal version of DOX that was approved by the FDA for treatment of Kaposi's sarcoma, ovarian cancer and multiple myeloma has show to reduce DOX-associated cardiotoxicity and increased circulation times.[98] DOX exhibits absorbance at 480nm and has a ~200nm bandwidth, both of which can be visualized and quantified with microscopy and flow cytometry.[99] DOX's extensive use, hydrophobicity, and optical properties make it an ideal candidate for use as a model for incorporating chemotherapeutics into PgP.

The addition of folate moiety (FA-PgP) should increase specificity of DDV, resulting in fewer systemic side effects and help establish a standard protocol pertaining to the incorporation of therapeutically relevant targeting moieties to PgP's structure. Delivering ABCB1 targeted siRNA by complexing with PgP should reduce drug efflux pump

quantity and assist in the mitigation of drug resistance. Doxorubicin loaded FA-PgP/siABCB1 complexes will be a potential targeted therapeutic intervention developed from PgP designed to overcome drug resistant breast cancer more safely and substantially improve the length and quality of life of cancer victims. Success of this pilot study illustrates a potential scheme of PgP constructs that can deliver multidrug, multigene-targeted cocktails. [100]

Altogether, this suggests that a variety of therapeutically relevant PgP target/gene/drug configurations merit investigation. The development of PgP as a lyophilizable system will begin to address shelf life and production issues while maintaining the standard chemotherapeutic format, accomplished by DDV reconstitution and subsequent administration via intravenous injection. Development of this system could strike a balance between the realities of medicine today with the potential of the personalized treatments of tomorrow. This incorporation of genetic and targeting technologies in a product that in a familiar format to practitioners could ease the transition, adoption and incorporation of nanotheraputic drug delivery vehicles into the clinical workspace.

Specific Aims

Aim 1: Synthesize and characterize poly (lactide-co-glycolide) -graft-polyethylenimine (*PgP) as nucleic acid carrier*

Approach: Poly(lactide-co-glycolide) (PLGA) of a various molecular weights will be conjugated to branched polyethylenimine (PEI, 25kDa) yielding poly (lactide-co-glycolide) -graft-polyethylenimine) to characterize the effects of

PLGA length on nucleic acid delivery and DDV toxicity. Polymer structure and physicochemical properties will be investigated using ^{1}H-NMR, GPC, DLS, various gel based assays, hemolytic and hemoaggregation assays. Utilizing a panel of breast cancers (MCF-7, MDA-MB-468, MDA-MB-435 wild type and a Doxorubicin resistant variant), transfection efficacy will be assessed by using pGFP as a reporter gene while cytotoxicity of DDV will be assessed via MTT assays.

Aim 2: Evaluate poly (lactide-co-glycolide) -graft-polyethylenimine (PgP) as a drug carrier

Approach: DOX-loaded PgP and DOX-loaded PgP/pGFP particles will be prepared, characterized, and tested against panel of breast cancers to determine the additional cytotoxicity of DDV imbued by the loading of DOX. Data acquired in aims 1 and 2 will be used to screen PgP weights for overall viability as a multifunctional drug delivery vehicle. The best candidate will be synthesized with a folate-targeting moiety undergo further testing.

Aim 3: Synthesize and characterize folate functionalized poly (lactide-co-glycolide) -graft-polyethylenimine nanoparticles (FA-PgP) as drug and siRNA carrier for combinatorial therapy for the efficient treatment of various types of breast cancer cells in vitro.

Approach: Folate will be conjugated to PEI portion of the most viable PgP format using a PEG spacer to illustrate the effect on DDV physicochemical

properties, pGFP plasmid delivery, and DOX loading capabilities. Doxorubicin loaded FA-PgP and Doxorubicin loaded FA-PgP/pGFP particles will be prepared and tested to determine if complexation with pDNA at a fixed N/P ratio alters it toxicity relative to an equivalent amount of polymer, as size and surface charge have been shown to effect uptake. Finally, Doxorubicin loaded FA-PgP/ABCB1 targeted siRNA particles will be prepared and tested against drug resistant MDA-MB-435 ADR cells.

CHAPTER THREE

SYNTHESIS AND CHARACTERIZATION POLY(LACTIDE-CO-GLYCOLIDE)-GRAFT-POLYETHYLENIMINE (PgP) AS A NUCLEIC ACID CARRIER

Introduction

With self-assembly in mind, poly (lactic-co-glycolic) acid-g-polyethylenimine (PgP) will be constructed out of hydrophobic and hydrophilic blocks. While no single polymer has been universally approved by the FDA for drug use there are several materials that have consistent track records of being a component in approved drugs, one such compound is Poly (Lactic-co-Glycolic) acid (PLGA). PLGA can be used as a hydrophobic core-forming block. PLGA is a random block copolymer comprised of lactide and glycolide units in different ratios based on relative molar frequency. For example, 75:25 represents a copolymer that has 75% lactide groups and 25% glycolide group for the given molecular weight. Synthesis produces polymers with narrow dispersity indices cheaply, making them ideal for large-scale production. PLGA degrades via hydrolysis into lactic and glycolic acid, of which the rate is dependent upon the ratio of lactide to glycolide in the polymer. Generally speaking, as lactide portion increases there is a corresponding increase in time for hydrolytic decay. Such a quality can be used to tune time frame for decay. The degradation products exist in a form that is naturally produced in the body and should not cause localized irritation and is often cited as a polymer with ideal biocompatibility. [74]

The polycationic polymer, branched polyethylenimine (bPEI) can be used as a shell-forming block. PEI exists in a variety of lengths and morphologies ranging from linear units to branched units scaled from less than one to several hundred kDa. [43,75] It has been investigated for decades and represents the gold standard for non-viral transfection in terms of efficacy. [76] Despite its potential there has yet to be any significant break through in the translation to a commercial product due to deleterious interactions with proteins in the body, reducing its efficacy. Nonetheless, PEI and its many forms have been cited in over 100,000 papers, giving a broad base of knowledge to work from. [77]

Utilization of polymers with primary, secondary, and tertiary amines (1:2:1 ratio of 581 amines [145.25:290.5:145.25]) such as branched polyethylenimine promotes early endosome escape via the "proton sponge" effect. [40] The presence of primary and secondary amines with different pKa values provides a buffering effect that results in the influx of protons, counter ions, and water as pH drops in the endosome resulting in the increase in branch repulsion as positive amines increase electrostatic repulsion and force the bPEI to open up much like an umbrella. This influx causes swelling of the endosome and results in rupture and release of nanotherapeutics into the cytosol. [41]

This mechanism is still contentious and an alternative hypothesis has been proposed that suggests that PEI facilitates escape via membrane interactions into the cytosol. [42] Once in the cytosol it is unclear as to whether the positive charge of a protonated PEI promotes attraction between its cargo and the proteins in the intracellular space including the

nucleus (providing potentially increased nuclear localization) or at which point or by what means the genetic cargo is released from the complex.

It is clear, however, that PEI localizes at the nucleus and in some cases provides adequate co-localization of plasmid within the intranuclear space to result in transgene protein expression. [43] PEI's use in a gene delivery context is usually defined in terms of nitrogen to phosphate ratios. This is a description on the number of nitrogens per mole polymer and the number of phosphates per mole of genetic component. This nomenclature is used because electrostatic complexation is a dynamic process that is influenced by the pH of the solution and a generalizing the number of charged moieties provides a better description of general polymeric behavior. [78] It has been shown that in monoculture settings that it ultimately is the number of uncomplexed free amines that drives both efficacy and cytotoxicity in a positive fashion. [77] Increased free amines, whether added as uncomplexed groups in a system along with complexed groupings adding up to a certain N/P ratio or as a homogenous system of particles, have been shown to increase efficacy of transgene expression. [77] These same exposed amines can cause damage to the cell by membrane disruption and interruption of cellular movement potentially inducing apoptotic or necrotic damage. [79]

PgP will be synthesized in a variety of weights and investigation into the physicochemical properties will determine if PgP-12k, PgP-25k, and PgP-50k are potential candidates for successful DDV platform technologies prior to moving forward to assess gene delivery capabilities using pGFP as a reporter gene.

Three different PgPs are to be synthesized with branched PEI 25kDa and three different molecular weights of PLGA (4kDa (lactide:glycolide 50:50), 25kDa (lactide:glycolide 75:25) and 50k (lactide:glycolide 50:50)). A designation was given to each PgP based on the total PLGA composition. For example, "PgP-12k" is made up of 12kDa of PLGA (3 PLGA 4kDa:1 bPEI), "PgP-25k" has 25kDa of PLGA per molecule (1 PLGA 25kDa:1PEI) and "PgP-50k" has 50kDa of PLGA per molecule (1 PLGA 50kDA:1PEI).

Such permutations provide an investigation across block length as well as block number. Both parameters have implications on the kinetics of the polymer in reference to micelle structure. PgP is designed to increase transfection levels and reduce cytotoxicity relative to the current gold standard of non-viral gene therapies, branched $PEI_{25k,}$ in tested breast cancer lines. [76]

PgP theoretically should compact and protect its cargo from degradation, maintain a hydration shell to help evade immune recognition, be of correct size to capitalize on EPR effect, avoid renal and RES clearance, and possesses high degree of stability to allow it to circulate in the blood stream to reach the intended target. [86] The amine-based chemistry should allow for relatively easy production of base polymer system (PgP) and subsequent modification with a targeting moiety of interest (folate, HER-2 targeting antibody, etc.).[47628788] Such a system could then be customized further with the pertinent genetic material (plasmid DNA or siRNA regulating P-gp, MCL-1, BCL-2, etc.) or hydrophobic pharmaceutical agents (Doxorubicin, Paclitaxel, Vincristine etc.) to imbue customized multifunctional capabilities to the drug delivery vector. [9,17,86,89-94] Treatment combinations

can be combined to co-deliver multiple genes of interest and multiple drugs to maximize efficacy and reduce unintended side effects. This dynamic system can potentially be used as an approach to a variety of ailments, not only limiting itself to the treatment of a wide variety of breast cancers.

DDVs are often preliminarily screened through a set of standardized experiments. These investigations provide insight to potential sources of variation that effect delivery system performance especially pertaining to gene delivery- a multistep process that requires a precise order of intracellular events in order to transpire. It is imperative to verify composition post synthesis. ^{1}H-NMR and Gel Permeation Chromatography (GPC) are commonly used to quantify polymeric composition.

Aggregate properties such as Critical Micelle Concentration (CMC), a measure of the minimum concentration of amphiphile at which spontaneous aggregation is favored and a phase transition occurs from surface aligned free unimers to micelles, are investigated as a proxy for the potential longevity of blood borne complex based on the relationship with higher kinetic stability and lower CMC. [24] These properties dictate the size distribution of aggregates, which can be investigated via Dynamic Light Scattering (DLS). This same principle is applied to measure size dispersity differences introduced by the addition of nucleic acids (pDNA or siRNA). Size and surface charge have a direct implication on reticuloendothelial system elimination rates, intracellular uptake and processing, as well as interfacial qualities such as the ability to bind and protect nucleic acids. [33,44] In addition to providing insight to charge dynamics between gene element and polymer zeta potential

assessment can provide insight to the potential of aggregation via self-attraction. With the presence both negative and positive charge components, complexes with low zeta potentials run the risk of surface electrostatic repulsion being insufficient in overcoming attractive forces of the negative genetic moiety on surface of one complex to the positive polymer corona of another complex. Polymer based delivery systems with insufficient electrostatic repulsion of units, induced by either great negative or positive charge, tend to aggregate and floc out of solution, rending them ineffective. [45] Both size and electrostatic potential (ζ-potential) must be assessed to determine if DDV exhibits ideal electrostatic characteristics to avoid complex flocculation and enhance cellular uptake.

Limitations of polyplex size follow the same dynamics, previously described in chapter one, that curb the average polymeric micelle size. Polyplex formation with siRNA has also been show to take part in a two-step process that is reminiscent of micellization. Primary polyplexes first associate in a semi-ordered fashion before aggregating into larger polyplexes. Complexation with DNA tends to be a more multilayered and sophisticated process, as longer DNA requires extensive folding for effective condensation.[28]

If intravenous administration is desired, DDV interaction with the solid elements of blood must result in minimal hemolysis or hemoaggregation, as either of these phenomena can result in catastrophic patient reactions.

Hemolysis is a direct measure of cytotoxicity on erythrocytes, while hemoaggregation provides insight into the physical interactions of the delivery vehicle with solid elements in the blood. Both are important factors necessary to assess the safety of the delivery vehicle prior to *in vivo* evaluation.

When utilizing polyionic complexes it is important to determine the minimum ratio of polymer to genetic element in which the nucleic acid becomes completely complexed. Without complete complexation, genetic elements are exposed and quickly degraded by endogenous enzymes, rendering a loss of therapeutic potential. [43] The ability to bind and shelter genetic components is directly measured through a variety of gel-based assays. Gel retardation assays measure basic charge neutralization and help corroborate zeta potential studies. Polyplex formation does not necessarily indicate adequate protection of genetic cargo from degradation or protein replacement. DNase was utilized order to more directly measure the protective effects against endogenous enzymes. Endogenous nucleases are present in the body to rapidly deteriorate free DNA in the body to avoid unintended protein production and to mitigate risk of infectious genetic activity. [101] In order to determine the stability of the DDV complex in preventing competitive binding with large polyanions and to assess the ability of the complex to dissociate in order to free the nucleic acid cargo, a heparin competition assay was performed. Such an assay utilizes a strong anionic complex, heparin (pI=1), in a weight-to-weight manner relative to polymer, to determine at which charge ratio the genetic cargo is stripped from DDV.[102]

These investigations into the physicochemical properties of any potential polymeric system will provide metrics that help to determine likelihood of DDV delivery while also providing insight into the differences in performance in cell based testing.

After identification of suitable candidates through physicochemical analysis, DDV drug and gene delivery performance are often assessed in relevant tissue lines for their potential induced cytotoxicity and therapeutic effect. High levels of unintended uptake and toxicity, poor drug delivery, low levels of transfection, or poor transgene expression in monoculture settings can suggest a poor candidate for a multifunctional DDV.

The efficiency as a gene delivery carrier was assessed by transfection with complexes of pGFP (2μg/well) and PgP-(12k, 25k, 50k) in various N/P ratios using branched-25kD PEI (Sigma Aldrich, cat no: 408727) at N/P of 5/1 as a positive control, a commonly used standard notably used by Dr. Bae's Group from University of Utah and Dr. Godbey's group at Tulane University. [82,107]

Cells were transfected with media in a physiologically relevant 10% FBS serum condition, ~3% higher than blood serum concentration and allowed to incubate at 37 °C for 24 hours; at which time media was replaced to full media containing 10% FBS and 1% Penicillin/Streptomycin. [31]

Drug delivery is a complex problem with an unknown number of total effectors. Any manipulation of an independent variable can result in the possibility of erroneous conflation. For example, positive alteration of the N/P ratio, a common form of

investigation in polymeric gene delivery, is usually undertaken with the notion that ratio of charge is the predominate factor is delivery regardless of the fact that such manipulation also changes concentration of the delivery vector and the charge distribution for each individual particle. It is known that even subtle changes in surface charge distribution can have profound effects in transfection outcomes and fails to capture the basic differences contributed by vector dose. This makes it easy to inappropriately conflate correlation down to a single factor of causation. One could easily mistake the change in charge ratio as the predominate factor driving in difference of outcome, while dose could be the sole driver. End point assays of metrics that are the result of multiple, potentially linked, factors can also result in similar outcomes despite varying mechanisms of actions. Generically, increasing one factor may diminish another factor in a way that results in the same outcome for the given timeframe. In the example of polymeric DDVs, increasing N/P ratio could increase particle surface charge in a way that decreases cell uptake rate, but since the number of complexed particles increased with the increase in dose, the resulting outcome could theoretically be the same, as each cell could end up with the same number of polyplexes. In a similar fashion, each cell type has variable response concerning charge distribution and its effect on uptake rate and the downstream endosome escape and subtle differences that drive performance go often overlooked. It is necessary to verify all permutations along a list of parameters to isolate each factors contribution in a particular model. With this in mind, transfections investigating the efficacy in delivering pDNA will be fixed to an equal dose of plasmid. Since an increase in number of micelles would also decrease average plasmid content per

polyplex and toxicity and gene delivery performance is driven by free amine content, two additional forms of DDV toxicity will be investigated: 1) All PgP polyplexes were formed at 25/1 N/P ratio and diluted 2) uncomplexed PgP; each regime was tested at equivalent concentrations of PgP as N/P 5/1, 15/1, 25/1 transfections. These investigations will help elucidate the primary driver of DDV cytotoxicity. Understanding the primary driver in DDV toxicity will help refine insights in later studies involving Doxorubicin loaded PgP and help inform the selection of the best PgP format in which to conjugate folate to as a targeting moiety for additional investigation as a multifunctional drug delivery vehicle.

Before further investigation into drug loading or targeting, a pilot study was performed to determine the efficacy of PgP *in vivo*. Immunodeficient mice were injected with MDA-MB-435 ADR breast cancer cells in the mammary fat pad and were injected with PgP/pDNA polyplexes to determine the degree to which polyplex induced unwanted transfection in organs via migration in the bloodstream and the efficacy of nucleic acid delivery.

Materials and Methods

Three different molecular weights of poly(lactide-co-glycolide) (PLGA) were purchased from Durect Corporation (Pelham, AL), including PLGA 4 kDa, (50% lactide: 50% glycolide), 25kDa (75:25), and 50kDa (50:50), each with a carboxylic end group. Branched poly(ethylenimine) (PEI) (Mw 25 kDa), dicyclohexylcarbodiimide (DCC), N-hydroxysuccinimide (NHS), Thiazolyl Blue Tetrazolium Bromide, and RPMI 1640 were

purchased from Sigma (Milwaukee, WI). HPLC grade DMSO was purchased from Fisher Scientific (Pittsburg, Pennsylvania). Dialysis tubing (MWCO=50,000) was purchased from Spectrum (Houston, TX). QIAgen maxi plasmid purification kit was purchased from QIAgen (Valencia, CA). Plasmid DNA encoding the Monster Green Fluorescent Protein (phMGFP Vector: pGFP) and marker dye for gel electrophoresis (Blue/Orange 6X Loading Dye) were purchased from Promega (Madison, WI). A molecular weight ladder (1kb DNA Ladder) and human recombinant insulin were purchased from Gibco BRL (Grand Island, NY). 100X stock solution of penicillin/streptomycin, and 0.05% trypsin/0.53 mM EDTA in Hank's Balanced Salt Solution were purchased from Mediatech Inc. (Manassas, VA). EMEM, MCF-7 and MDA-MB-468 human breast cancer cells were purchased from ATCC (Manassas, VA). FBS was acquired from Atlanta Biologicals (Norcross, GA). Confocal microscope utilized was Olympus IX81 (Center Valley, PA) with Hamamatsu DCAM (Middlesex, NJ) Camera using Metamorph image processing software (Center Valley, PA). Fluorodishes were purchased from World Precision Instruments, Inc. (Sarasota, Florida). MDA-MB-435 (WT and ADR) human breast cancer cells were provided by Dr. Hassan Uludag's group at the University of Alberta (Alberta, Canada).

Synthesis and characterization of poly(lactide-co-glycolide)-g-poly(ethylenimine):
PLGA was conjugated to the primary amine group of bPEI via ester bonding. PLGA (800 mg, 200 μmole) was dissolved in 20 ml dried anhydrous DMF. N-hydroxysuccinimide (NHS, 27.6 mg, 240 μmole) and N,N'-Dicyclohexylcarbodiimide (DCC, 49.6 mg,

240μmole) were added to the reaction solution, and this mixture was stirred for 2 hours to activate the carboxylic end group of PLGA. The resulting precipitate, dicyclohexyl urea (DCU), was removed by filtration. bPEI (1.25 g, 50 μmole) was dissolved in 20 ml dried DMF. The activated PLGA solution was added dropwise to the bPEI solution over 30 min, and then the mixture was allowed to react for 24 hours at room temperature while stirring. Poly(lactide-co-glycolide)-g-poly(ethylenimine) (PgP) was purified by dialysis against deionized water using a membrane filter (MWCO=50,000), centrifuged at 5,000 rpm for 10 minutes to remove unreacted PLGA precipitate, solution was then lyophilized.

Following synthesis and purification, the structure of PgP was determined by ^{1}H-NMR on a Bruker 300 MHz using D_2O as solvent. The structure and grafting ratio of PLGA to bPEI was confirmed by observing peaks (δ=2.4~3.5 (m, bPEI backbone -CH_2), δ=1.4~1.6 (d, 3H, PLGA -CH_3), δ=4.3 (q, 1H, PLGA-CH), δ=3.9 (s, 2H, PLGA –CH_2)).

The molecular weight of PgP was determined by gel permeation chromatography. GPC was performed on an Ultrahydrogel 250 column (7.8x300 mm) and guard column (6x40 mm) with water as the mobile phase. A 20-μl sample of PgP solution was utilized, with the flow rate set to 0.7 ml/minute. A Waters 1525 HPLC pump and Waters 2414 refractive index detector were used. Dextrans at molecular weights of 5, 12, 25, 50 and 80kDa were used as standards.

Critical Micelle Concentration

The critical micelle concentration (CMC) was determined using a dye solubilization method. Each weight of PgP was dissolved into a 1 mL aqueous solution at a variety of

concentrations, to which 10 uL of 0.4 mM DPH (1,6-diphenyl-1,3,5-hexatriene) solution was added and shaken for six hours in darkness. The absorbance at 356 nm was measured and plotted against the PGP concentration, and the CMC was determined as the point of intersection between linear extrapolations of the absorbance in low- and high-concentration regions illustrating the concentration micelle complexes form.

Particle size and surface charge of PgP/pDNA complex

PgP/pGFP complexes were prepared using three different PgPs at various N/P (nitrogen atoms of polymer/phosphorus atoms of pDNA) ratios ranging from 5 to 30 (PgP-12k) and from 20 to 70 (PgP-25k and PgP-50k). Varying amounts of PgP solution were mixed with DNA (20 μg pGFP) solution and incubated for 30 min at room temperature. Particle size was determined by dynamic laser light scattering using Zeta PALS and reported as effective mean diameter. ζ-potential was measured electrophoretically using the same apparatus.

Hemolytic activity

The extent of hemolysis was determined by adapting a protocol used by Aravindan et al. [103] Blood collected from Sprague-Dawley rats was combined with heparin (v/v ratio 1:10) was and then centrifuged at 700 x g for 20 minutes at 4ºC to separate buffy coat. The plasma was removed and the red blood cell pellets were washed three times using 150 mM PBS (7.4 pH) with ten times the original volume of pellet, followed by aspiration of the supernatant post-centrifugation at 1000 x g for 10 minutes at 4ºC. Red blood cells were resuspended in 3% (w/v) solution in PBS for combination with polymers dissolved

in the same solution. Equal volumes (80 μL each) of cell solution and polymer were mixed and incubated for one hour at 37ºC. Following incubation, suspensions were centrifuged at 1000 x g for 10 minutes and 100 μL of supernatant was transferred to a 96 well plate and absorbance was assessed at 540 nm using Synergy HT plate reader. Hemolysis was quantified using the following formula: $(A_{Sample}-A_{PBS})/(A_{Triton-X}-A_{PBS})*100\%$, where A_{Sample}, A_{PBS}, A_{Triton} are the absorbance of the sample, PBS, and Triton-X, respectively. Triton-X and PBS treatments were utilized as positive and negative control, respectively.

Hemoaggregation was analyzed using the procedure described by Delgado et. al. utilizing the previously described red blood cell isolation procedure. [104] Equal volumes (80 μL each) of cell solution and various polymer solutions were mixed and incubated for fifteen minutes at room temperature and then imaged.

Plasmid amplification and purification

Escherichia coli DH5α was transformed with plasmids encoding the Monster Green Fluorescent Protein (phMGFP Vector, pGFP) or beta-galactosidase (pSV40-pβGal, pβGal) and amplified in Lysogeny broth at 37°C overnight with shaking at 250 rpm. Plasmids were harvested using the Endofree Maxi Plasmid Purification Kit following the manufacturer's protocol. Plasmid concentration and purity were assessed using a Biotek Synergy HT plate reader in conjunction with a Biotek Take3 microvolume plate system.

Gel retardation assays

To evaluate pDNA binding, heparin competition, or DNase stability, PgP/pGFP or PEI/pGFP complexes were formed at various N/P ratios in RNase/DNase-free water and incubated for 30 minutes at 37°C to allow complex formation. To evaluate complex stability in the presence of DNase, PgP/pGFP polyplexes or pGFP alone was incubated in the absence or presence of DNase (2U) for one hour at 37°C. For the heparin competition assay, PgP/pGFP polyplexes or pGFP alone were incubated in the presence of increasing concentrations of heparin for one hour at 37°C. To complete each assay, the polyplexes were electrophoresed on a 1% (w/v) agarose gel for 25 minutes at 100 V, stained with ethidium bromide (0.5 μg / mL) and imaged on a UV illuminator (Alpha Innotech FluorChem SP imager). The 1kb DNA molecular weight ladder was purchased from Gibco.

Cell Culture

MCF-7, MDA-MB-468, MDA-MB-435 WT, and MDA-MB-435 ADR breast cancer cells were all grown in media supplemented with 10% Fetal Bovine Serum (FBS) and 1% penicillin-streptomycin at 37 °C with 5 % CO_2. MCF-7 cells were grown using Eagle's Minimum Essential Medium supplemented with 10 μg/mL insulin while MDA-MB-468, MDA-MB-435 wild type, and MDA-MB-435 ADR) were grown using RPMI 1640 media supplemented with 1% L-glutamine. Drug resistance was maintained in MDA-MB-435 ADR cells by treating them with 0.2 μg/mL of Doxorubicin-HCl once a week.

Transfection efficiency and cytotoxicity of PgP/pDNA complexes in breast cancer cells in vitro

The transfection efficiency of 3 different formulations of PgP (PgP-12k, PgP-25k, and PgP-50k) was assessed by transfecting various breast cancer cell types with plasmid green fluorescent protein (pGFP) in media containing 10% serum. PEI/pDNA complexes at an N/P of 5/1 were also transfected as a positive control. Untreated cells were used as a negative control. Polyplexes were prepared by mixing PgP and pGFP, (2 μg/mL) at various N/P ratios and then incubating them for 30 minutes at 37°C. Cells (9x 10^5 cells/well) were seeded in 12-well plates and allowed to attach overnight. The cells were then incubated with PgP/pGFP complexes in media containing 10% serum for 24 hours. Afterward, the media was removed and replaced with fresh media containing 10 % FBS and cells were incubated an additional 24 hours. The GFP-expressing cells were imaged using an inverted fluorescence microscope. Following imaging, cells were trypsinized and GFP-expressing cells were counted using a flow cytometer. The results were expressed as a percentage of transfected cells.

Cytotoxicity was also analyzed by MTT assays in parallel experiments following the same transfection protocol. 48 hours post-transfection, cells were washed with PBS and incubated with 1 mL of serum-free media containing 240 μL of Thiazolyl Blue Tetrazolium Bromide in PBS (2 mg/mL) for 4 hours at 37 °C. After incubation, MTT-containing medium was removed, and 1 mL of DMSO was added to dissolve the formazan crystals formed by live cells. Absorbance was measured at 570 nm using a Biotek Synergy HT plate reader. Cell viability was assessed according to the following

formula: Cell viability (%) = ($OD_{570\ (sample)}$/ $OD_{570\ (control)}$) X 100%. Statistical analysis was performed using ANOVA for multiple comparisons using Tukey's Post Hoc analysis using Dunnet's correction.

MCF-7 cells were transfected with PgP-12k/pGFP at N/P ratio of 30/1 while the pGFP expression was evaluated by epifluorescent microscopy over 20 days to investigate the transfection duration.

Determination of the driver of PgP toxicity

Transfections investigating the efficacy in delivering pDNA were fixed to an equal dose of plasmid; an increase in number of micelles would also decrease average plasmid content per polyplex. PEI toxicity and performance is driven by free amine content. With this in mind two additional forms of DDV toxicity were investigated: 1) All PgP polyplexes were formed at 25/1 N/P ratio and diluted 2) uncomplexed PgP; each regime was tested at equivalent N/P 5/1, 15/1, 25/1 PgP transfection doses.

Intracellular trafficking and nuclear localization study

PgP-12k was conjugated with Rhodamine-123 in a manner similar to Yang et al. [11] Rhodamine-labeled PgP-12k was mixed with PgP-12k (1:5 w/w ratio) for visualization. MDA-MB-435 WT and ADR cells (9x 10^5 cells/dish) were plated in Fluorodishes. Polyplexes were formed by mixing pGFP, and Rhodamine-labeled PgP-12k at N/P ratio of 25/1 and transfected as described above. Cells were fixed using 4% paraformaldehyde solution at 36 hours post-transfection, and nuclei were counterstained with 4',6-Diamidino-2-Phenylindole, Dihydrochloride (DAPI).

Uptake poly (lactide-co-glycolide) -graft-polyethylenimine/siGLO nanoparticles (FA-PgP) in MDA-MB-435 ADR breast cancer cells

The siGLO Red transfection indicator, consisting of a fluorescently labeled siRNA duplex with a chemical modification for nuclear localization, was used to evaluate siRNA transfection efficiency. PgP/siGLO complexes (1 μg siGLO Red) at various N/P ratio were transfected in cells in 10% serum condition. bPEI/siGLO at N/P 5/1 was used as positive controls. The cells were incubated at 37 °C for 24 hours and then the media were replaced with fresh media containing 10 % FBS. At 4 and 24 hours post-transfection, siGLO Red-transfected cells were collected and assessed by flow cytometry and the results expressed as % uptake positive and mean fluorescence.

Transfection efficiency of PgP/pDNA polyplexes in an athymic nude mouse breast cancer model in vivo

Athymic nude mice (female, 25 grams) were anesthetized using isoflurane gas. MDA-MB-435 ADR cell solution (1 x 10^6cells/50 μl PBS) was injected into four mammary fat pads per mouse. After four weeks, PgP/pGFP or PgP/pβgal polyplexes (10 μg, 20 μL) were intratumorally injected at an N/P ratio of 30/1. Naked pGFP or pβgal were used as negative controls. Seven days post-injection of polyplexes, animals were anesthetized using isoflurane gas and euthanized by CO2 asphyxiation. To evaluate GFP expression *ex vivo*, tumors and organs from mice treated with pGFP were excised and imaged using a Vevo IVIS Lumina XRMS In Vivo Imaging System. To evaluate β-galactosidase expression; tumors treated with pβgal were excised, frozen in OCT, sectioned, and stained using a β-Gal staining kit to detect β-Gal+ transfected cells and imaged using an inverted

microscope. All surgical procedures and postoperative care were conducted according to NIH guidelines for the care and use of laboratory animals (NIH publication No. 86-23, revised 1996) and under the supervision of the Clemson University Animal Research Committee (Approved animal protocol no. AUP2015-025).

Statistical analysis

Statistical analysis was performed using ANOVA for multiple comparisons using Tukey's Post Hoc analysis unless otherwise noted. A p-value of less than 0.05 was considered statistically significant. The data were represented as mean + SEM.

Results and Discussion

Three different PgPs were synthesized using procedure described in a previous work done by our group. [84] Briefly, the carboxylic acid group of PLGA was activated using *N*-hydroxysuccinimide (NHS) and *N,N'*-Dicyclohexylcarbodiimide (DCC) and then reacted to the amine group of PEI. The resulting Poly (lactide-co-glycolide)–g-poly(ethylenimine) (PgP) was purified by dialysis The structure of PgP was determined by ^{1}H- NMR (300 MHz, Bruker) using D_2O as a solvent (Fig 3.1).

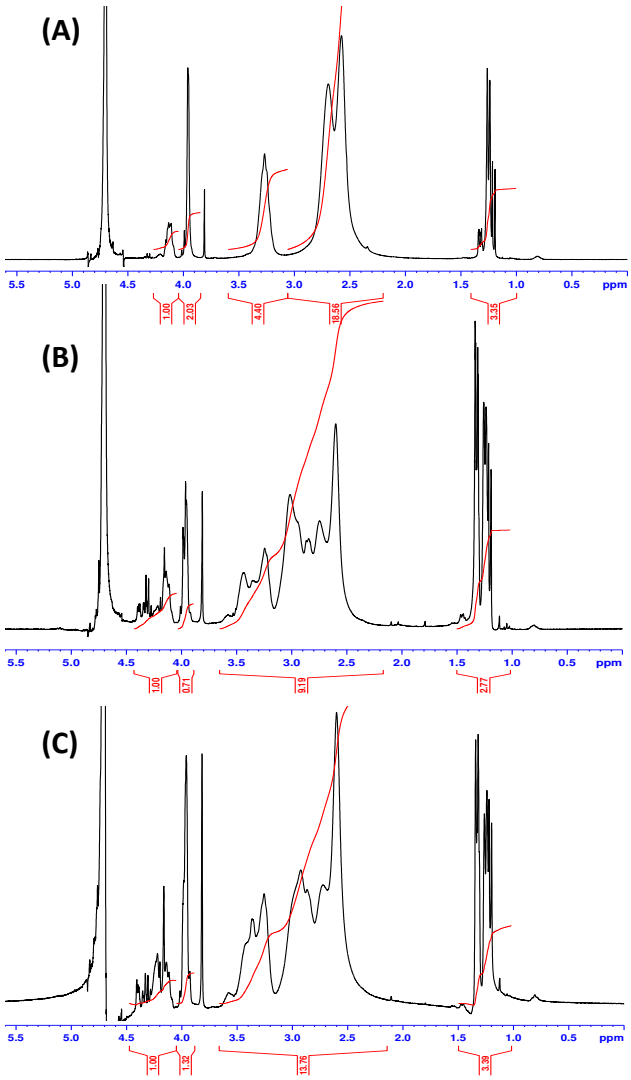

Figure 3.1: ^{1}H-NMR spectra of PgP-[12k, 25k, 50k] (A) PgP-12k (B) PgP-25k (C). PgP-50k

In our characterization of PgP-12k, we found that approximately three 4 kDa blocks of PLGA are grafted to one PEI and the molecular weight of PgP-12k was approximately 38,681 Da measured by ^{1}H-NMR and 38,168 Da measured by GPC. The analysis of PgP-25k revealed that approximately one block of 25kDa PLGA was grafted to one PEI and the molecular weight of PgP-25k was approximately 49,275 Da measured by ^{1}H-NMR

and 48,791 Da measured by GPC. Lastly, one block of 50kDa PLGA was grafted to one PEI and the molecular weight of PgP-50k was approximately 73,000 Da measured by ^{1}H-NMR. The nomenclature for each PgP was ascribed by the weight of PLGA per one PEI molecule. PgP-12k, PgP-25k, and PgP-50k, have the following PLGA compositions: three blocks of 4 kDa PLGA, one block of 25 kDa PLGA, and one block of 50 kDa PLGA, respectively (Table 3.1).

Table 3.1: Table summarizing composition of PgP-(12k, 25k, 50k)

	PgP-12k	**PgP-25k**	**PgP-50k**
PLGA Weight (kDa)	4	25	50
PLGA Repeats	3.6	0.96	0.96
PLGA Weight (kDa)	14.4	24	48
Total Weight (kDa)	39.4	49	73
HLB	12.7	10	6.84

These permutations provide an investigation across block length as well as block number. Both parameters have implications on the kinetics of the polymer in reference to micelle structure.

Essentially, we have three similar compositions of a singular drug delivery vector. These vectors are self-assembled amphiphilic unimers; these unimers are comprised of an average number of hydrophobic blocks (PLGA) covalently bound to a hydrophilic block

(PEI). These PgP unimers form aggregates called micelles; of which the composition number and stereo-arrangement, is unique to each composite, and is ultimately resultant of thermodynamic and electrostatic equilibrium between the polymer and its environment.

Micelle formation is a dynamic process that is in in continual flux, like any physical interaction between molecules and solvent. Unimers have distinct hydrophobic and hydrophilic domains that are in constant interaction with the solvent molecules. Below CMC, it is more energetically favorable for hydrophobic moieties interact with air than to sequester hydrophobic tails in a micellar solution. Once CMC/CMT conditions are met micellization occurs with colloidal suspensions providing hydrophobic space in solution. DPH exhibits differential ultraviolet absorbance depending upon its surrounding environment; an increase in absorbance associated with hydrophobic sequestration or incorporation into the hydrophobic space within micelles. [105] CMC was determined as the point of intersection between incorporated DPH associated with singularly dissolved unimer and the much brighter incorporated DPH localized in micelles.

The CMCs of PgP were calculated to be 0.69 mg/ml (1.86 X 10^{-5} M), 0.45 mg/mL (9.39x 10^{-6} M), and 0.16 mg/mL (2.07x 10^{-6} M) for PgP-12k, PgP-25k, and PgP-50k, respectively). HLB correlated negatively with an increase in hydrophobic block length and exceeded the stability range (~10^{-3}-10^{-4}M) of small molecular weight surfactants, such as sodium dodecyl sulfate (8.2 mM). The low CMC indicates a high degree of thermodynamic stability, a measure that describes tendency for unimers to undergo

micellization. The same forces that dictate thermodynamic stability are related to kinetic stability, the rate at which micelles disband into unimers once diluted below CMC. Polymeric micelles illustrate increased kinetic stability with increasing size of hydrophobic block. [25] Other factors such as core plasticity or incorporation of hydrophobic drugs may also slow destabilization, which is advantageous for increasing circulation times of a delivery vector for drugs and nucleic acids. [106]

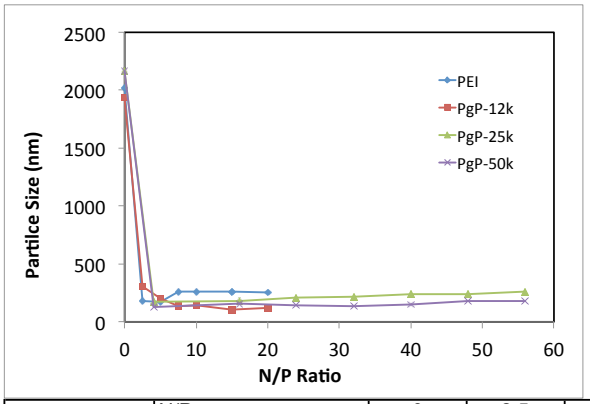

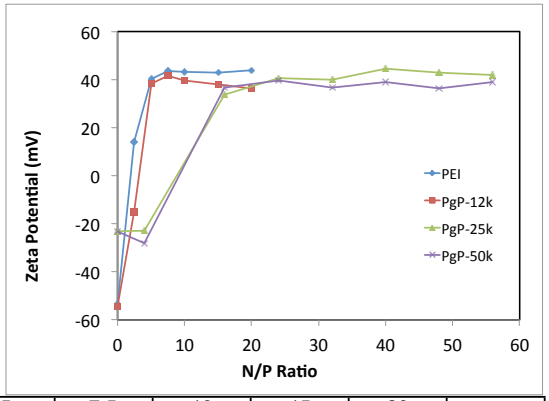

PgP-12k	N/P	0	2.5	5	7.5	10	15	20	
	Size (nm)	1937.5	307.2	203.6	138.3	146	102.7	120.4	
	Zeta Potential (mV)	-54.29	-14.94	38.46	41.53	39.73	38.12	36.21	
PgP-25k	N/P	0	4	16	24	32	40	48	56
	Size (nm)	2167	174.0	178.8	207.3	218.9	239.6	241.6	262.7
	Zeta Potential (mV)	-23.12	-23.08	33.73	40.56	39.94	44.61	43.05	41.80
PgP-50k	N/P	0	2.5	10	15	20	25	30	35
	Size (nm)	2167	125.0	159.5	142.2	132.1	151.3	183.0	178.7
	Zeta Potential (mV)	-23.12	-28.09	36.64	39.70	36.83	39.02	36.21	39.01
PEI	N/P	0	2.5	5	7.5	10	15	20	
	Size (nm)	2016.3	176.1	168.7	262.4	257.6	260.5	256.7	
	Zeta Potential (mV)	-53.51	14.07	40.26	43.67	43.26	42.89	44.01	

Figure 3.2: Particle size and zeta potential of PgP-(12k, 25k, 50k) and PEI polyplexes

The size and surface charge of PgP/pDNA polyplexes at various N/P ratios are shown in Figure 3.2. PgP/pGFP complexes were prepared at various N/P (nitrogen atoms of polymer/ phosphorus atoms of pDNA) ratios ranging from 1 to 30. DNA (20 μg pGFP)

and varying amounts of PgP were each separately diluted in 500 μl of deionized water. After 10 min, solutions were mixed and incubated for 30 min at room temperature. Particle size was determined by dynamic laser light scattering using Zeta PALS (Brookhaven Instruments Corp, Holtsville, NY) and reported as effective mean diameter. ζ-potential was measured electrophoretically using the same apparatus.

The mean particle size of PgP-12k/pDNA polyplexes decreased with an increase in N/P ratio and was about 150-200 nm at an N/P ratio of 7.5/1 and above (Fig 3.2). Zeta potentials of PgP/pDNA complexes were dependent on the N/P ratio and were positively charged at an N/P ratio of 5/1 or greater suggesting that negatively charged plasmid DNA is completely neutralized by positively charged PgP above an N/P ratio of 5/1 (Fig 3.2). Particle size and ζ-potential of PgP-25k and PgP-50k were found to neutralize DNA at an N/P of 12/1 with particle sizes ranging from 200nm to 150nm respectively. All of which are similar to the size of bPEI/pGFP complexes (Fig 3.2). It is of note that in some size and zeta potential experiments a bimodal distribution of neutrally charged and positively charged aggregates was exhibited (data not shown). This phenomenon has been observed in other polymeric micelle systems, as primary aggregates undergo secondary conformation changes into larger complexes.[106]

Size and surface charge characteristics of polyionic complexes are important in determining the fate of the delivery system both in terms of extracellular delivery, cellular uptake, and intracellular fate. [44] In addition to providing insight to charge dynamics between gene element and polymer zeta potential assessment can provide

insight to the potential of aggregation via self-attraction. With the presence both negative and positive charge components complexes with low zeta potentials run the risk of surface electrostatic repulsion being insufficient in overcoming attractive forces of negative moiety on surface of complex (nucleic acid) of one complex to the positive corona of another complex. [78] Such a situation increases the likelihood of flocculation, reducing concentration of drug within system and reducing efficiency.

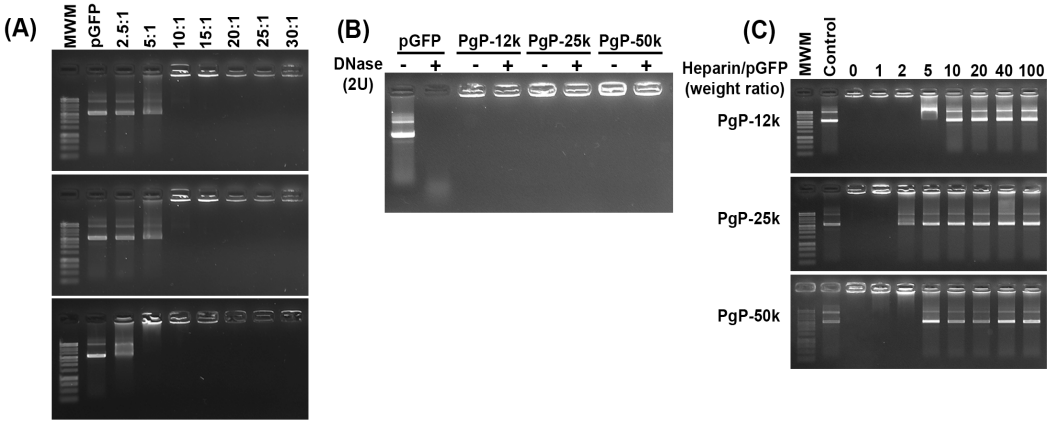

Figure 3.3: A) Gel retardation assay using PgP-(12k, 25k, 50k) /pGFP complexes. Lane 1: DNA ladder, Lane 2:naked pDNA, Lane 3 -9: PgP/pGFP (N/P: 2.5, 5, 10, 15, 20, 25, 30 respectively) B) DNase protection assay with PgP-(12k, 25k, 50k)/pGFP complexed at N/P 25/1. Lane 1:pGFP, Lane 2:pGFP with 2 units DNase, Lane 3: PgP-12k/pGFP, Lane 4: PgP-12k/pGFP with 2 units DNase, Lane 5: PgP-25k/pGFP, Lane 6: PgP-25k/pGFP with 2 units DNase, Lane 7: PgP-50k/pGFP, Lane 8: PgP-50k/pGFP with 2 units DNase C) Heparin competition assay using PgP-(12k, 25k, 50k) /pGFP complexes. Lane 1: DNA ladder, Lane 2:naked pDNA, Lane 3: PgP/pGFP (N/P:25/1), Lanes 4-10: PgP-12k/pGFP (N/P: 25/1 with W/W Heparin 1, 2, 5, 10, 20, 40, 100 respectively)

Minimum N/P ratios required for complex formation between PgP and pDNA were investigated using a gel retardation assay. PgP/pDNA complexes were formed at a variety of N/P ratios and the minimum ratio for complex formation was determined by identifying the lowest N/P ratio at which no pDNA migration was observed,

demonstrating complete binding of free pDNA by PgP. PgP-12k, 25k, and 50k completely bound free pDNA at N/P ratios of 10/1 (Fig 3.3A). Binding strengths were further assessed in a Heparin competition assay.

In order to determine the stability of the PgP/pDNA complex in preventing competitive binding with large polyanions and the ability of the complex to dissociate in order to free the nucleic acid cargo, a heparin competition assay was performed. PgP-25k polyplexes began to dissociate at a Heparin/pGFP weight ratio of 2/1, while PgP-12k and PgP-50k both began to dissociate at a weight ratio of 5/1 (Fig 3.3B). The additional weight of heparin required to dissociate PgP-12k and PgP-50k relative to PgP-25k, reflects the increased stability of these complexes over PgP-25k. PgP micelles composed of any weight PLGA have exhibited the ability to dissociate from pDNA, demonstrating the potential utility of PgP for delivery and release of nucleic acid cargo.

Both gel retardation and heparin are indirect measure of protective ability of DDV. PgP-12k, 25k, and 50k all exhibited protective effects against DNase-mediated degradation of pDNA at an N/P ratio of 25/1, demonstrating the potential of PgP to protect genetic cargo for *in vivo* delivery (Fig 3.3C).

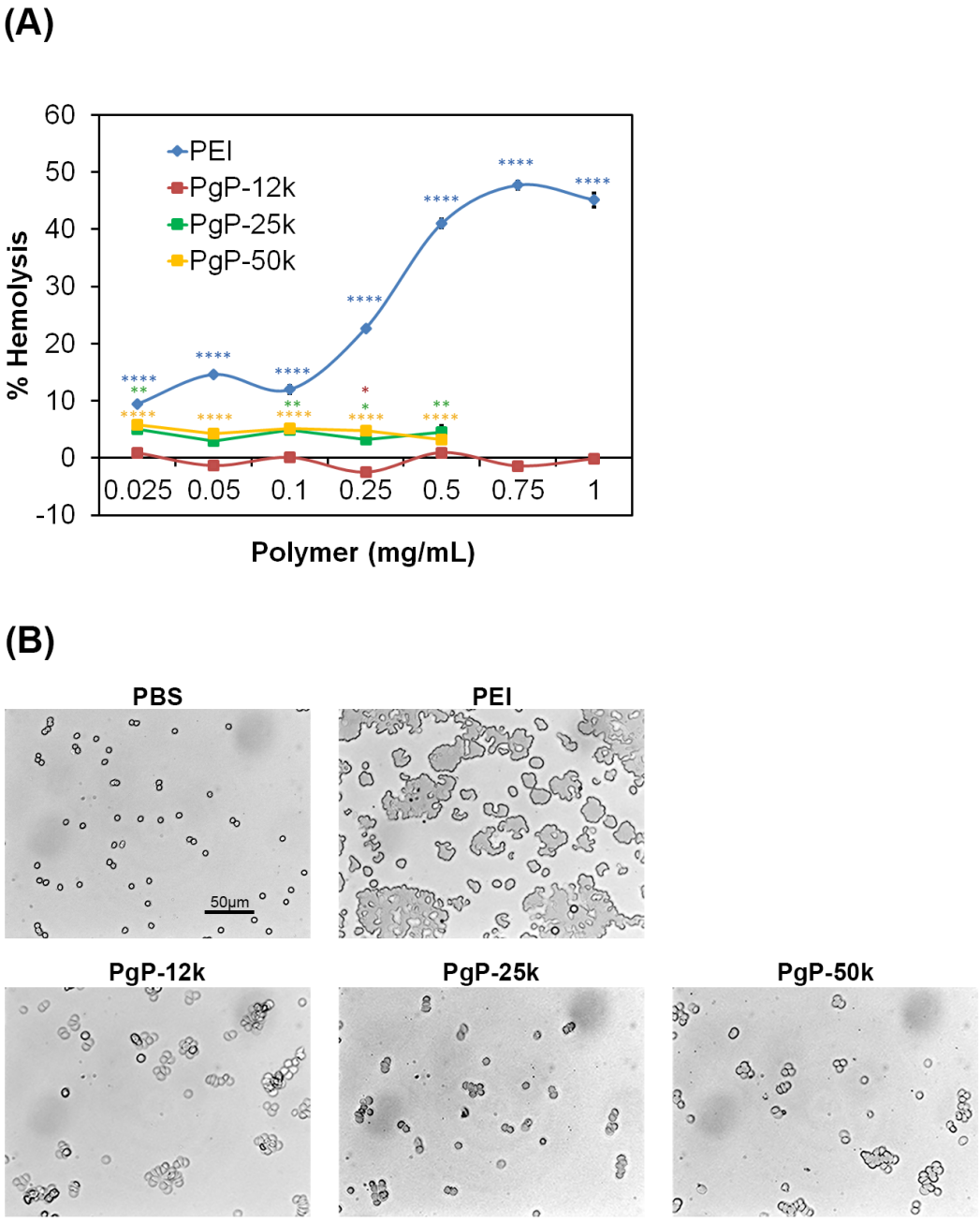

Figure 3.4: A) Hemolytic activity of PEI, PgP-[12k, 25k, 50k] at 0.025, 0.05, 0.1, 0.25, 0.5, 0.75, 1 mg/mL in 7.4 pH 150 mM phosphate buffered saline (PBS). Red blood cells collected from Sprague-Dawley rats. * P≤ 0.05, ** P≤0.01, *** P≤0.001, **** P≤0.0001 B) Hemoaggregation of red blood cells in 7.4 pH 150 mM PBS incubated with 1 mg/mL of PEI, PgP-[12k, 25k, 50k] for fifteen minutes

Hemolysis is a direct measure of cytotoxicity on erythrocytes, while hemoaggregation provides insight into the physical interactions of the delivery vehicle with solid elements in the blood. Both are important factors necessary to assess the safety of the delivery vehicle prior to *in vivo* evaluation. Interestingly, increasing the dose of PgP at any MW between the concentrations 0.025 mg/mL to 0.5 mg/mL did not result in increased hemolysis, as was demonstrated with PEI. PgP-12k induced little to no hemolytic activity while both PgP-25k and 50k induced 4-7% hemolysis. The hemolytic activity of PEI generally increased with polymer concentration and ranged from ~10% at 0.025 mg/mL to ~40% at 0.5 mg/mL (3.4A). At 1 mg/mL, PgP-12k, 25k, and 50k induce some erythrocyte aggregation relative to untreated cells; however, it is to a far lesser degree compared to PEI at the same concentration (Fig 3.4B).

Together, these results demonstrate that PgP micelles have minimal hemolytic activity, especially when compared to equivalent concentrations of PEI. However, the linearized block conjugates (25k and 50k) exhibited more hemolytic activity despite relatively reduced charge. This may suggest nanotopology has an effect, likely on a steric level to reduce blood cell exposure to primary amines.

The transfection efficiency of pGFP and cytotoxicity of PgP-12k, PgP-25k, and PgP-50k polyplexes in MCF-7, MDA-MB-468, MDA-MB-435 WT and MDA-MB-435 ADR cells was determined by flow cytometry and MTT assays, respectively. These results are shown in Figure 3.5. PEI polyplexes at an N/P ratio of 5/1 were evaluated as a positive control and untreated cell were used as a negative control. Generally, there was a positive

correlation between N/P ratio and transfection efficiency, and a negative correlation between N/P ratio and cell viability. PgP polyplexes also achieved much higher transfection efficiencies in comparison to PEI polyplexes, which achieved maximum transfection of less than 5% in all cell lines (Fig 3.5).

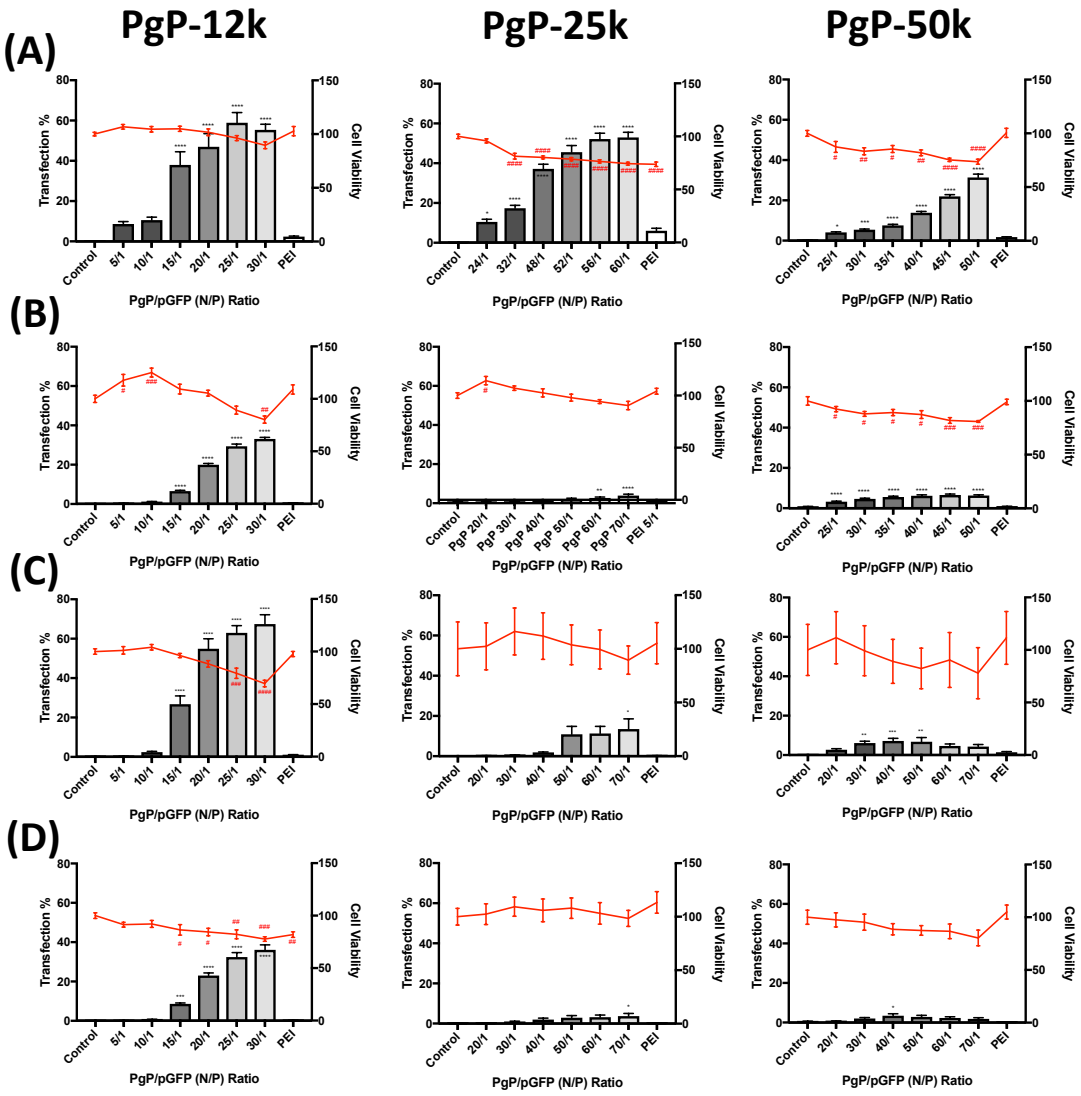

Figure 3.5: Transfection efficiency (primary axis) and metabolic activity (secondary axis) of three PgP /pGFP complexes at varying N/P ratios in (A) MCF-7, (B) MDA-MB-468, (C) MDA-MB-435 Wild Type, and (D) MDA-MB-435 ADR cells. * or ## P≤ 0.05, ** or ## P≤0.01, *** or ### P≤0.001, **** or #### P≤0.0001

PgP-12k polyplexes demonstrated the highest levels of pGFP transfection in MCF-7 and MDA-MB-435 WT cells, with 54% and 65% transfection efficiency, respectively, at an N/P ratio of 30/1 (Fig 3.5). Although to a lesser degree, PgP-12k polyplexes were also able to transfect MDA-MB-468 and MDA-MB-435 ADR cells with transfection efficiencies of 30% and 35% at an N/P ratio of 30/1. PgP-12k demonstrated minimal cytotoxicity in all cell lines tested. The highest toxicity was observed in MDA-MB-435 WT cells, with 75% viability at an N/P ratio of 30/1. For all other breast cancer cell lines, the viability ranged between 80-120% for all N/P ratios evaluated.

PgP-25k polyplexes required higher N/P ratios to achieve transfection efficiency similar to PgP-12k polyplexes. Transfection of PgP-25k polyplexes was greatest for MCF-7 cells, with a transfection efficiency of 50% at an N/P ratio of 70/1 (Fig 3.5). However, PgP-25k was not very effective in transfecting all other cell types evaluated. Transfection efficiencies observed for MDA-MD-468, MDA-MB-435 WT, and MDA-MB-435 ADR cells were approximately 3%, 13%, and 4%, respectively. Cytotoxicity of PgP-25k polyplexes was similar to measured values for PgP-12k polyplexes, with viability ranging between 75-120%.

PgP-50k was the least efficient in transfecting pGFP into breast cancer cells lines when compared to PgP-12k and PgP-25k. Like PgP-25k, the highest transfection efficiency was observed in MCF-7 cells, with 30% transfection at an N/P ratio of 50/1 (Fig 3.5). PgP-50k polyplexes achieved transfection efficiencies of only 6%, 4%, and 2% at the maximum N/P ratio tested in MDA-MB-468, MDA-MB-435 WT, and MDA-MB-435

ADR cells, respectively. Treatment with PgP-50k polyplexes resulted in a wide range of measured cell viabilities from 75% in MCF-7 cells up to 120% in MDA-MB-435 WT cells at N/P ratios from 20/1 to 70/1.

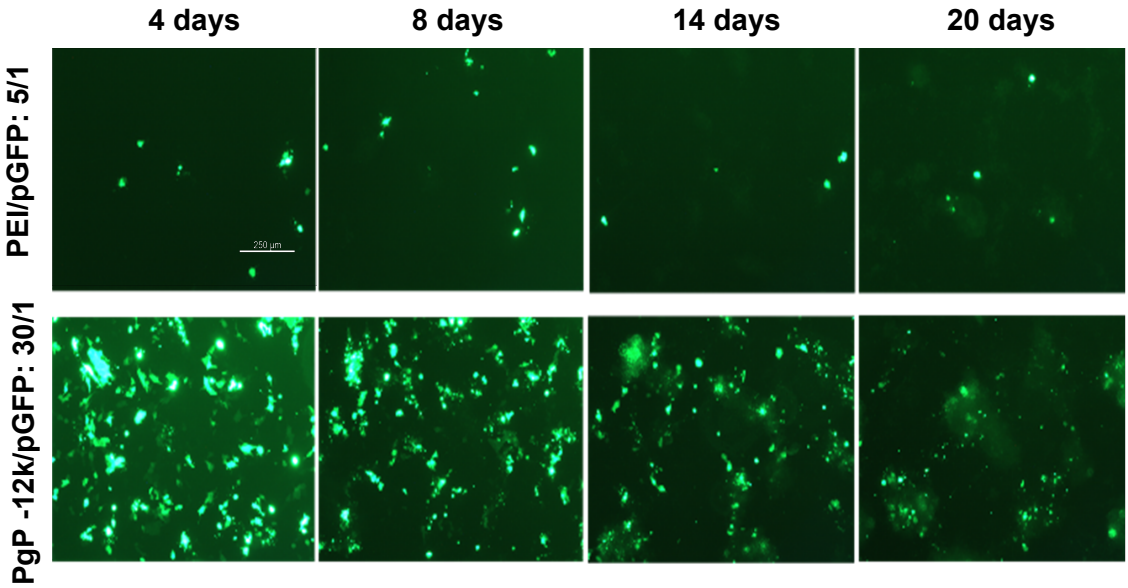

Figure 3.6: Time-course study of GFP expression in MCF-7 cells with PEI/pGFP and PgP-12k/pGFP in 10% serum condition at 4, 8, 14, 20 days. Top: PEI/pGFP N/P 5/1, Bottom: PgP/pGFP N/P 30/1

Transgene GFP expression was found to last up to 20 days in MCF-7 breast cancer cells (Fig 3.6).

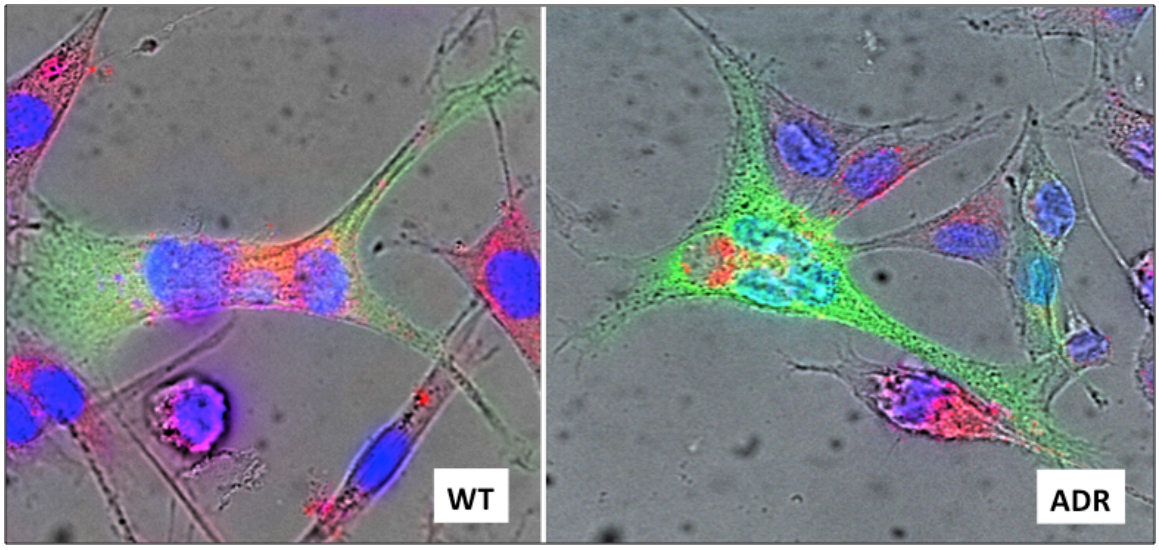

Figure 3.7: Confocal microscopy depicting intracellular trafficking of Rhodamine-PgP/pGFP polyplexes in MDA-MB-435 WT and MDA-MB-435 ADR breast cancer cells

Intracellular uptake, nuclear localization and subsequent transfection were observed in both MDA-MB-435 WT and MDA-MB-435 ADR breast cancers via confocal microscopy 48 hours post transfection (Fig 3.7).

Overall, the results demonstrate that PgP-12k was the most efficient vector for transfecting breast cancer cell lines in comparison to PgP-25k and PgP-50k. PgP-12k mediated high levels of pGFP transfection in MCF-7 cells and MDA-MB-435 WT cells and mediated moderate transfection in MDA-MB-468 and MDA-MB-435 ADR cells. PgP-25k and PgP-50k were only able to mediate transfection into MCF-7 cells, with PgP-50k demonstrating the lowest efficiency. PgP-12k and PgP-25k were approximately 1.7-fold more efficient in transfecting MCF-7 cells compared to PgP-50k. Further, PgP-12k polyplexes were at least 5-fold more efficient in transfecting all other cell lines in comparison to both PgP-25k and PgP-50k.

Differences in cell lines are result of differences in uptake and subsequent intracellular trafficking. The size distribution of polyplexes is a dynamic entity related to synthetic composition, initial formation conditions, temperature, pH, protein and salt contents.[9] Serum content is high in albumin, whose presence has been shown to have a strong detrimental effect on the kinetic stability of polymeric delivery due to induced aggregation effects and formation of a ternary structure.[102,108] Differences in media composition between cell lines may have some effect on the aggregation but stronger effects are likely due to serum content, which remains constant throughout experimentation. These minute differences in size and charge may have more profound effects depending on each cell's optimal trafficking modality. Altering the relative proportion of polyplexes trafficked to each endocytic pathway will have obvious effects dependent on the efficacy of each route, with optimal pathway conditions likely varying between cell lines.[36]

Furthermore, cells that divide more quickly have been associated with improved transfection outcomes. Nuclear import and subsequent transcription are two rate limiting steps to transfection. [77,109] Nuclear pores generally only allow free trafficking of molecules under 9 nm in diameter or 50kD in size, much smaller than the observed size of polyplexes. [83,101] Magnitudes higher transfections have been associated with S or G_2/M phases compared to other cell cycles. [110] During these phases genetic material is no longer sequestered within the nuclear envelope, thus it is now widely accepted that increased cell division and growth have a positive correlation with transfection success. [36] Generally, observed cell division rates increase across MDA-MB-435 ADR, MDA-MB-

468, MCF-7, and MDA-MB-435 WT cells. This observation may serve to explain some of the resulting transfection differences between lines.

Within each experimental set, plasmid concentration is fixed to 2ug/well and increasing the amounts of PgP used in higher N/P ratios. With each increase of PgP there is also a decrease of relative number of plasmid copies compared to unimer number. Despite this fact, with each increase in dose there is increase in the percentage of cells positive. This would suggest that despite there being few plasmid copies per micelle the added functionality of increasing the vector somehow yields greater protein production. It has been shown that uncomplexed PEI, even added a few hours after initial polyplex exposure can enhance transfection up to 500 times. It is still not clear why but proposed explanations involve enhanced uptake of complexed PEI, improved endosomal escape, or activation of trafficking pathways more conducive to transfection. [77] The cytotoxic mechanism of PEI is still in contention. It has been observed that membrane exposure to primary amines has a destabilizing effect, which results in a decrease of metabolic activity. [111] PEI is more toxic in its free form due to increased numbers of exposed primary amines compared to PgP. [112] It is these free amines that have also been correlated to increased endosomal escape and transfection rates, regardless of mechanism. [77]

Initial micellization is driven by the presence of hydrophobic blocks. This effect reduces primary amine exposure via steric limitations induced by hydrophobic effect. Such a reduction is reflected in the higher N/P ratios required for complete charge neutralization when utilizing PgP compared to PEI. Microcytic regularity is partially enforced by

preformation of micelles prior to complexation with DNA. These motifs enforce regularity in the chaotic and multilayered aggregation process associated with DNA. Decreasing HLB across increasing PgP size dictates the morphology of these microstructures with star-like micelles being more limited by hydrophilic block sterics transitioning into tighter-cored crew-cut micelles, limited by hydrophobic block sterics. Particle size measurements reflect a reduction in aggregate size from ~200nm for PgP-12k and PgP-25k to ~150nm for PgP-50k, potentially as a result of tighter cores associated with crew-cut micelles relative to star-like micelles allowing better polyplex compaction. With an HLB of 10, PgP-25k may represent a transition from star-like to crew-cut micelles. An increase in hydrophobic block length in one-block systems with a consistent hydrophilic block has been shown to increase aggregation number as well as core size while decreasing CMC. This however, often comes with a negative effect on the total number of micelles. [106] This transition has an effect final aggregate structure and may help explain the easier dissociation of genetic material associated with PgP-25k relative to PgP-12k and PgP-50k in Heparin competition assay as aggregate behavior potentially trends from more, loosely-associated to fewer, more strongly associated micelles.

Use of lipophilic moieties to reduce primary amine exposure and membrane compatibility has been extensively investigated to mitigate polyplex toxicity. [113] Enhanced transfection with PgP relative to PEI is partially due to a hybridization of reduced primary amine exposure and enhanced membrane compatibility induced by hydrophobic moieties.

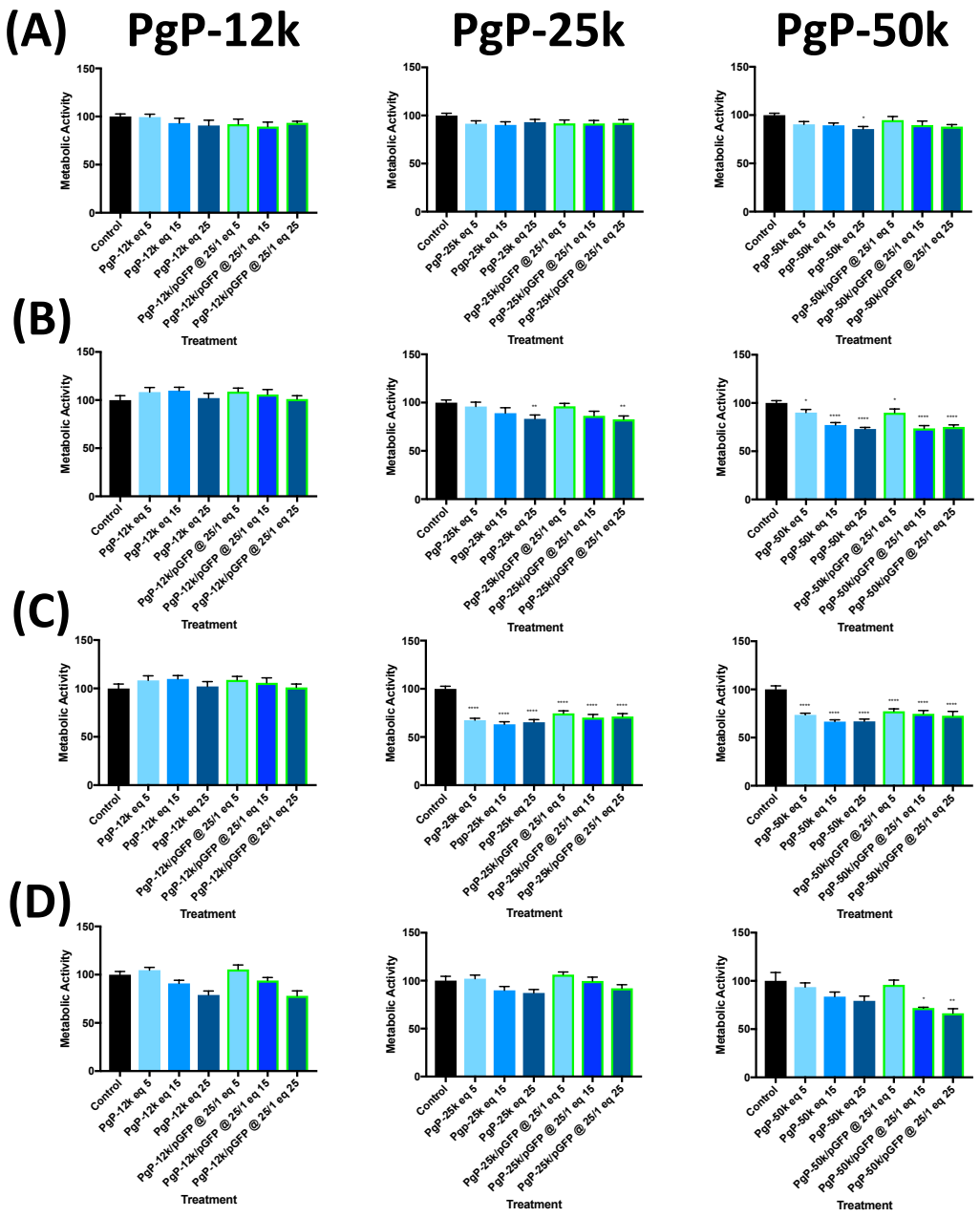

Figure 3.8: Metabolic activity of three PgP /pGFP complexes in (A) MCF-7, (B) MDA-MB-468, (C) MDA-MB-435 Wild Type, and (D) MDA-MB-435 ADR cells. PgP/pGFP complexes were formed at N/P 25/1 and both PgP alone and PgP/pGFP complexes were diluted down to concentration of PgP found in designated N/P equivalent * $P \leq 0.05$, ** $P \leq 0.01$, *** $P \leq 0.001$, **** $P \leq 0.0001$

In cytotoxicity experiments designed to decouple N/P ratios from dose of PgP, PgP-12k and PgP-12k/pGFP complexes were not significantly cytotoxic in any ratio in any cell line (Fig 3.8). There were no significant differences in cytotoxicity between PgP-12k alone and PgP-12k/pGFP in any ratio equivalent. Using PgP-25k, similar cytotoxicities were observed in all ratios tested with no significant differences found between any groups. PgP-50k alone and PgP-50k/pGFP were only found to be significantly toxic at PgP-50k at PgP dose equal to a N/P 25/1. In MDA-MB-468 cells, neither PgP-12k nor PgP-12k/pGFP were significantly cytotoxic at any dose. PgP-25k and PgP-25k/pGFP induced significant cytotoxicity at 25/1. Unlike MCF-7 cells, PgP-50k was found to be significantly cytotoxic at all ratios tested in both formats. In MDA-MB-435 WT cells, PgP-25k, PgP-50k, and PgP-50k/pGFP were found to be significantly cytotoxic at all doses tested ($p \leq 0.0001$). In MDA-MB-435 ADR cells, only PgP-50k/pGFP at equivalent doses 15/1 and 25/1 were able to be found statistically different from control. This study supports the notion that larger PgPs are more toxic per mole, regardless of N/P relationship.

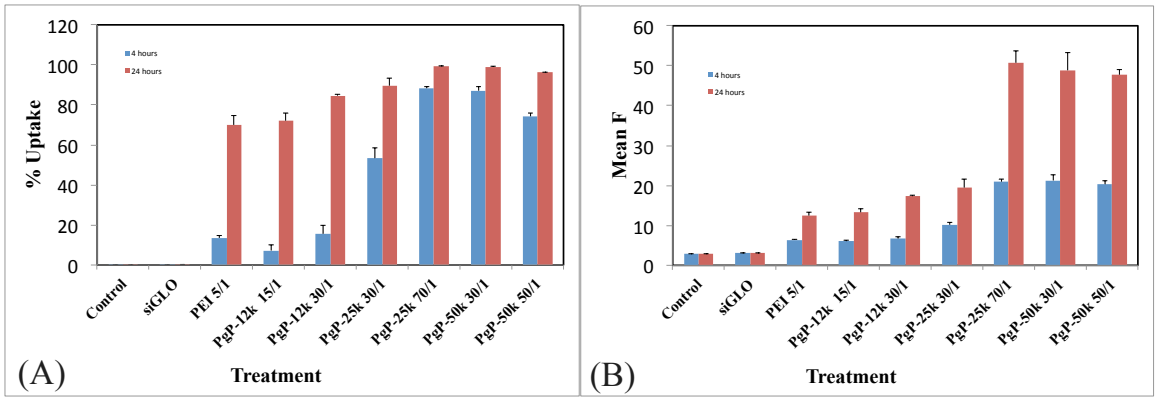

Figure 3.9: Cell uptake of siGLO/PgP complexes in MDA-MB-435 ADR cells (A)% uptake (B) mean fluorescence value (F).

In a siGLO uptake study in MDA-MB-435 ADR cells, as N/P ratio increased within each PgP type or as weight of PgP used at each N/P increased there was an increase in percent of cells positive for siGLO as well as the mean brightness of cells (Fig 3.9). This suggests that given equitable levels of nucleic acid components for any increase in polymer concentration there will be an increase in both the population of cells that uptake DDV as well as a greater amount of nucleic acid per each cell, despite the nucleic acid reduction relative to polymer. This study, taken together with cytotoxicity data suggests that, despite greater amount of PgP uptake associated with increased PgP weight there is a reduction in transgene expression. Indicating that differences in PgP-12k transfection vs PgP-25k and PgP-50k are likely the result of reduced endosomal escape or poor nuclear localization of pGFP plasmid.

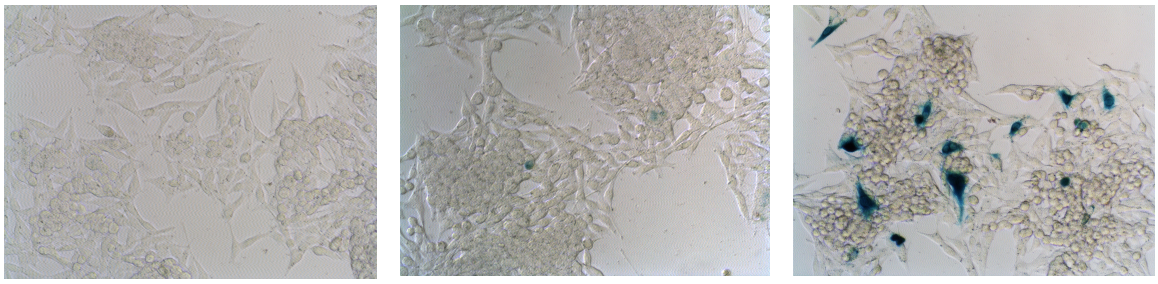

pβGal PEI/pβGal PgP-12k/pβGal

Figure 3.10: Transfection efficacy of PEI/pβGal and PgP-12k/pβGal in MDA-MB-435 ADR cells

Prior to injecting PgP-12k polyplexes in vivo, transfection with pβGal pDNA transfection was undertaken in vitro. Observed transfection rates were highest in PgP-12k/pβGal with reduced transfection in PEI/pβGal and pβGal alone (Fig 3.10).

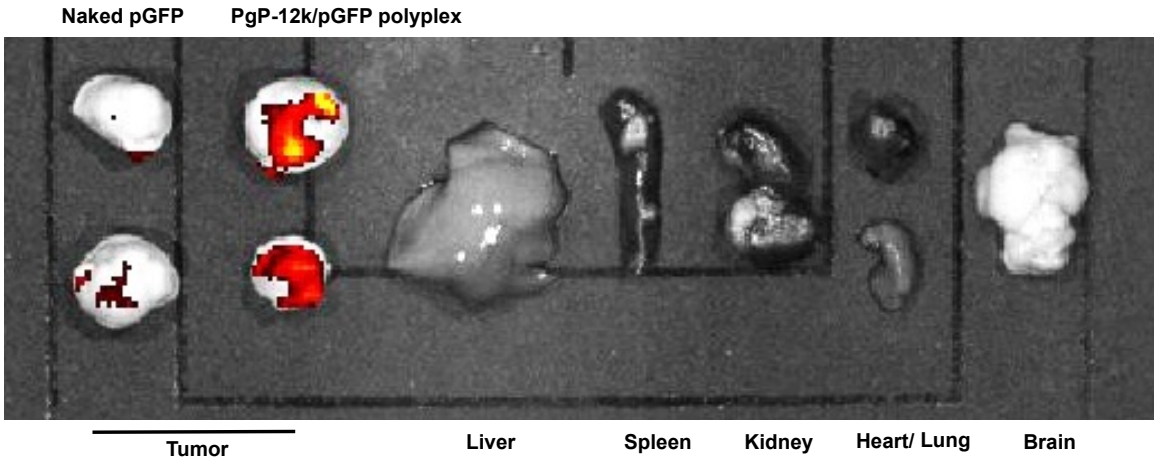

Figure 3.11: GFP expression after local injection of PgP12k/pGFP in mice, excised tumor and organs at 1week post-injection

Immunodeficient mice were injected with MDA-MB-435 ADR breast cancer cells in the mammary fat pad. Tumors were injected with naked pGFP or PgP-12k/pGFP polyplexes. One week later tumors and organs were excised. GFP was found to be concentrated in

tumors with increased visible GFP expression in tumors injected with PgP-12k/pGFP relative to tumors injected with pGFP alone. Little to no GFP was expressed on surfaces of organs, suggesting limited exposure of injected pDNA to rest of the body via the circulatory system (Fig 3.11).

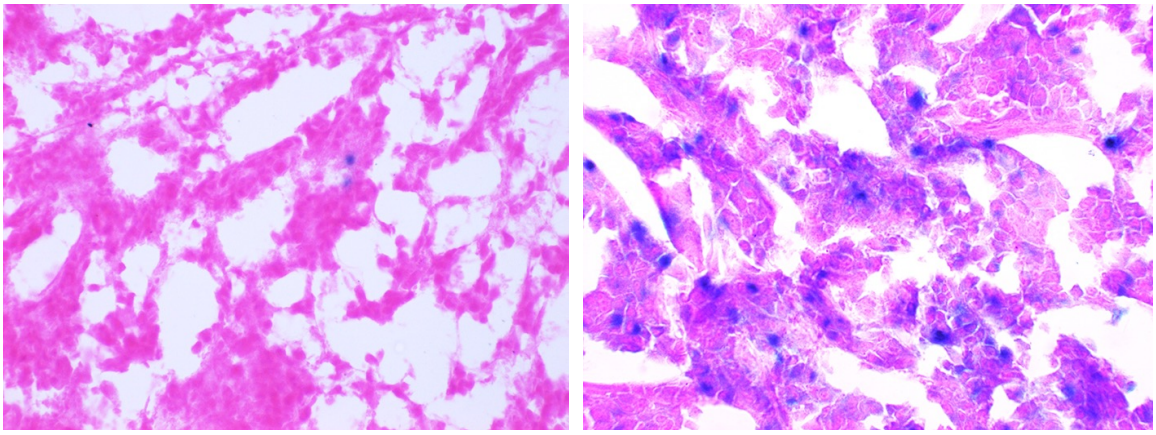

pβGal PgP-12k/pβGal

Figure 3.12: Transfection efficacy of pβGal and PgP-12k/pβGal in MDA-MB-435 ADR tumors

A similar study was performed using pβGal in lieu of pGFP. Excised tumor sections illustrate increased transfection in tumors injected with PgP-12k/pβGal polyplexes compared to naked pβGal alone (Fig 3.12). Both of these *in vivo* studies indicate that PgP-12k is potentially and effective DDV for nucleic acid delivery.

Conclusions

PgP was successfully synthesized and characterized utilizing a variety of PLGA lengths. In all cell lines and PgP types, transfection efficiency ascends with a rise in N/P ratio (sans the top end of PgP-12k in MCF-7 [30/1] and PgP-50k in MDA-MB-468 at highest

N/P ratios tested [70/1]). As weight of PLGA component increased there was a decrease in transfection efficiency compared to its associated cytotoxicity. PgP-12k has ten to one hundred fold higher transfection efficiency relative to cytotoxicity than that of branched PEI-25k, known as the best non-viral gene carrier, in all cell lines tested in 10% serum condition. [86,114] This represents marked improvement of Dr. Bae's (PLGA)-b-PEI micelles which exhibited a reduction in concentration of GFP produced compared to PEI N/P 5:1 in non-serum conditions. [114]

PgP-12k illustrates itself to be a superior polymeric gene delivery vector than the current gold standard PEI in more physiologically relevant conditions (10% serum) across wide variety of breast cancer contexts. [76] Utilization of longer PLGA blocks may increase hydrophobic drug loading capability but at the detriment to its ability to effectively deliver pDNA. As incorporation of a hydrophobic drug within the polymeric core would increase functionality of DDV, future studies involve loading of Doxorubicin within complexes. Increasing PLGA block length is expected to enhance drug-loading capability per weight of polymer and may redeem functionality of lesser transfecting PgP-25k and PgP-50k. Additionally, PgP-12k will be conjugated to folate to illustrate the feasibility of incorporating a targeting moiety.

CHAPTER FOUR

EVALUATE POLY(LACTIDE-CO-GLYCOLIDE)-GRAFT-POLYETHYLENIMINE (PgP) AS A DRUG CARRIER

Introduction

The composition of poly (lactide-co-glycolide) -graft-polyethylenimine (PgP) is described by increasing poly (lactic-co-glycolic) acid (PLGA) ratios. PLGA exists as different blends of block copolymers from lactide (L) and glycolide (G) monomers. These blends are described by the relative number of blocks of each type whose nomenclature is derived from this proportion. PgP-12k and PgP-50k are comprised of 50%:50% L to G while PgP-25k is comprised of 75:25 L to G. Lactide groups weigh per unit more because of additional methyl group within the structure. This additional hydrophobic branching results in greater hydrophobicity to some extent and may increased steric hindrance due to a more branched structure. [115] The reason for variable block composition is due to materials available.

Beyond PLGA composition differences there also exist some synthetic differences between each type. PgP-12k is comprised of ~3[.6] (4 kDa) blocks per 1 PEI. PgP-25k ~1 (25 kDa) to 1 PEI and PgP-50 ~1 (50 kDa) to 1 PEI; yielding total weights of 38.6 kDa, 49.2 kDa and 73 kDa for PgP-12k, PgP-25k, PgP-50k respectively (Table 3.1). Many chemotherapeutic drugs are hydrophobic. [9] This results in a diminishment of medical utility due to solubility limits, which may be improved via encapsulation within DDV. In this study, increasing amounts of hydrophobic PLGA were used load more

Doxorubicin (DOX) per mg of polymer. A fixed mass (1 mg/mL) of each PgP type was dissolved to a fixed volume (1 mL) and subjected to variable hydrophobic Doxorubicin content in order to determine optimal DOX loading procedure. In chapter 3, all transfections were fixed to an equal dose of plasmid; an increase in number of micelles would also decrease average plasmid content per polyplex. PEI toxicity and performance is associated with free amine content, with N/P 5/1 being cited as the most efficacious format with increased ratios incurring unacceptable toxicity; indicating the importance of both dose and form in nanomedicine. It was found larger PgPs are more toxic per mole, regardless of N/P relationship. It was then important to determine if this concept carries forward to it DOX loaded counterparts and additionally determine if DOX loaded PgP (complexed or uncomplexed) induces an equivalent cytotoxic response to DOX Hydrochloride (DOX HCl), a more water-soluble version of DOX often used chemotherapeutic treatment. These comparisons 1) provide further evidence that even within a refined context of "breast cancer" that our delivery goals are different relative to each target population, 2) illustrate that introduction of a new compound may assist or hinder advancement on other goals, 3) determine if PgP delivers effective dose to a current at-market counterpart DOX HCl, and 4) determine if effective dosages optimized for gene delivery can deliver a dose of DOX in sufficient quantity to induce a significant cytotoxic response.

Materials and Methods

Three different molecular weights of poly(lactide-co-glycolide) (PLGA) were purchased from Durect Corporation (Pelham, AL), including PLGA 4 kDa, (50% lactide: 50%

glycolide), 25kDa (75:25), and 50kDa (50:50), each with a carboxylic end group. Branched poly(ethylenimine) (PEI) (Mw 25 kDa), Dicyclohexylcarbodiimide (DCC), N-hydroxysuccinimide (NHS), Thiazolyl Blue Tetrazolium Bromide, Doxorubicin HCl, and RPMI 1640 were purchased from Sigma (Milwaukee, WI). Doxorubicin free base was purchased from MedKoo Biosciences (Chapel Hill, North Carolina). HPLC grade DMSO was purchased from Fisher Scientific (Pittsburg, Pennsylvania). Dialysis tubing (MWCO=50,000) was purchased from Spectrum (Houston, TX). QIAgen maxi plasmid purification kit was purchased from QIAgen (Valencia, CA). Plasmid DNA encoding the Monster Green Fluorescent Protein (phMGFP Vector: pGFP) and marker dye for gel electrophoresis (Blue/Orange 6X Loading Dye) were purchased from Promega (Madison, WI). A molecular weight ladder (1kb DNA Ladder) and human recombinant insulin were purchased from Gibco BRL (Grand Island, NY). 100X stock solution of penicillin/streptomycin, and 0.05% trypsin/0.53 mM EDTA in Hank's Balanced Salt Solution were purchased from Mediatech Inc. (Manassas, VA). EMEM, MCF-7 and MDA-MB-468 human breast cancer cells were purchased from ATCC (Manassas, VA). FBS was acquired from Atlanta Biologicals (Norcross, GA). Fluorodishes were purchased from World Precision Instruments, Inc. (Sarasota, Florida). MDA-MB-435 (WT and ADR) human breast cancer cells were provided by Dr. Hassan Uludag's group at the University of Alberta (Alberta, Canada).

Doxorubicin loading in Poly (lactide-co-glycolide)-g-poly(ethylenimine)

Hydrophobic Doxorubicin freebase was dissolved into methanol to form a 10 mg/mL solution and then serially diluted. One hundred µl of various concentrations of DOX

solution was added to 1 mg/mL PgP-(12k, 25k, and 50k) solutions and shaken for 4 hours at 37 degrees Celsius. Samples stood at 37 degrees Celsius overnight to allow methanol to evaporate. The solution was filtered using a 0.2 μm filter to remove unloaded DOX. DOX loaded PgP (DOX/PgP) samples were then analyzed at 480nm absorbance and the amount of DOX loaded in PgP was calculated using a DOX standard curve. Samples were then frozen for further use.

Cytotoxicity of Doxorubicin loaded PgP in various breast cancer cells

Polyplexes were prepared by mixing various PgPs and pGFP (1 μg) at a N/P ratio of 25/1 and then allowing them to incubate for 30 minutes at 37°C. Cells (2.25x 10^5 cells/well) were plated in 48-well plates and allowed to attach overnight. The cells were incubated with PgP, DOX/PgP, PgP/pDNA or DOX/PgP/pDNA in media containing 10% serum for 48 hours; at which point media was replaced to 0.25 mL of serum-free media containing 60 μL of MTT solution (2 mg/mL Thiazolyl Blue Tetrazolium Bromide in PBS) and incubated for 4 hours at 37 degrees. Doses apportioned via polymer concentrations at each N/P of PgP (5/1, 15/1, 25/1) using 0.5 μg pGFP/well; polyplexes formed at N/P ratio of 25/1 then subsequently diluted down to match PgP concentrations used in lower N/P ratio equivalent transfections. DOX HCl was used as control and the dose is equivalent to amount of DOX loaded by DOX/PgP at specified N/P ratio.

Statistical analysis

Statistical analysis was performed using ANOVA for multiple comparisons using Tukey's Post Hoc analysis unless otherwise noted. A p-value of less than 0.05 was considered statistically significant. The data were represented as mean + SEM.

Results and Discussion

Doxorubicin loaded in PgP-[12k, 25k, 50k] micelles correlated positively with an increase in amount available at the cost of efficiency (Fig 4.1A). Values shown in table 4.1 exhibit maximum amount of DOX loaded relative to weight of PgP-12k, 25k, and 50k and associated efficiency, constrained by maximum solubility of DOX in methanol for chosen loading scheme (Fig 4.1B).

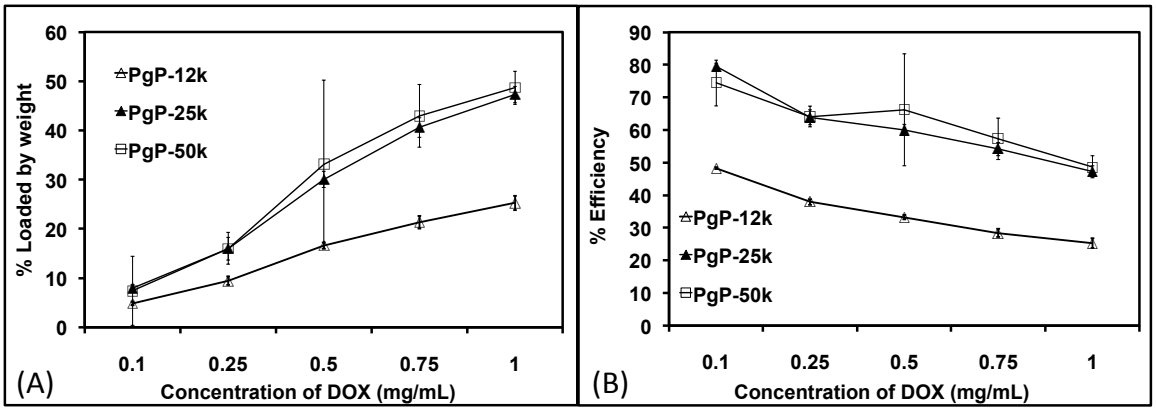

Figure 4.1: (A) Doxorubicin loading in PgP-(12k,25k,50k) (B) Doxorubicin loading efficiency in PgP-(12k, 25k, 50k)

Hydrophobic weight in each type of PgP is intrinsic to it composition i.e. as we ascend in PgP weight, there is greater proportion of molecular weight comprised of PLGA.

	% Loaded by Weight	% Efficiency
PgP-12k	31.85	21.23
PgP-25k	79.26	52.84
PgP-50k	69.98	46.65

Table 4.1: Table summarizing Doxorubicin loading in PgP-[12k, 25k, 50k] at 1 mg/mL with 1 mg/mL DOX

As expected, with an increase in solute content (DOX), increasing amounts are loaded into PgP with decreasing efficiency (Table 4.1).

	PgP-12k	PgP-25k	PgP-50k
Relative PLGA per N/P	1	1.24	1.85
DOX Loading Ratio/PLGA	1	2.5	2.2
Relative DOX dose per N/P	1	3.1	4.1

Table 4.2: Table summarizing relative Doxorubicin loading amounts in PgP-[12k, 25k, 50k]

There is approximately 2.5 times DOX loading observed in PgP-25k and 2.2 times loading in PgP-50k relative to PgP-12k (Table 4.2). Unloaded DOX was removed via 0.2 μm filtration. The ability to undergo 0.2 micron filtration is another desirable quality for a DDV, as it can significantly reduce manufacturing costs. [10]

Equal concentrations of polymer were dissolved above CMC (1 mg/mL). The composition of each different polymer yields increasing PLGA content positively correlated to hydrophobic block length. PLGA weight ratios between PgP-12k, PgP-25k

(1.47x PLGA/mol), and PgP-50k (2x PLGA/mol) samples begins to explain loading differences but this difference is insufficient to attribute all additional loading effects considering the relatively increased amount of DOX loading against additional PLGA content observed in PgP-25k (2.5x DOX loading/mol) vs PgP-50k (2.2x DOX loading/mol) (Table 4.2). PgP-25k has a higher percentage lactide composition in its PLGA, increasing hydrophobic character, potentially facilitating drug loading. However, no additional imbued multiplicity of loading per lactide will ever explain the observed difference in loading. Therefore, there must be some additional factor at play.

Particle size measurements at higher N/P ratios reflect a reduction in polyplex size from ~200nm for PgP-12k and PgP-25k to ~150nm for PgP-50k, potentially as a result of tighter cores associated with crew-cut micelles relative to star-like micelles (Fig 3.2).

This suggests that relative aggregate core volume differences can potentially be elucidated in a comparison of DOX loading relative to PLGA weight and molar PgP content. In loading conditions, the molar content of PgP-25k and PgP-50k relative to PgP-12k are 0.75 and 0.5 for PgP-25k and 50k respectively. Relative PLGA content in loading conditions are 1.47x and 2x for PgP-25k and PgP-50k. This suggests PgP-25k and PgP-50k hydrophobic space is 1.7x and 1.1x that of PgP-12k per PLGA molecule Decreasing HLB correlated with increasing PgP size enforces the morphology of these microstructures, star-like micelles being more limited by hydrophilic block sterics transitioning (~HLB=10) into tighter-cored crew-cut micelles, limited by hydrophobic block sterics. Below an HLB of 10, an increase in hydrophobic block length in one-block

systems with a consistent hydrophilic block has been shown to increase aggregation number as well as core size while decreasing CMC. This however, often comes with a negative effect on the total number of micelles. [106] Differences in loading could be the result from the effects of increasing PLGA block length: decreasing CMC, increasing unimer proportion in micelle form, decreasing number of total micelles as increased aggregation number results in more unimers per micelle. The apparent lesser loading in PgP-50k compared to PgP-25k may be the byproduct of less numerous but larger and more tightly cored micelle population, resulting in less overall hydrophobic space. Increased thermodynamic stability may be imbued with the addition of a hydrophobic drug such as DOX. [46]

DOX doses in free or complexed form were enough to induce significant cytotoxicity in all groups and doses except MDA-MB-435 ADR. In all groups, except in PgP-12k and PgP-25k transfections in MDA-MB-435 ADR cells, DOX loaded PgP groups of any weight were significantly more cytotoxic then the control and their PgP counterparts. No differences were found comparing free PgP versus complexed PgP in any group, dose, or cell line further supporting chapter 4 findings that dose has more bearing on cytotoxicity than N/P ratio.

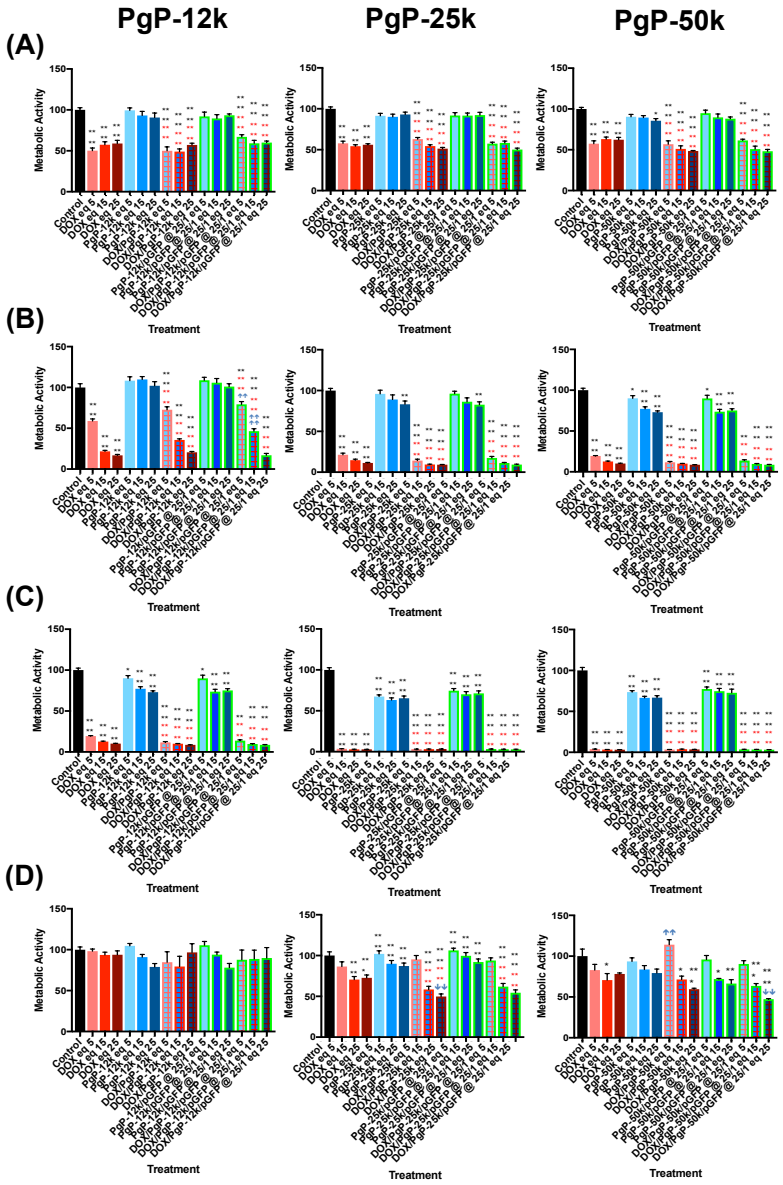

Figure 4.2: Cytotoxicity of Doxorubicin HCl, PgP-(12k, 25k, 50k), PgP-(12k, 25k, 50k) /pGFP, Doxorubicin loaded PgP-[12k, 25k, 50k], Doxorubicin loaded PgP-(12k, 25k, 50k) /pGFP complexes in (A) MCF-7, (B) MDA-MB-468, (C) MDA-MB-435 Wild Type, and (D) MDA-MB-435 ADR cells. Concentration of Doxorubicin HCl used was equivalent to amount of Doxorubicin used in DOX loaded PgP groups. PgP/pGFP complexes were formed at N/P 25/1 and both PgP alone and PgP/pGFP complexes were diluted down to concentration of PgP used in designated N/P equivalent. * P≤ 0.05, ** P≤0.01, *** P≤0.001, **** P≤0.0001 vs control, * P≤ 0.05, ** P≤0.01, *** P≤0.001, **** P≤0.0001 vs PgP or PgP/pGFP counterpart, ↑ P≤ 0.05, ↑↑ P≤0.01, ↑↑↑ P≤0.001, ↑↑↑↑ P≤0.0001 vs equivalent DOX HCl dose

In MCF-7 cells, there were no significant differences between toxicity of DOX/PgP-12k and DOX/PgP-12k/pGFP and the equivalent dose of DOX HCl. DOX/PgP and DOX/PgP/pGFP were significantly more cytotoxic than its PgP counterparts at all doses, which were only able to be found cytotoxic in PgP-50k 25/1 equivalent. This suggests vector toxicities are primarily due to the addition of DOX in MCF-7 cells (Fig 4.2A).

In MDA-MB-468 cells, DOX-loaded PgP of any form was more cytotoxic than its PgP counterpart. DOX HCl was more toxic than DOX/PgP-12k/pGFP in 5/1 and 15/1 equivalent dose ranges with comparable cytotoxicity noted in DOX/PgP-12k/pGFP at 25/1 dose and all DOX/PgP-12k doses. The DOX/PgP-12k/pGFP group was found to be significantly less cytotoxic than DOX HCl at 5/1 and 15/1 but was equitably cytotoxic at 25/1 dose. PgP toxicity versus control was only significant at PgP-25k and PgP-25k/pGFP at 25/1 dose and PgP-50k and PgP-50k/pGFP at all doses with DOX loaded counterparts all inducing greater cytotoxicity, suggesting a large part of vector toxicity is due to loaded DOX (Fig 4.2B).

MDA-MB-435 WT cells, all permutations were found to be significantly cytotoxic, however, DOX loaded counterparts all induced greater cytotoxicity, again suggesting a large part of vector toxicity is due to loaded DOX (Fig 4.2C).

In MDA-MB-435 ADR cells, DOX/PgP-12k groups induce comparable cytotoxicities than their DOX HCl counterparts at all doses tested. DOX/PgP-25k are comparably cytotoxic at 5/1 and 15/1 and more cytotoxic at 25/1 than their DOX HCl counterpart ($p \leq 0.0001$ for DOX/PgP-25k and DOX/PgP-25k/pGFP respectively). Only DOX/PgP-25k

of either form or DOX/PgP-50k of either form were significantly cytotoxic over PgP counter parts. DOX/PgP-50k was less cytotoxic compared to DOX HCl at 5/1 dose while DOX/PgP-50k/pGFP at 25/1 dose was significantly more cytotoxic (Fig 4.2D).

In the comparison of cytotoxicities, there were only divergences seen in MDA-MB-435 wild type in PgP-12k dose equivalency of 25/1 and PgP-25k at N/P equivalence of 5/1 in PgP/pGFP and PgP alone groups. However, there were more profound differences in comparisons with DOX loaded groups. Interestingly, in MCF-7 and MDA-MB-435 lines, introduction of DOX into the system diminished GFP expression while the opposite effect occurred in MDA-MB-468 cells, where it was observed in greater quantities (data not shown). This may be the result of alternative endocytic dispersion profiles exposing more pDNA to nuclear machinery, or possibly an effect of DDV's differed kinetic evolution with incorporation of DOX (Fig 4.2).

The dosages applied at the 5/1 equivalent dosage for DOX-loaded groups in each regime were not enough to induce a LD50 response but in the case of MDA-MB-468's and MDA-MB-435 WT cell lines was enough for all other applied doses. For MCF-7's there seemed to be a thresholding of dose; while MDA-MB-435 ADR's illustrated a proliferative response after some dose. Additionally, DOX loaded groups tended to follow toxicity curves more closely related to DOX HCl. While gene therapy seeks non-toxic vectors, this is may not the goal in enhancing chemotherapeutic delivery. In this context, pDNA and DOX are co-administered and requires similar nuclear co-localization to be effective. In transfection studies, uptake profiles and toxicities of PgP micelles

appear to be most strongly correlated with DDV concentration. It is likely that the same groups that receive adequate polyplex to induce GFP transfection also will be the same populations that get increased DOX loaded PgP micelles, inducing greater cytotoxicity. Thus, polymer induced cytotoxicity via exposure to free primary amines may be less of a concern when incorporating a cytotoxic chemotherapeutic, assuming differential trafficking to target cancer populations. It is with this mind, PgP-12k will be conjugated to folate to illustrate the feasibility of incorporating a targeting moiety in an effort to selectively channel DDVs towards targeted cancerous populations.

All things considered, this reinforces the concept the "magic bullet" is not a singular entity but rather a dynamic system and provides further evidence that the introduction of a new compound may assist or hinder advancement on other goals; even within a refined context of "breast cancer" we can clearly see delivery goals are specific to each target population.

Conclusions

Higher PLGA percentage was correlated with greater overall DOX loading per mg, potentially redeeming functionality of lesser transfecting PgP-25k and PgP-50k compared to PgP-12k. In doses optimized for transfection, Doxorubicin loaded PgPs were able to induce increased or similar cytotoxicity compared its free drug counterpart in MCF-7, MDA-MB-468, and MDA-MB-435 ADR lines and was able to induce over a LD50 response in MDA-MB-468 and MDA-MB-435 WT cells. Comparable performance to free DOX suggests adequate incorporation of chemotherapeutic agents and with vastly

improved transfection rates further supports PgP as a candidate for a multifunctional delivery system targeted towards breast cancer.

CHAPTER FIVE

SYNTHESIZE AND CHARACTERIZE FOLATE FUNCTIONALIZED POLY(LACTIDE-CO-GLYCOLIDE)-GRAFT-POLYETHYLENIMINE NANOPARTICLES (FA-PgP) AS DRUG AND siRNA CARRIER FOR COMBINATORIAL THERAPY FOR THE EFFICIENT TREATMENT OF VARIOUS TYPES OF BREAST CANCER CELLS IN VITRO

Introduction

An increase in efficacy alone was insufficient in creating a delivery system that minimized therapeutic risk. Therefore, targeted therapies were set forth to further mediate specific delivery and promote cell internalization in a cell specific fashion. The addition of a targeting ligand has been long sought as an answer to specificity problems. However, because of the similar genetic profile cancer shares with its host, the existence of an exclusive moiety has yet to be discovered. Fortunately, there are a plethora of overexpressed moieties and transporters that are associated with common cancer types that can easily be conjugated to polymeric micelles. The ultimate goal of chemical based interventions is to accumulate enough of agent in target population to resolve existence with minimal damage to the host's healthy populations. Because of their selective upregulation in some cancers and relative absence in normal tissue; surface proteins such as Human Epidermal Factor-2 (HER-2), prolactin, and folate receptors have been utilized as a means of actively transporting DDV's into cells [47].

Some cancers possess unregulated extracellular receptors that are relatively absent in normal tissue; folate receptor alpha is an exemplar protein and has been frequently utilized as a means of selectively transporting DDV's into cells. [47] Folate (FA) is an essential cofactor to DNA replication and is needed in large quantities by rapidly dividing cancer masses. Elevated levels of folate receptor (up to 100x expression) are correlated with aggressive cancers in the brain (75% of cases), ovaries (90%), lung (37%) and breast (32%).[61,62] Breast cancers positive for folate receptor alpha overexpression (FA+) are associated with grim outcomes. [63] Furthermore, triple negative breast cancers represent a cohort of breast cancers that lack defined targeted therapeutic approach and have been also noted to have (FA+) in over 80% of cases. [64-66] Fortunately, both alpha and beta folate receptors (~38 kDa) exhibit limited distribution in normal tissues. [61] This level of upregulation and relative tissue specificity compounded with the great binding affinity of folate (Kd = 10^{-10} M), makes folate an attractive ligand to add targeting functionality to DDV's. [67] There is little difference in the mechanism by which free folate and folate-conjugated particles are trafficked. Free folate (and folate conjugated particles) initiates active transport into cell and is moved along the endosomal pathway; thus allowing conjugated DDV's containing branched PEI to escape endosomal degradation. [47,67]

Over the pasts few decades three subsequent generations of non-viral delivery vectors have been engineered to address the shortcomings of previous technologies and incorporate lessons learned from a continuously evolving understanding of the delivery challenges associated with drug resistant breast cancer. [71] Initially relying solely on passive diffusion via the EPR effect, it became clear that further modification would be

required to sufficiently increase intracellular accumulation. [72] This addition of active targeting via antibody or small molecule ligands improved the specificity of DDVs, but still left much to be desired in therapeutic efficacy. [73] It is currently recognized that a multifunctional drug delivery system that interacts with the target in a combinatorial way, i.e. co-delivery of a variety of genetic therapeutics and conventional pharmacological agents is necessary to address the complexities of breast cancer treatment in an effective manner. [1, 13]

Proposed is a unique combination of the amphiphilic copolymer, poly (lactic-co-glycolic) acid-g-polyethylenimine) (PgP) micelle delivery system as a flexible platform technology. PgP theoretically has potential advantages as a delivery system: 1) it should maintain some degree of morphological regularity as a result of associated thermodynamic forces, potentially limiting primary amine exposure via steric hindrance reducing DDV toxicity 2) its hydrophobic core can serve as a reservoir for hydrophobic anticancer drugs 3) its positively charged PEI hydrophilic shell could be used for complexation with negatively charged nucleic acids (therapeutic plasmid DNA or siRNA) which may further reduce primary amine exposure and DDV toxicity, and 4) targeting moieties can be easily conjugated on the surface of micelle. [84,85]

The addition of folate moiety (FA-PgP) will increase specificity of DDV, resulting in fewer systemic side effects and help establish a standardized protocol for the incorporation of therapeutically relevant targeting moieties to PgP's structure.

In chapter 3, it was found that compared to the current gold standard of non-viral gene therapies, branched PEI_{25k}, PgP-12k exhibits increased transfection and reduced cytotoxicity in tested breast cancer lines. [76]. It was also found larger PgPs are more toxic per mole, regardless of N/P relationship. In chapter 4 it was then determined this concept carries forward to it DOX loaded counterparts. Confirmation that dose is more critical than form will again be sought in FA-conjugated PgP-12k and will be investigated in a similar manner before commencing siRNA studies. Delivering P-glycoprotein (ABCB1) targeted siRNA via complexation with PgP-12k should reduce efflux pump quantity and assist in the mitigation of drug resistance. Doxorubicin loaded FA-PgP-12k/ABCB1 siRNA complexes will be a potential targeted therapeutic intervention developed from PgP designed to overcome drug resistant breast cancer more safely and substantially improve the length and quality of life of cancer victims. Success of this pilot study unveils the potential of PgP DDV constructs to deliver multidrug, multigene-targeted cocktails, improving upon the treatments of today and evolving with the personalized needs of the medicine of tomorrow.[100]

Materials and Methods

Three different molecular weights of poly(lactide-co-glycolide) (PLGA) were purchased from Durect Corporation (Pelham, AL), including PLGA 4 kDa, (50% lactide: 50% glycolide), 25kDa (75:25), and 50kDa (50:50), each with a carboxylic end group. Branched poly(ethylenimine) (PEI) (Mw 25 kDa), Dicyclohexylcarbodiimide (DCC), N-hydroxysuccinimide (NHS), Thiazolyl Blue Tetrazolium Bromide, Doxorubicin HCl, folate, cysteamine-HCL, and RPMI 1640 were purchased from Sigma (Milwaukee, WI).

Doxorubicin free base was purchased from MedKoo Biosciences (Chapel Hill, North Carolina). Malmide-PEG-SVA was acquired from Laysan Bio Inc. (Arab, AL). Rotovapor RII was purchased from Bucci (Switzerland). Paraformaldehyde, chloroform, dimethyl sulfoxide and ethyl acetate were purchased from Acros (Geel, Belgium). HPLC grade DMSO was purchased from Fisher Scientific (Pittsburg, Pennsylvania). Dialysis tubing (MWCO=50,000) was purchased from Spectrum (Houston, TX). QIAgen maxi plasmid purification kit was purchased from QIAgen (Valencia, CA). Plasmid DNA encoding the Monster Green Fluorescent Protein (phMGFP Vector: pGFP) and marker dye for gel electrophoresis (Blue/Orange 6X Loading Dye) were purchased from Promega (Madison, WI). A molecular weight ladder (1kb DNA Ladder) and human recombinant insulin were purchased from Gibco BRL (Grand Island, NY). 100X stock solution of penicillin/streptomycin, and 0.05% trypsin/0.53 mM EDTA in Hank's Balanced Salt Solution were purchased from Mediatech Inc. (Manassas, VA). Confocal microscope utilized was Olympus IX81 (Center Valley, PA) with Hamamatsu DCAM (Middlesex, NJ) Camera using Metamorph image processing software (Center Valley, PA). EMEM, MCF-7 and MDA-MB-468 human breast cancer cells were purchased from ATCC (Manassas, VA). FBS was acquired from Atlanta Biologicals (Norcross, GA). Fluorodishes were purchased from World Precision Instruments, Inc. (Sarasota, Florida). MDA-MB-435 (WT and ADR) human breast cancer cells were provided by Dr. Hassan Uludag's group at the University of Alberta (Alberta, Canada).

Synthesis and Characterization of folate functionalized PgP

Synthesis of FA-PEG-PgP-12k (FA-PgP-12k) was performed using a method similar to the synthesis of FA-PEG-PEI published by Zhang et al. in 2010, differing only in size of PEG based spacer and final conjugation to PgP-12k rather than PEI (Fig 5.1). [40]

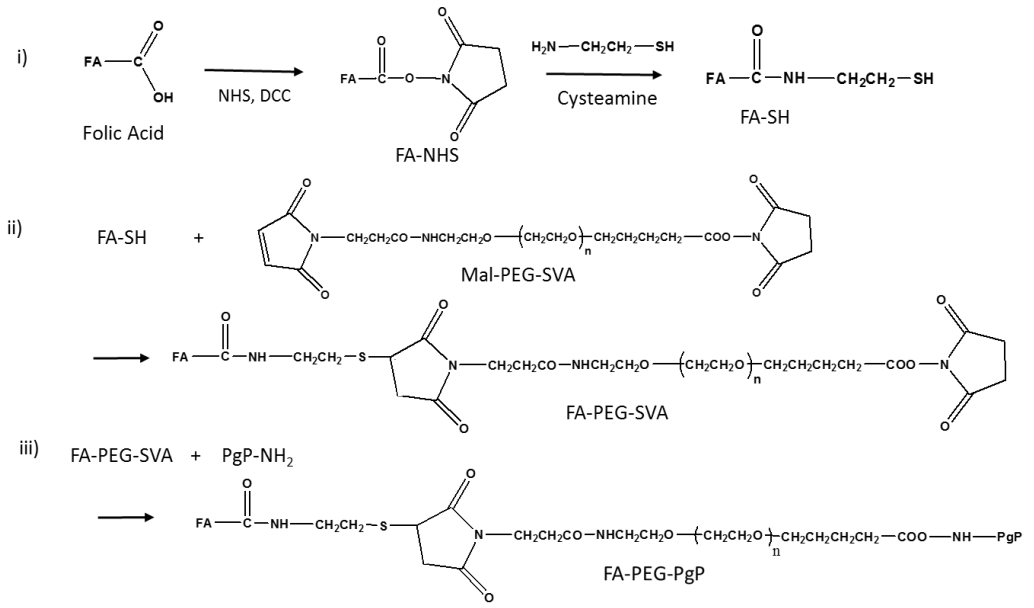

Figure 5.1: Scheme of synthesis of generic FA-PgP

FA-NHS**:** Under darkness, 40 mL anhydrous DMSO was utilized as a solvent and stirred continuously to completely dissolve one gram of folate and 5 mL anhydrous triethylamine. Once homogeneous, 0.313g of NHS and .561g of DCC were introduced to the solution and allowed to mix for 48h. Product was collected via precipitation with 300 mL of ethyl acetate following filtration with a fine pore filter. FA-NHS was then purified by two washes of ethanol and an additional precipitation in ether.

FA-SH: Again using DMSO as a solvent (25mL), 450 mg of FA-NHS, 105 mg of cysteamine-HCL and 4.5 mL of anhydrous triethylamine were combined in darkness and stirred overnight. Product was further purified via two washes of ethanol and a subsequent precipitation in ether.

FA-PEG-NHS: 200 mg of Mal-PEG-SVA and 56 mg of FA-SH were individually dissolved using 8 mL of phosphate buffered saline as a diluent. The reaction was allowed to proceed overnight at 35 degrees C after combining solutions with 100 µl of triethylamine. Precipitate was extracted with chloroform and excess solvent removed via vacuum evaporation. Final product was collected via ether precipitation.

FA-PgP-12k: Stirring in darkness for 48 hours, 2.5mL anhydrous DMSO was utilized to dissolve 45 mg of FA-PEG-NHS and 517mg of PgP-12k or 346mg of bPEI to synthesize FA-PgP-12k or FA-PEI respectively. Products were then dialyzed against water (MWCO=50,000) and lyophilized before redissolved in chloroform and precipitated in ether twice.

Gel retardation assays

To evaluate pDNA binding, PgP-12k, FA-PgP-12k, one part FA-PgP-12k to two parts PgP-12k by weight (same format as FA-PgP-12k MIX used in transfection experiments discussed in the latter portion of this chapter), and one part FA-PgP-12k to four parts PgP-12k by weight/pGFP polyplexes were formed at various N/P ratios (N/P: 2.5, 5, 7.5, 10, 12.5, 15, 17.5/1) in RNase/DNase-free water and incubated for 30 minutes at 37°C to allow polyplex formation. For the heparin competition assay, PgP-12k, FA-PgP-12k, one part FA-PgP-12k to two parts PgP-12k by weight, and one part FA-PgP-12k to four parts

PgP-12k by weight/pGFP polyplexes or pGFP alone was incubated in the presence of increasing concentrations of heparin for one hour at 37°C at N/P ratio 15/1. Heparin competition assays were also performed using PgP-12k, FA-PgP-12k/pGFP polyplexes at N/P 30/1 and FA-PgP-12k and one part FA-PgP-12k to two parts PgP-12k by weight,/pGFP polyplexes at N/P 25/1. To complete each assay, the polyplexes were electrophoresed on a 1% (w/v) agarose gel for 25 minutes at 100 V, stained with ethidium bromide (0.5 μg / mL) and imaged on a UV illuminator.

To evaluate siRNA binding, PgP-12k, FA-PgP-12k, one part FA-PgP-12k to two parts PgP-12k by weight, and one part FA-PgP-12k to four parts PgP-12k by weight/siABCB1 polyplexes were formed at various N/P ratios (N/P: 2.5, 5, 7.5, 10, 12.5, 15, 17.5/1) in RNase/DNase-free water and incubated for 30 minutes at 37°C to allow complex formation. For the heparin competition assay, PgP-12k, FA-PgP-12k, one part FA-PgP-12k to two parts PgP-12k by weight,, and one part FA-PgP-12k to four parts PgP-12k by weight/siABCB1 polyplexes or siABCB1 alone was incubated in the presence of increasing concentrations of heparin for one hour at 37°C at N/P ratio 15/1. Heparin competition assays were also performed using PgP-12k/pGFP polyplexes at N/P 30/1 and PgP-12k, FA-PgP-12k/pGFP polyplexes at N/P 60/1. To complete each assay, the polyplexes were electrophoresed on a 1% (w/v) agarose gel for 25 minutes at 100 V, stained with ethidium bromide (0.5 μg / mL) and imaged on a UV illuminator (Alpha Innotech FluorChem SP imager). The 1kb DNA molecular weight ladder was purchased from Gibco (Grand Island, NY).

Hemolytic activity

The extent of hemolysis was determined by adapting a protocol used by Aravindan et al. [103] Blood collected from Sprague-Dawley rats was combined with heparin (v/v ratio 1:10) was and then centrifuged at 700 x g for 20 minutes at 4ºC to separate buffy coat. The plasma was removed and the red blood cell pellets were washed three times using 150 mM PBS (7.4 pH) with ten times the original volume of pellet, followed by aspiration of the supernatant post-centrifugation at 1000 x g for 10 minutes at 4ºC. Red blood cells were resuspended in 3% (w/v) solution in PBS for combination with polymers dissolved in the same solution. Equal volumes (80 µL each) of cell solution and polymer were mixed and incubated for one hour at 37ºC. Following incubation, suspensions were centrifuged at 1000 x g for 10 minutes and 100 µL of supernatant was transferred to a 96 well plate and absorbance was assessed at 540 nm using Synergy HT plate reader. Hemolysis was quantified using the following formula: $(A_{Sample}-A_{PBS})/(A_{Triton\text{-}X}-A_{PBS})*100\%$, where A_{Sample}, A_{PBS}, A_{Triton} are the absorbance of the sample, PBS, and Triton-X, respectively. Triton-X and PBS treatments were utilized as positive and negative control, respectively.

Hemoaggregation was analyzed using the procedure described by Delgado et. al. utilizing the previously described red blood cell isolation procedure. [104] Equal volumes (80 µL each) of cell solution and various polymer solutions were mixed and incubated for fifteen minutes at room temperature and then imaged.

Plasmid amplification and purification

Escherichia coli DH5α was transformed with plasmids encoding the Monster Green Fluorescent Protein (phMGFP Vector, pGFP) or beta-galactosidase (pSV40-pβGal, pβGal) and amplified in Lysogeny broth at 37°C overnight with shaking at 250 rpm. Plasmids were harvested using the Endofree Maxi Plasmid Purification Kit following the manufacturer's protocol. Plasmid concentration and purity were assessed using a Biotek Synergy HT plate reader in conjunction with a Biotek Take3 microvolume plate system.

In vitro transfection efficiency and cytotoxicity of folate-functionalized poly (lactic-co-glycolic) acid-g-polyethylenimine) complexes in various breast cancer cells

Cell Culture: MCF-7, MDA-MB-468, MDA-MB-435 wild-type (WT), and MDA-MB-435 Doxorubicin (ADR) resistant cells were all grown in media supplemented with 10% Fetal Bovine Serum (FBS) and 1% penicillin-streptomycin at 37 °C with 5 % CO_2. MCF-7 cells were grown using Eagle's Minimum Essential Medium supplemented with 10 μg/mL insulin while MDA-MB-468, MDA-MB-435 wild type, and MDA-MB-435 ADR) were grown using RPMI 1640 media supplemented with 1% L-glutamine. Drug resistance was maintained in MDA-MB-435 ADR cells by treating them with 0.2 μg/mL of Doxorubicin-HCl once a week.

In vitro transfection efficiency and cytotoxicity of PgP/pDNA complexes in breast cancer cells

Transfection efficacies of PgP-12k, FA-PgP-12k and FA-PgP-12k MIX: Transfection efficiency of 3 different formulations of PgP-12k (PgP-12k, FA-PgP-12k, and FA-PgP-12k MIX) were assessed by transfecting various breast cancer cell types with green fluorescent protein in media containing 10% serum. PEI/pDNA and FA-PEI/pDNA complexes at an N/P of 5/1 were also transfected as a positive control. Untreated cells were used as a negative control. Polyplexes were prepared by mixing PgP and pGFP, (2 μg/mL) at 25/1 N/P ratio and then incubating them for 30 minutes at 37°C. Cells (9x 10^5 cells/well) were seeded in 12-well plates and allowed to attach overnight. The cells were then incubated with PgP/pGFP complexes in media containing 10% serum for 24 hours. Cells were incubated for 4 hours in folate free media prior to transfection to starve folate receptors. Treatment groups designated with INHIB were changed to RPMI 1640 media containing 760 micromole/Liter (0.33 mg/mL) of free folate 10 minutes prior to transfection to block folate receptor alpha

Afterward, the media was removed and replaced with fresh media containing 10 % FBS and cells were incubated an additional 24 hours. The GFP-expressing cells were imaged using an inverted fluorescence microscope. Following imaging, cells were trypsinized and GFP-expressing cells were counted using a flow cytometer. The results were expressed as a percentage of transfected cells.

Cytotoxicity was also analyzed by MTT assays in parallel experiments following the same transfection protocol. 48 hours post-transfection, cells were washed with PBS and incubated with 1 mL of serum-free media containing 240 µL of Thiazolyl Blue Tetrazolium Bromide in PBS (2 mg/mL) for 4 hours at 37 °C. After incubation, MTT-containing medium was removed, and 1 mL of DMSO was added to dissolve the formazan crystals formed by live cells. Absorbance was measured at 570 nm using a Biotek Synergy HT plate reader. Cell viability was assessed according to the following formula: Cell viability (%) = ($OD_{570\ (sample)}$/ $OD_{570\ (control)}$) X 100%. Statistical analysis was performed using ANOVA for multiple comparisons using Tukey's Post Hoc analysis using Dunnet's correction.

Comparison of transfection efficacies of PgP-12k, FA-PgP-12k and FA-PgP-12k MIX

Three (FA+) breast cancer types: MCF-7, MDA-MB-435 wild type and its Doxorubicin resistant counterpart (ADR) and one (FA-) breast cancer MDA-MB-468, were utilized to test gene delivery performance in cancerous cells (Fig 1.1). The paired breast cancer set of wild type (FA+) MDA-MB-435 WT and ADR cells were assessed for candidacy in future experimentation involving targeted delivery of ABCB1 targeted siRNA.

Serum aggregation plays a significant role in reducing the efficacy of non-viral delivery systems, often resulting in failure *in vivo* where protein accounts for approximately 7% of blood volume. [32,116] In order to simulate a more clinically relevant environment, transfections were performed in media containing 10% Fetal Bovine Serum (FBS).

The specificity of FA-functionalized PgP-12k/pGFP polyplex was determined by transfecting (FA+) MCF-7, MDA-MB-435 (WT,ADR) and (FA-) MDA-MB-468 with PgP-12k, FA-PgP-12k or FA-PgP-12k MIX, each complexed with pGFP at an N/P ratio of 25/1. FA conjugated PEI was used as a positive control. [117] Cells were incubated for 4 hours in FA free media prior to transfection to starve folate receptors.

Inhibition of FA-PgP-12k and FA-PgP-12k MIX transfections with free folate

Target specificity was further investigated by performing transfection in media containing 760 micromole/Liter free folate to act as a competitive inhibitor for folate receptor alpha specific uptake. Treatment groups designated with INHIB were changed to RPMI 1640 media containing 760 micromole/Liter (0.33 mg/mL) of free folate 10 minutes prior to transfection to block folate receptor alpha. After 24 hours media was replaced to RPMI 1640 containing 10% FBS and 1% Penicillin. Data acquisition occurred 48 hours post transfection using aforementioned techniques.

Intracellular trafficking and nuclear localization study

PgP-12k was conjugated with Rhodamine 123 in a manner similar to Yang et al. [118] Rhodamine labeled PgP-12k was mixed with FA-PgP-12k (1/5 w/w ratio) for visualization. MDA-MB-435 WT and ADR cells (9x 10^5 cells/dish) were plated in Fluorodishes. Polyplexes were formed by mixing pGFP and Rhodamine labeled PgP at N/P ratio of 25/1 and transfected as described above. Cells were fixed using 4% paraformaldehyde solution at 36 hours post transfection and nuclei were counter stained

with DAPI. Cells were imaged using an Olympus IX81 confocal microscope with Hamamatsu DCAM Camera using Metamorph image processing software.

Determination of the driver of PgP toxicity

Transfections investigating the efficacy in delivering pDNA were fixed to an equal dose of plasmid; an increase in number of micelles would also decrease average plasmid content per polyplex. PEI toxicity and performance is driven by free amine content. With this in mind two additional forms of DDV toxicity were investigated: 1) All PgP polyplexes were formed at 25/1 N/P ratio and diluted 2) uncomplexed PgP; each regime was tested at equivalent N/P 5/1, 15/1, 25/1 PgP transfection doses. Confirmation of differences in toxicity related to increase in primary amine exposure is necessary in the event cellular exposure is restricted to only free, uncomplexed micelle populations. These investigations will help elucidate the primary driver of DDV cytotoxicity and provide further support of PgP as a potential gene and drug delivery agent.

Doxorubicin loading in FA-PgP

Hydrophobic Doxorubicin freebase was dissolved into methanol to form a 10 mg/mL solution and then serially diluted. One hundred µl of various concentrations of DOX solution was added to 1 mg/mL FA-PgP and FA-PgP MIX solutions and shaken for 4 hours at 37 degrees. Samples stood at 37 degrees overnight to allow methanol to evaporate. The solution was filtered using a 0.2 um filter to remove unloaded DOX. DOX loaded PgP (DOX/PgP) samples were then analyzed at 480nm absorbance and the amount of DOX loaded in PgP was calculated using a DOX standard curve. Loading

efficiency and percent loaded by weight were determined in triplicate. Samples were then frozen for further use.

Cytotoxicity of Doxorubicin-loaded folate-functionalized poly-(lactide-co-glycolide)-g-poly(ethylenimine) in various breast cancer cells

Polyplexes were prepared by mixing PgP-12k, FA-PgP-12k, or FA-PgP MIX, with pGFP (1 μg) at a N/P ratio of 25/1 and then allowing them to incubate for 30 minutes at 37°C. Cells (2.25x 10^5 cells/well) were plated in 48-well plates and allowed to attach overnight. The cells were incubated with PgP, DOX/PgP, PgP/pDNA or DOX/PgP/pDNA in media containing 10% serum for 48 hours, at which point, media was replaced to 0.25 mL of serum-free media containing 60 μL of MTT solution (2 mg/mL Thiazolyl Blue Tetrazolium Bromide in PBS) and incubated for 4 hours at 37 degree. Doses apportioned via polymer concentrations at each N/P of PgP (5/1, 15/1, 25/1) using 0.5 μg pGFP/well; polyplexes formed at N/P ratio of 25/1 then subsequently diluted down to match polymer concentrations at lower N/P ratio equivalent transfections. DOX HCl was used as control and the dose is equivalent to amount of DOX loaded by DOX/PgP at specified N/P ratio.

Uptake of folate-functionalized poly(lactide-co-glycolide) -graft-polyethylenimine/siGLO nanoparticles (FA-PgP) in MDA-MB-435 ADR breast cancer cells

The siGLO Red transfection indicator, consisting of a fluorescently labeled siRNA duplex with a chemical modification for nuclear localization, was used to evaluate siRNA transfection efficiency. PgP/siGLO complexes (1 μg siGLO Red) at various N/P ratio were transfected in cells in 10% serum condition. PEI/siGLO at N/P 5/1 was used as

positive controls. The cells were incubated at 37 °C for 24 hours and then the media were replaced with fresh media containing 10 % FBS. At 4 and 24 hours post-transfection, siGLO Red-transfected cells were collected and assessed by flow cytometry and the results expressed as % uptake positive. Groups designated with "INHIB" were co incubated with (0.33 mg/mL free folate) during transfection.

Doxorubicin-loaded folate-functionalized poly (lactide-co-glycolide) -graft-polyethylenimine nanoparticles (FA-PgP) as drug and siRNA carrier for combinatorial therapy for the efficient treatment of MDA-MB-435 ADR breast cancer cells

A siRNA knockdown study was performed in which the cell viability of various N/P ratios of ABCB1 targeted or scrambled siRNA complexes (1 μg siRNA/48 well) in MDA-MB-435 (ADR) cells. Cells were transfected and 48 hours post transfection media containing 50 μg/mL Doxorubicin was added to specified group. At 96 hours, post transfection, % knockdown was assessed via RT-PCR while cell viability was assessed via MTT to compare differences in metabolic activity.

Statistical analysis

Statistical analysis was performed using ANOVA for multiple comparisons using Tukey's Post Hoc analysis unless otherwise noted. A p-value of less than 0.05 was considered statistically significant. The data were represented as mean + SEM.

Results and Discussion

The structure of FA-PgP was characterized by ^{1}H NMR (300 MHz, D_20). Presence of folate related peaks (6-8.6 ppm) represent indicate successful synthesis (Fig 5.2). [119] UV

spectroscopy indicated FA-PEG conjugation to 1 in 12.5 molecules of PgP-12k (data not shown).

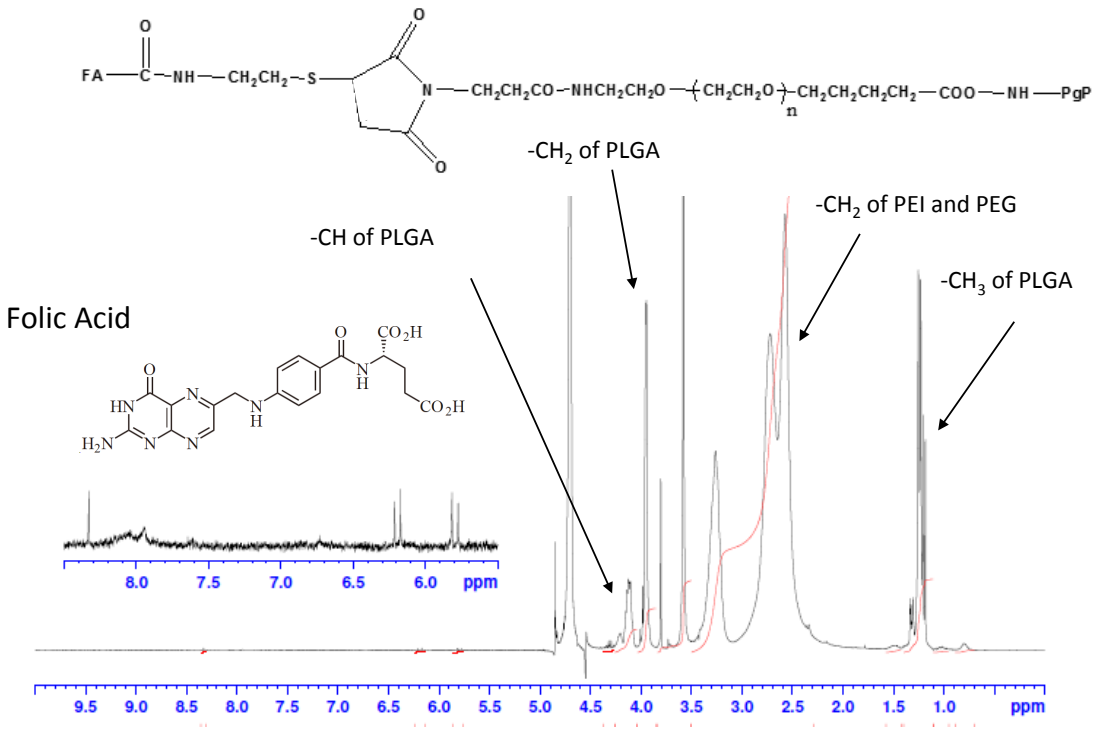

Figure 5.2: ^{1}H-NMR spectra of FA-PgP-12k

Minimum N/P ratios required for complex formation between PgP and pDNA were investigated using a gel retardation assay. PgP/pDNA complexes were formed at a variety of N/P ratios and the minimum ratio for complex formation was determined by identifying the lowest N/P ratio at which no pDNA migration was observed, demonstrating complete binding of free pDNA by PgP.

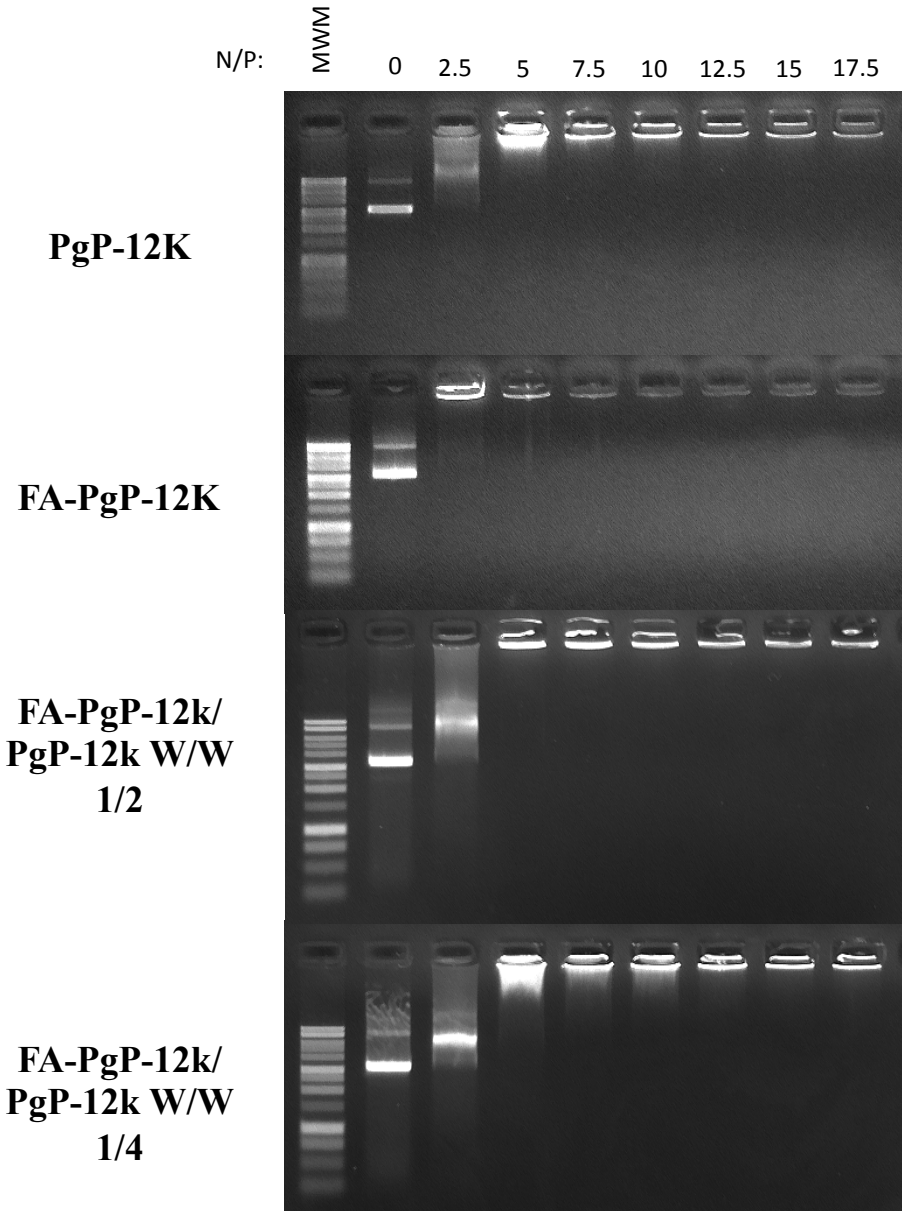

Figure 5.3: Gel retardation assay using PgP-12k, FA-PgP-12k, one part FA-PgP-12k to two parts PgP-12k by weight, and one part FA-PgP-12k to four parts PgP-12k by weight /pGFP complexes. Lane 1: DNA ladder, Lane 2:naked pDNA, Lane 3 -9: PgP/pGFP (N/P: 2.5, 5, 7.5, 10, 12.5, 15, 17.5 respectively)

Ratios at which complete binding is observed: PgP-12k N/P (2.5/1), FA-PgP-12k N/P (5/1), one part FA-PgP-12k to two parts PgP-12k by weight N/P (5/1), and one part FA-PgP-12k to four parts PgP-12k by weight N/P (5/1) (Fig 5.3).

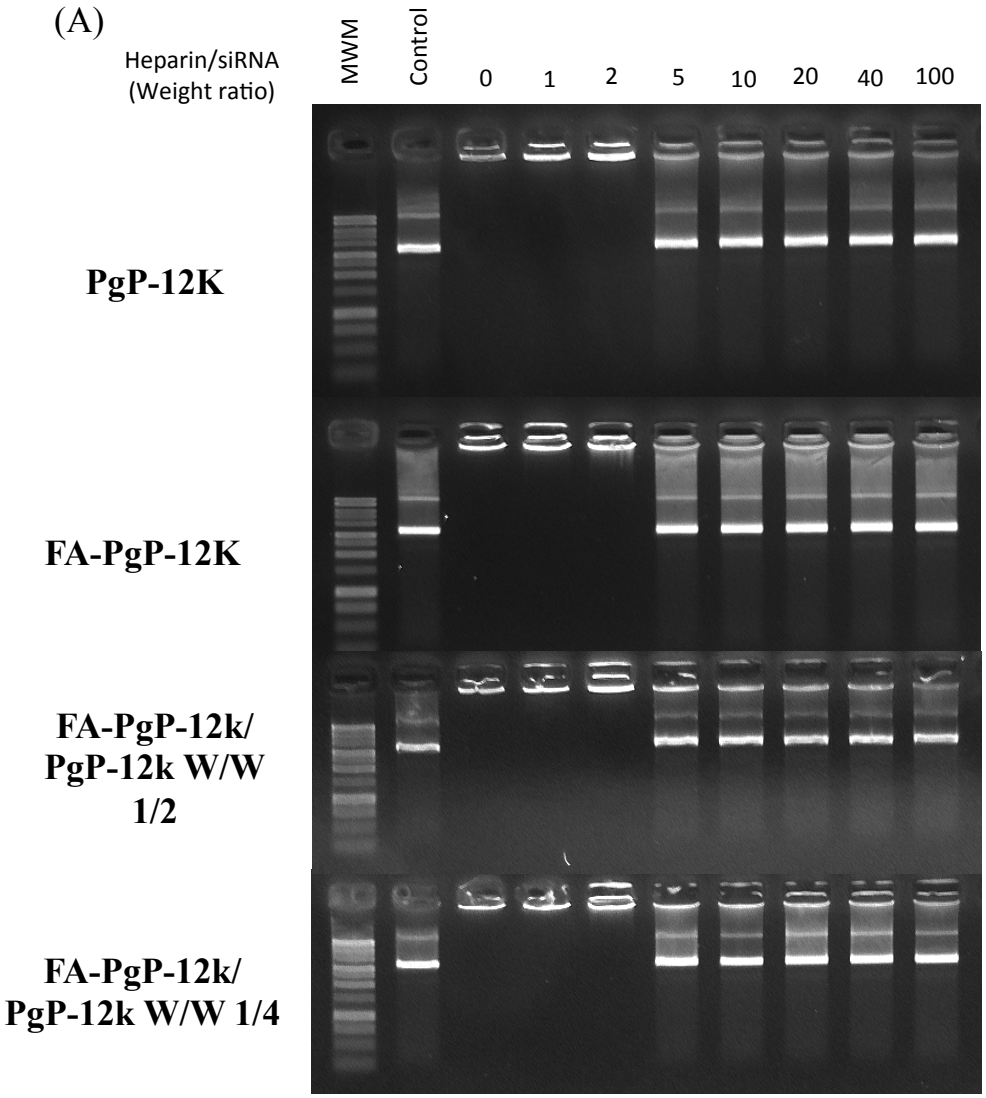

Figure 5.4a: Heparin competition assay using PgP-12k, FA-PgP-12k, one part FA-PgP-12k to two parts PgP-12k by weight, and one part FA-PgP-12k to four parts PgP-12k by weight /pGFP /pGFP complexes. Lane 1: DNA ladder, Lane 2:naked pDNA, Lane 3: PgP/pGFP (N/P:15/1), Lanes 4-10: PgP-12k/pGFP (N/P: 15/1 with W/W Heparin 1, 2, 5, 10, 20, 40, 100 respectively)

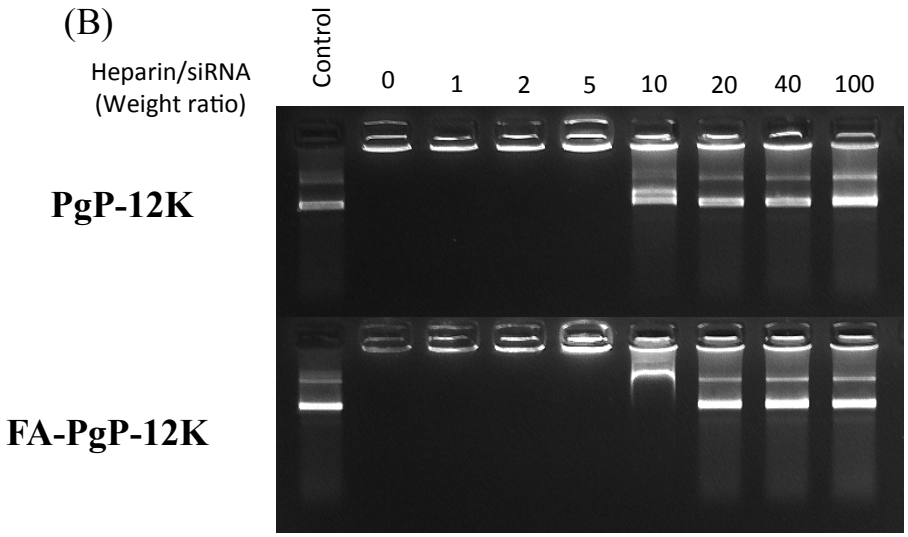

Figure 5.4b: Heparin competition assay using PgP-12k, FA-PgP-12k/pGFP complexes N/P 30/1 Lane 1: DNA ladder, Lane 2:naked pDNA, Lane 3: PgP/pGFP (N/P:30/1), Lanes 4-10: PgP-12k/pGFP (N/P: 30/1 with W/W Heparin 1, 2, 5, 10, 20, 40, 100 respectively)

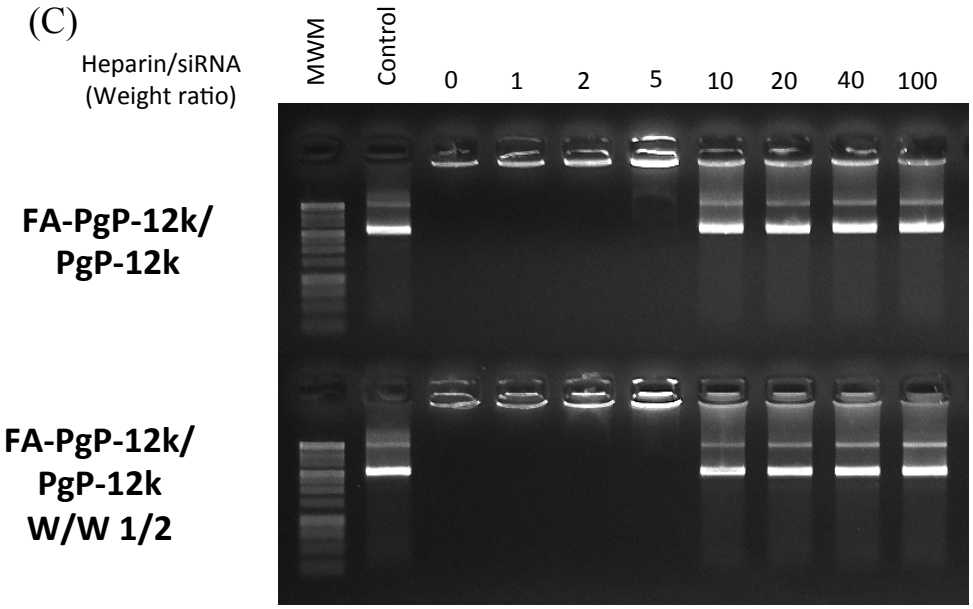

Figure 5.4c: FA-PgP-12k and one part FA-PgP-12k to two parts PgP-12k by weight/pGFP complexes. Lane 1: DNA ladder, Lane 2:naked pDNA, Lane 3: PgP/pGFP (N/P:25/1), Lanes 4-10: PgP-12k/pGFP (N/P: 25/1 with W/W Heparin 1, 2, 5, 10, 20, 40, 100 respectively)

For the heparin competition assay, PgP-12k, FA-PgP-12k, one part FA-PgP-12k to two parts PgP-12k by weight, and one part FA-PgP-12k to four parts PgP-12k by weight all formed at N/P 15/1 and subjected to various relative weights of Heparin, complete dissociation occurred at 5/1 for all permutations (Fig 5.4A). Using polyplexes formed at N/P 30/1, PgP-12k, FA-PgP-12k/pGFP polyplexes lose their cargo when subjected to a weight-to-weight treatment of Heparin at W/W 10/1 (Fig 5.4B). A similar experiment using one part FA-PgP-12k to two parts PgP-12k by weight, and one part FA-PgP-12k to four parts PgP-12k by weight all formed at N/P 25/1 also required a Heparin dose W/W 10/1 to dissociated cargo (Fig 5.4C).

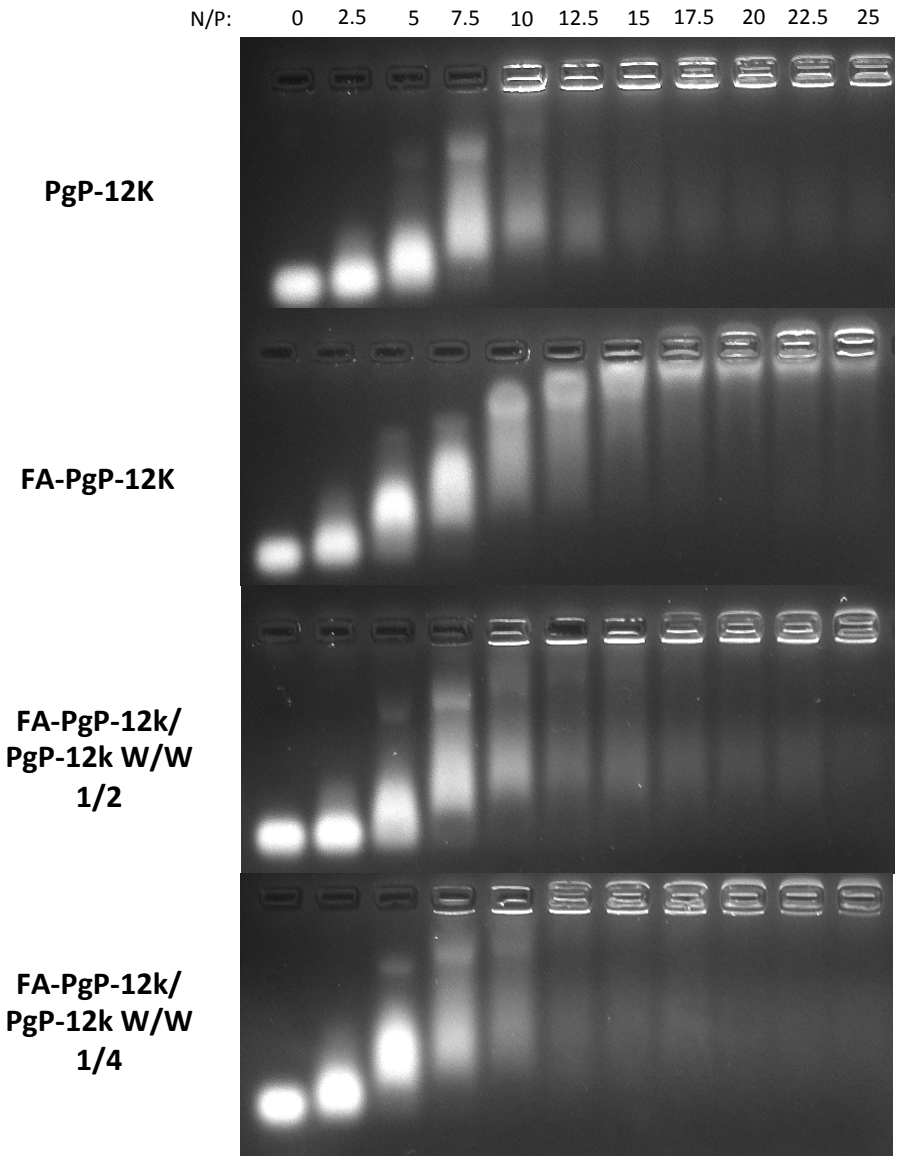

Figure 5.5: Gel retardation assay using PgP-12k, FA-PgP-12k, one part FA-PgP-12k to two parts PgP-12k by weight, and one part FA-PgP-12k to four parts PgP-12k by weight /siABCB1 complexes. Lane 1: DNA ladder, Lane 2:naked siABCB1, Lane 3 -9: PgP/siABCB1 (N/P: 2.5, 5, 10, 12.5, 15, 17.5, 20, 22.5, 25 respectively)

Minimum N/P ratios required for complex formation between PgP and siRNA were investigated using a gel retardation assay. PgP/siABCB1 complexes were formed at a variety of N/P ratios and the minimum ratio for complex formation was determined by

identifying the lowest N/P ratio at which no siABCB1 migration was observed, demonstrating complete binding of free siABCB1 by PgP (Fig 5.5).

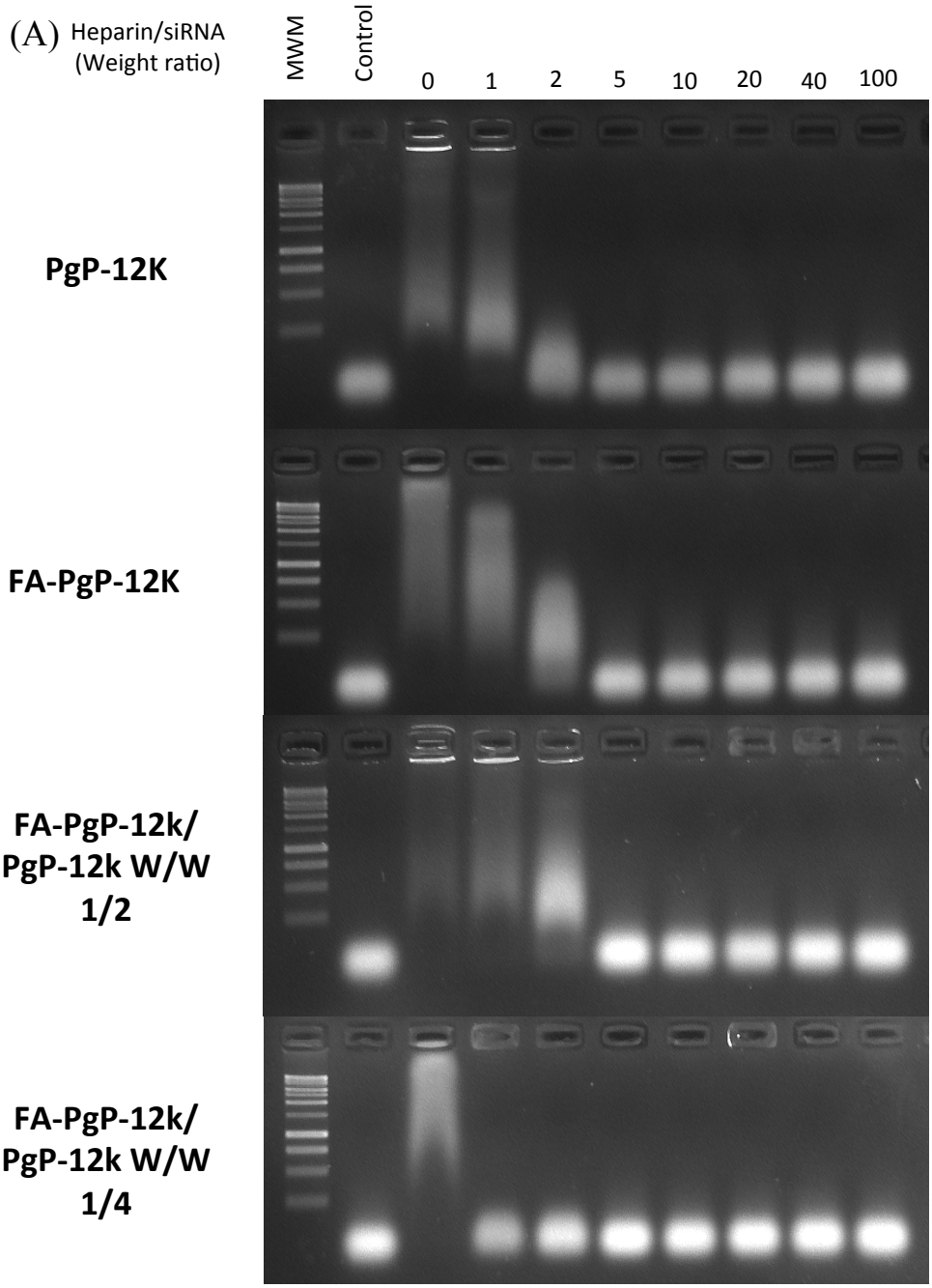

Figure 5.6a: Heparin competition assay using PgP-12k, FA-PgP-12k, one part FA-PgP-12k to two parts PgP-12k by weight, and one part FA-PgP-12k to four parts PgP-12k by weight / siABCB1 complexes. Lane 1: DNA ladder, Lane 2:naked siABCB1, Lane 3: PgP/ siABCB1 (N/P:15/1), Lanes 4-10: PgP-12k/ siABCB1 (N/P: 15/1 with W/W Heparin 1, 2, 5, 10, 20, 40, 100 respectively)

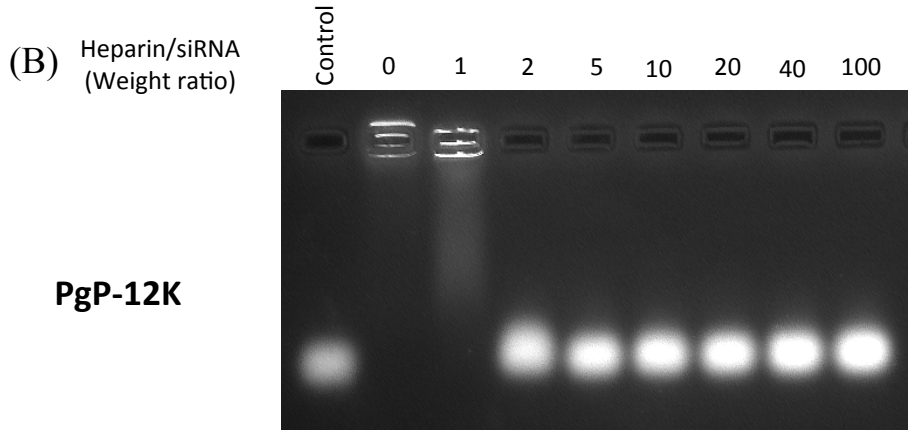

Figure 5.6b: Heparin competition assay using PgP-12k/ siABCB1 complexes. Lane 1: DNA ladder, Lane 2:naked siABCB1, Lane 3: PgP/ siABCB1 (N/P:30/1), Lanes 4-10: PgP-12k/ siABCB1 (N/P: 30/1 with W/W Heparin 1, 2, 5, 10, 20, 40, 100 respectively)

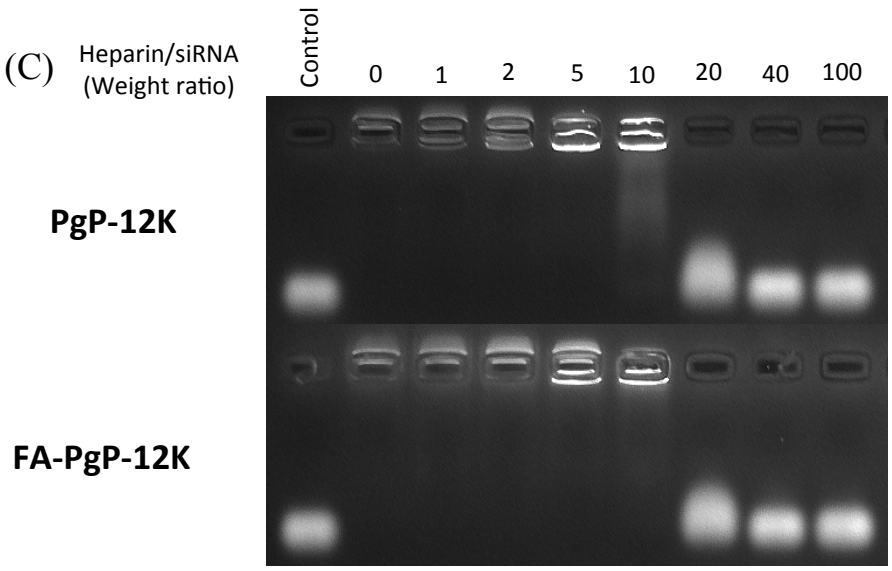

Figure 5.6c: Heparin competition assay using PgP-12k, FA-PgP-12k / siABCB1 complexes. Lane 1: DNA ladder, Lane 2:naked siABCB1, Lane 3: PgP/ siABCB1 (N/P:60/1), Lanes 4-10: PgP-12k/ siABCB1 (N/P: 60/1 with W/W Heparin 1, 2, 5, 10, 20, 40, 100 respectively)

Ratios at which complete binding is observed: PgP-12k N/P (15/1), FA-PgP-12k (N/P 17.5/1), one part FA-PgP-12k to two parts PgP-12k by weight (12.5/1), and one part FA-PgP-12k to four parts PgP-12k by weight N/P (12.5/1). When compared to pDNA results it requires 2-6.5x the concentration of PgP to fully bind siRNA.

For the heparin competition assay, PgP-12k, FA-PgP-12k, one part FA-PgP-12k to two parts PgP-12k by weight, and one part FA-PgP-12k to four parts PgP-12k by weight all formed at N/P 15/1 and subjected to various relative weights of Heparin, complete dissociation occurred at 1/1 for all permutations (Fig 5.6A). Compared to pDNA, siRNA dissociated using ~1/10 the Heparin. Taken with gel retardation data this indicates that pDNA binds more readily and more strongly to PgP than does siRNA. To investigate this concept further, PgP-12k/siABCB1 polyplexes were formed at N/P 30/1 (Fig 5.6B). PgP-12k/siABCB1 polyplexes lose their cargo when subjected to a weight-to-weight treatment of Heparin at W/W 2/1 or about double the weight required to dissociate PgP-12k/siABCB1complexes formed at one half the N/P ratio (15/1) suggesting a linear relationship. However, in another experiment, this time using PgP-12k and FA-PgP-12k formed at N/P 60/1 also required a Heparin dose W/W 10/1 to dissociated cargo (Fig 5.6C). In other words, double the concentration of PgP in 60/1 required 5x more expected Heparin by weight. This additional weight may be required as a result of higher average number of stable micelles over time associated with higher N/P, potentially another example of kinetic stability having an appreciable effect over experimental timeframes. Perhaps, some unknown factors resulting in a higher charge densities per micelle or greater number of micelles than to be expected from a linear increase, resulting in a

disproportional strength of binding. The similar performance of PgP-12k, FA-PgP-12k and its blends suggest that FA conjugation has little effect on the binding kinetics as all polyplexes exhibited the ability to dissociate from pDNA and siRNA at a similar Heparin concentration, demonstrating the potential utility of PgP for delivery and release of nucleic acid cargo.

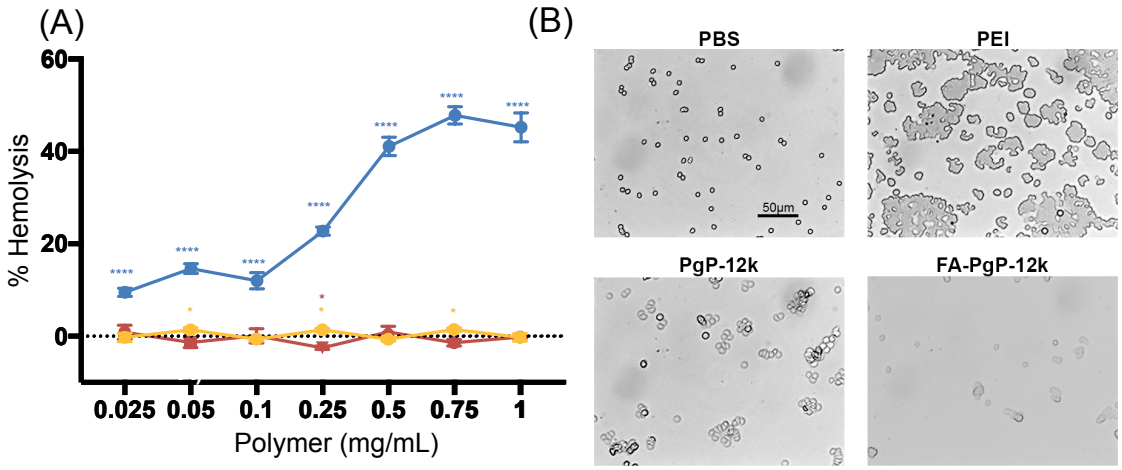

Figure 5.7: (A) Hemolytic activity of PEI, PgP-12k, and FA-PgP-12k at 0.025, 0.05, 0.1, 0.25, 0.5, 0.75, 1 mg/mL in 7.4 pH 150 mM phosphate buffered saline (PBS). Red blood cells collected from Sprague-Dawley rats. (B) Hemoaggregation of red blood cells in 7.4 pH 150 mM PBS incubated with 1 mg/mL of PEI, PgP-12k, or FA-PgP-12k for fifteen minutes

Hemolysis is a direct measure of cytotoxicity on erythrocytes, while hemoaggregation provides insight into the physical interactions of the delivery vehicle with solid elements in the blood. Both are important factors necessary to assess the safety of the delivery vehicle prior to *in vivo* evaluation. Interestingly, increasing the dose of PgP at any MW between the concentrations 0.025 mg/mL to 0.5 mg/mL did not result in increased hemolysis, as was demonstrated with PEI. PgP-12k and FA-PgP-12k induced little to no

hemolytic activity with differences from control only occurring at 0.05, 0.25, and 0.75 mg/mL for FA-PgP-12k and 0.25 for PgP-12k albeit statistically significant due to tight grouping of values (Fig 5.7A). FA-PgP-12k exhibited similar hemoaggregation properties to PgP-12k. Aggregation is limited especially compared to the high level of hemoaggregation and hemolysis induced by an equal concentration of PEI (Fig 5.7B). Again, there is little difference in the performance between PgP-12k and FA-PgP-12k suggesting that conjugation of FA to PgP-12k has little effect on overall physicochemical characteristics.

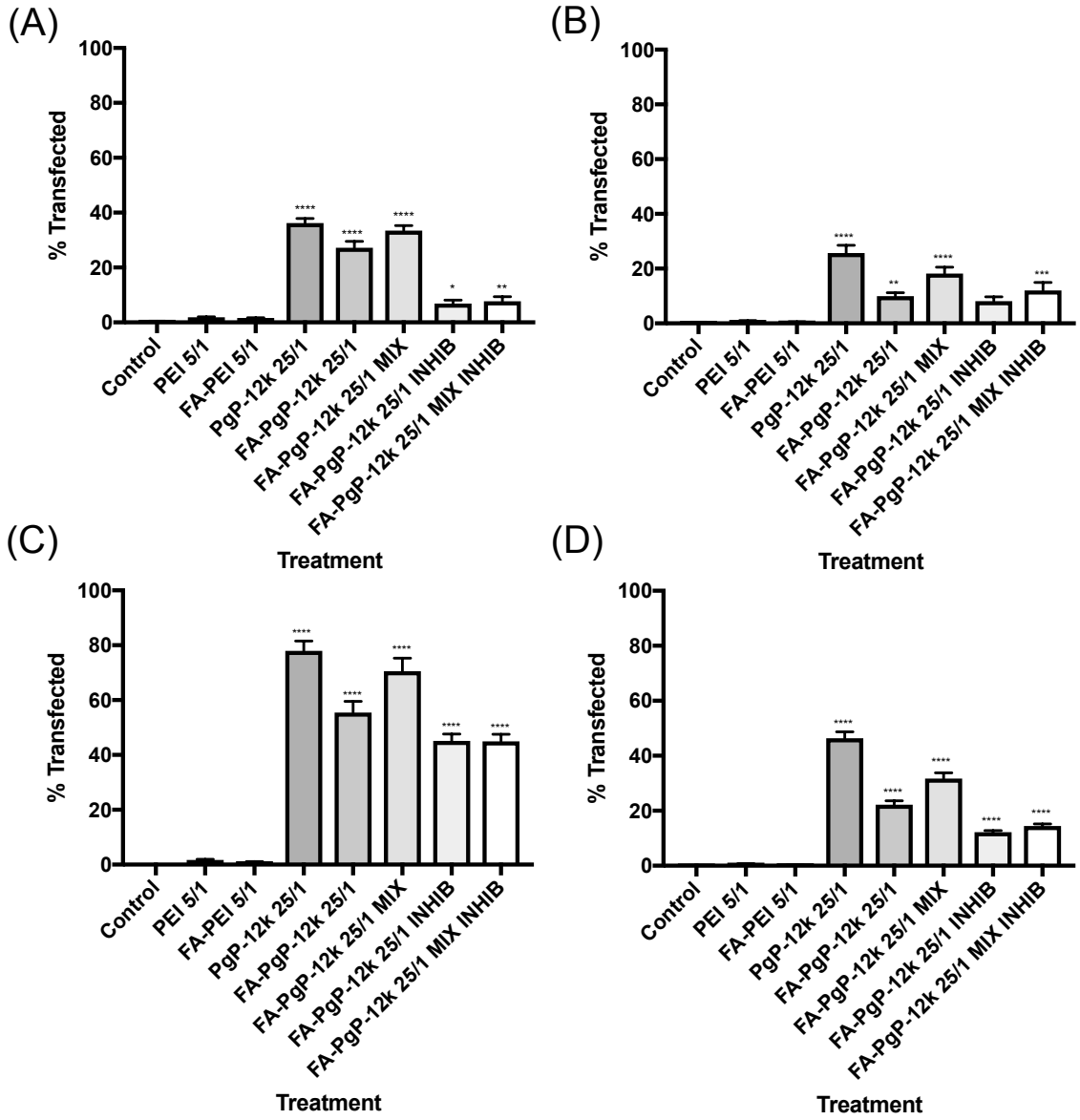

Figure 5.8: Transfection efficiency of PEI, FA-PEI (N/P: 5/1), PgP-12k/pGFP, FA-PgP-12k/pGFP, mixed micelles comprised of one part FA-PgP-12k to two parts PgP-12k by weight, (N/P: 25/1) in (A) MCF-7, (B) MDA-MB-468, (C) MDA-MB-435 Wild Type, and (D) MDA-MB-435 ADR cells. Groups designated with "INHIB" were co incubated with (0.33 mg/mL free folate) * P≤ 0.05, ** P≤0.01, *** P≤0.001, **** P≤0.0001

Folate functionalized PgP-12k maintained high levels of significant transfection in all

(FA+) MCF-7, MDA-MB-435 (wild type, Doxorubicin resistant variant) cells lines albeit

reduced compared to PgP-12k (Fig 5.8). FA-PgP-12k weight used exceeds PgP-12k at same N/P since FA has some additional non-contributing weight of PEG spacer and FA. Thus amount used in transfections are as follows: PgP-12k < FA-PgP-12k MIX < FA-PgP-12k. This adds more evidence to the concept of PgP-12k concentration driving transfection increase, as a higher concentration of FA-PgP-12k was used with less resulting transfection compared to PgP-12k.

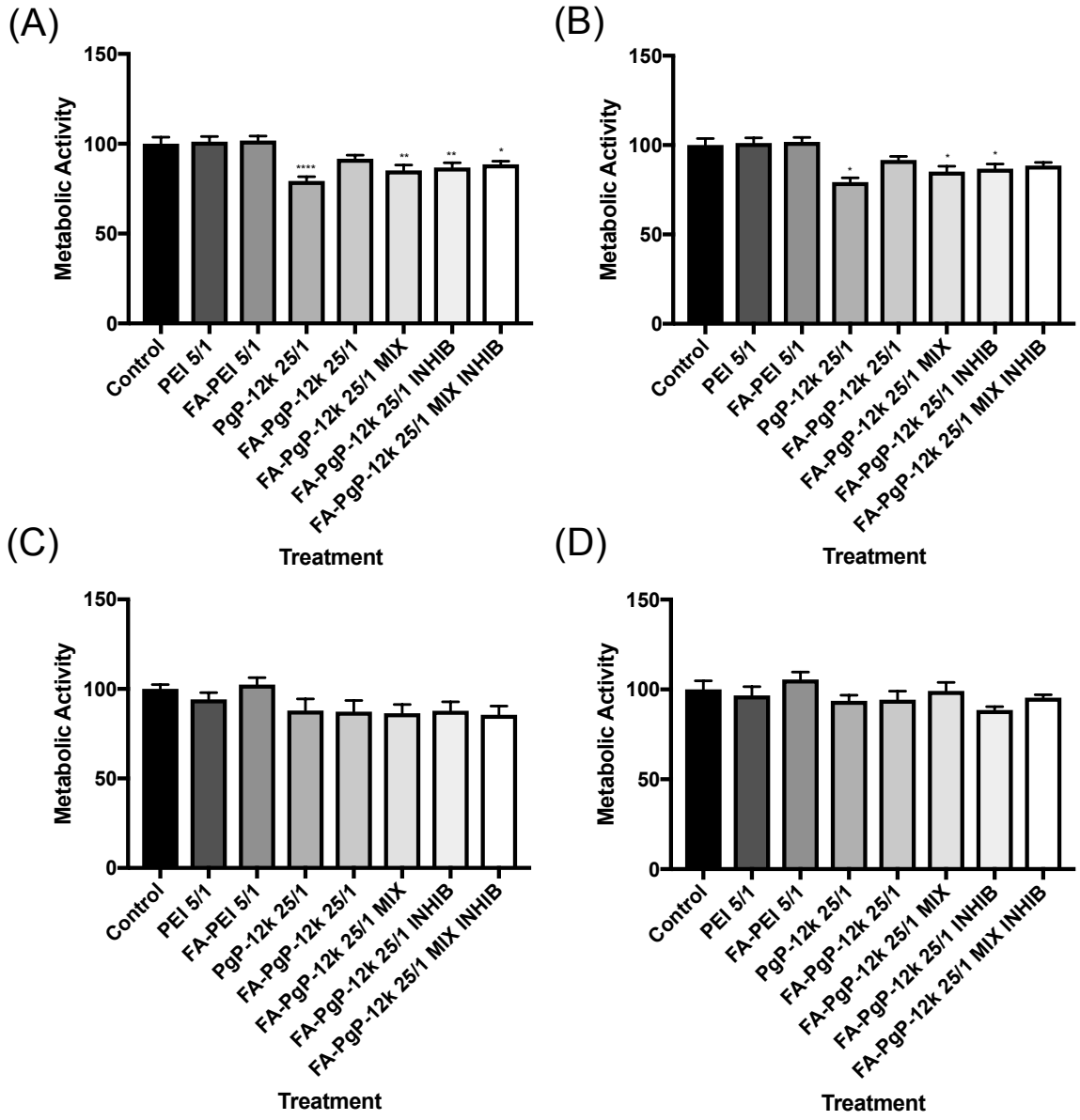

Figure 5.9: Metabolic activity of PEI, FA-PEI (N/P: 5/1), PgP-12k/pGFP, FA-PgP-12k/pGFP, mixed micelles comprised of one part FA-PgP-12k to two parts PgP-12k by weight/pGFP, (N/P: 25/1) in (A) MCF-7, (B) MDA-MB-468, (C) MDA-MB-435 Wild Type, and (D) MDA-MB-435 ADR cells. Groups designated with "INHIB" were co incubated with (0.33 mg/mL free folate) * P≤ 0.05, ** P≤0.01, *** P≤0.001, **** P≤0.0001

Significant cytotoxicity was induced in PgP-12k groups in both MCF-7 and MDA-MB-468 cells; with additional significant cytotoxicity in FA-PgP-12k MIX and FA-PgP-12k

INHIB groups in MDA-MB-468 cells (Fig 5.9). More substantial reduction in transfection percentage was noted in (FA-) MDA-MB-468, potentially the result of reduced presence of folate receptor alpha (Fig 5.10).

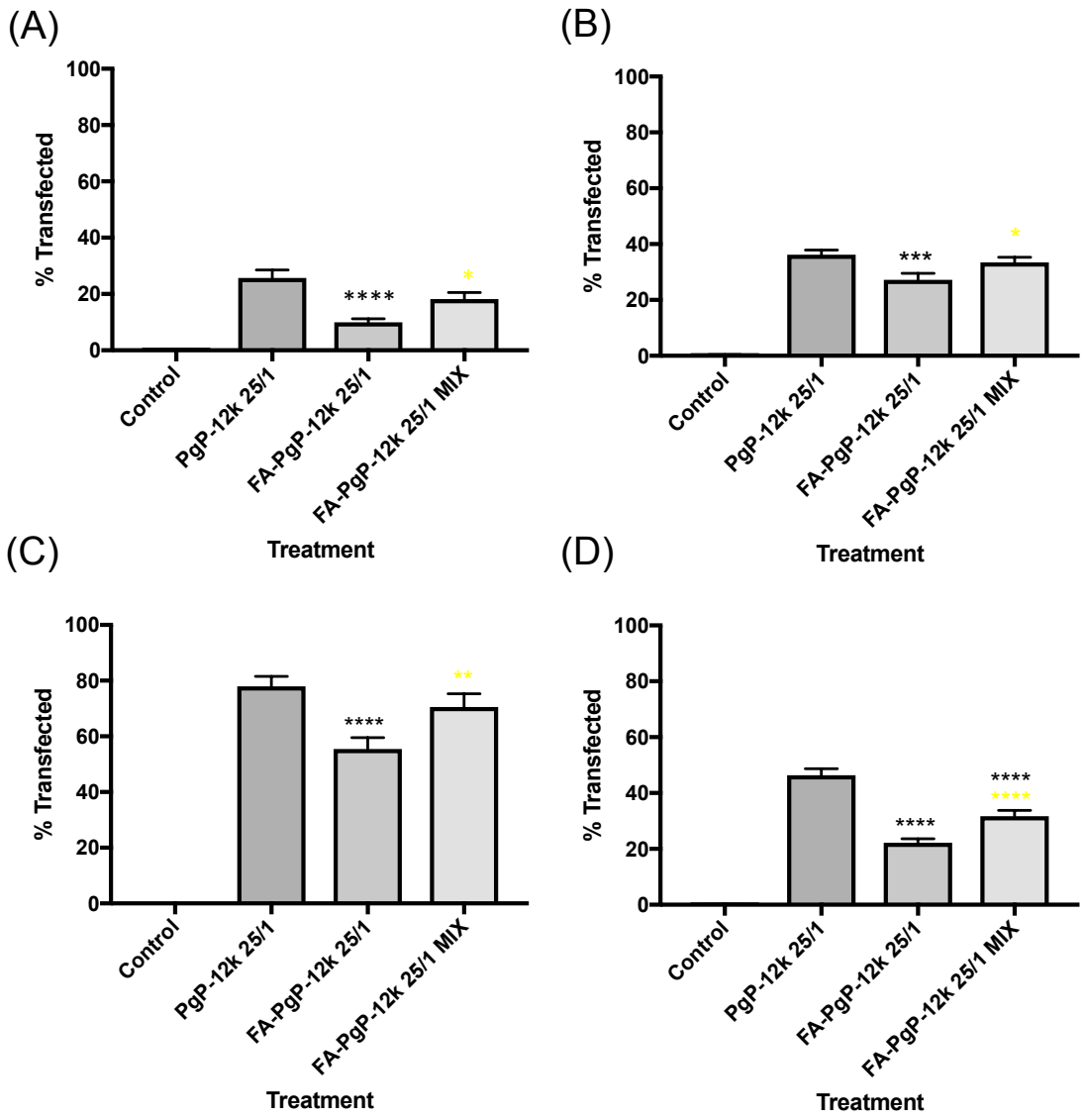

Figure 5.10: Transfection efficiency of PgP-12k/pGFP, FA-PgP-12k/pGFP and mixed micelles comprised of one part FA-PgP-12k to two parts PgP-12k by weight/pGFP (N/P: 25/1) complexes in (A) MCF-7 (B) MDA-MB-468 (C) MDA-MB-435 wild type (D) MDA-MB-435 Doxorubicin resistant variant. * P≤ 0.05, ** P≤0.01, *** P≤0.001, **** P≤0.0001 vs control. * P≤ 0.05, ** P≤0.01, *** P≤0.001, **** P≤0.0001 vs FA-PgP-12k

The decrease in transfection efficacy observed with FA-PgP is likely due to folate related steric hindrance or altered endosomal release dynamics, as a mixed micelle formulation restored performance in a PgP-12k proportional manner, a phenomena noted in Cheng et al.[120]

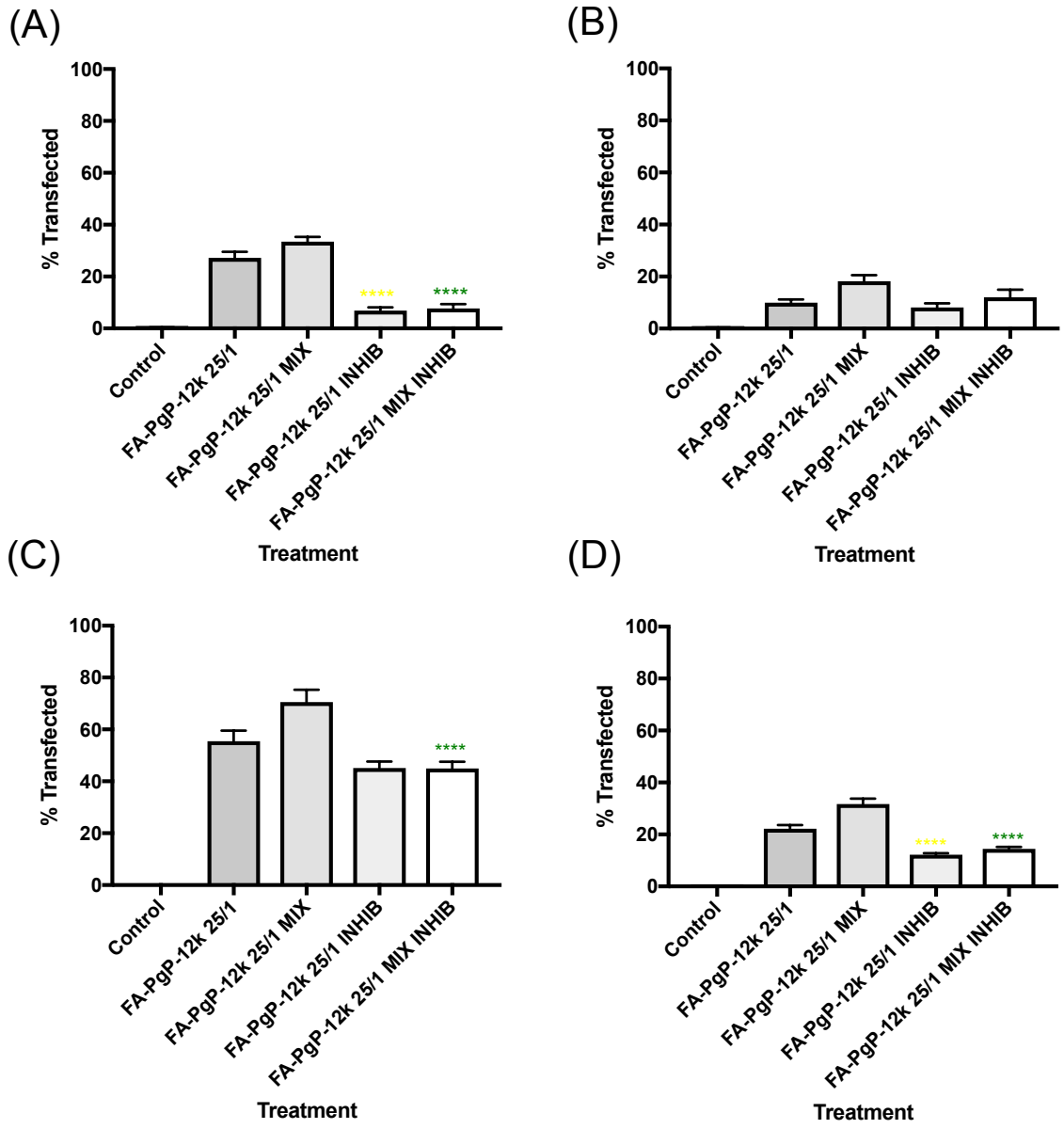

Figure 5.11: Transfection efficiency of FA-PgP-12k/pGFP and mixed micelles comprised of one part FA-PgP-12k to two parts PgP-12k by weight/pGFP (N/P: 25/1) complexes in (A) MCF-7 (B) MDA-MB-468 (C) MDA-MB-435 wild type (D) MDA-MB-435 Doxorubicin resistant variant. Groups designated with "INHIB" were co incubated with (0.33 mg/mL free folate). * : P<0.01 * P≤ 0.05, ** P≤0.01, *** P≤0.001, **** P≤0.0001 vs FA-PgP-12k, * P≤ 0.05, ** P≤0.01, *** P≤0.001, **** P≤0.0001 vs FA-PgP-12k Mix mixed micelles comprised of one part FA-PgP-12k to two parts PgP-12k by weight

The presence of FA moiety resulted in a substantial drop in transfection efficiency for all cells, indicating some kind pathway specific or deterministic uptake. Reduction of FA-PgP content in micelle system did not impede folate receptor alpha specific uptake, as mixed micelle exhibited equitable levels of inhibition of transgene expression in the presence of free folate compared to its fully functionalized counterpart in all (FA+) groups (Fig 5.11). There was no statistical difference between FA-PgP-12k groups and their free folate inhibited counterparts in (FA-) MDA-MB-468 groups. Reduced, but not statistically significant inhibition was noted in FA-PgP-12k free folate inhibited groups in MDA-MB-435 Wild Type cells compared to its uninhibited counterpart, partially a byproduct of higher variability associated with higher transfection percentages. Reduced differences in transfection percentage in (FA-) cells compared to the more dramatic and in most cases, statistically significant inhibition of transgene expression in (FA+) groups further supports a degree of pathway specificity related to folate receptor alpha presence.

Differences in cell lines are result of differences in uptake and subsequent intracellular trafficking. The size distribution of polyplexes is a dynamic entity related to synthetic composition, initial formation conditions, temperature, pH, protein and salt contents. [9] Serum content is high in albumin, whose presence has been shown to have a strong detrimental effect on the kinetic stability of polymeric delivery due to induced aggregation effects and formation of a ternary structure. [102,108] Differences in media composition may have some effect on the aggregation but stronger effects are likely due to serum content, which remains constant throughout experimentation. These minute differences in size and charge may have more profound effects depending on each cell's

optimal trafficking modality. Altering the relative proportion of polyplexes trafficked to each endocytic pathway will have obvious effects dependent on the efficacy of each route, with optimal pathway conditions likely varying between cell lines.[36]

Furthermore, cells that divide more quickly have been associated with improved transfection outcomes. Nuclear import and subsequent transcription are two rate limiting steps to transfection. [77,109] Nuclear pores generally only allow free trafficking of molecules under 9 nm in diameter or 50kD in size, much smaller than the observed size of polyplexes. [83,101] Magnitudes higher transfections have been associated with S or G_2/M phases compared to other cell cycles. [110] During these phases genetic material is no longer sequestered within the nuclear envelope, thus it is now widely accepted that increased cell division and growth have a positive correlation with transfection success. [36] Generally observed cell division rates increase across MDA-MB-435 ADR, MDA-MB-468, MCF-7, and MDA-MB-435 WT cells. This observation may serve to explain some of the resulting transfection differences.

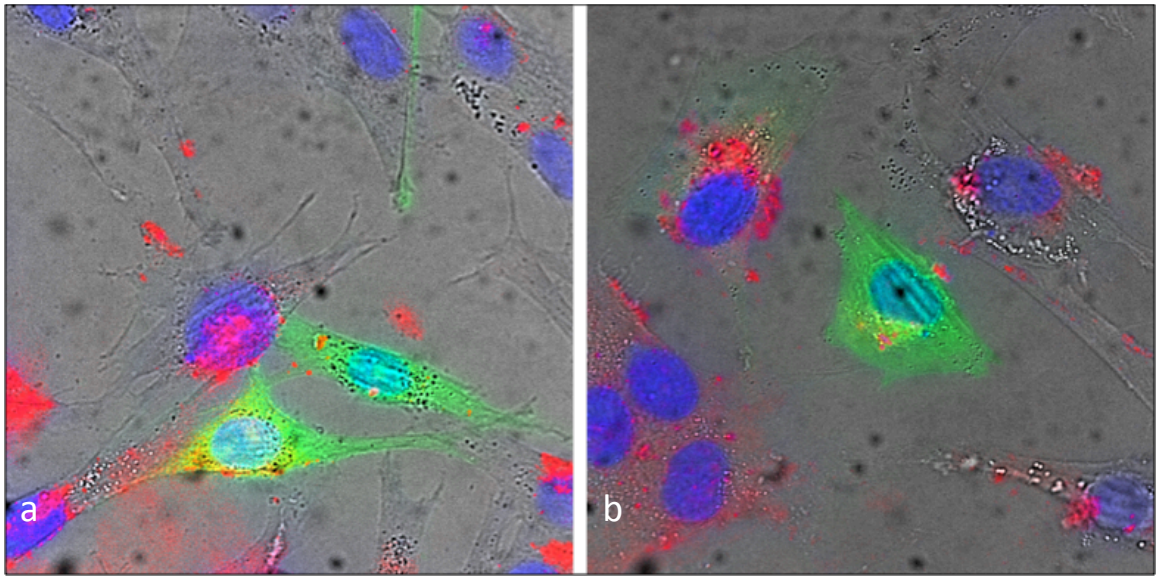

Figure 5.12: Intracellular trafficking of Rhodamine-PgP-12k/FA-PgP-12k/pGFP complexes in MDA-MB-435 wild type cells a) 24 hours and b) 48 hours post transfection

Intracellular uptake, nuclear localization and subsequent transfection were observed in both MDA-MB-435 Doxorubicin resistant variant breast cancers via confocal microscopy 24 and 48 hours post transfection (Fig 5.12). Intracellular uptake, nuclear localization and subsequent GFP production occurs in a visually similar pattern to PgP-12k (Fig 3.7). There is little apparent difference in intercellular trafficking and nuclear localization between base PgP-12k and FA-PgP-12k.

A fixed mass (1 mg/mL) of each PgP type was dissolved to a fixed volume (1 mL) and subjected to variable hydrophobic Doxorubicin content.

	% Loaded by Weight	% Efficiency
PgP-12k	31.85	21.23
FA-PgP-12k	30.47	20.31
FA-PgP-12k MIX	30.34	20.22

Table 5.1: Table summarizing Doxorubicin loading in PgP-12k, FA-PgP-12k, and mixed micelles comprised of one part FA-PgP-12k to two parts PgP-12k by weight

Values shown in Table 5.1 exhibit the content of DOX loaded in PgP-12k, FA-PgP-12k and FA-PgP-12k MIX micelles and associated efficiency, constrained by maximum solubility of DOX in methanol for chosen loading scheme.

Hydrophobic weight in each type of PgP is intrinsic to it composition, with slightly reduced composition of PLGA percentage by weight found in functionalized groups due to the weight of folate and PEG spacer. Table 5.1 describes the relative molar ratios of PLGA content across loading conditions with little difference noted between FA-PgP-12k and FA-PgP-12k MIX groups.

In chapter 4, it was found larger PgPs are more toxic per weight, regardless of N/P relationship. In chapter 5 it was then determined this concept carries forward to it DOX loaded counterparts. Confirmation that dose is more critical than form will again be sought in FA-conjugated Pg-12k and will be investigated in both manners.

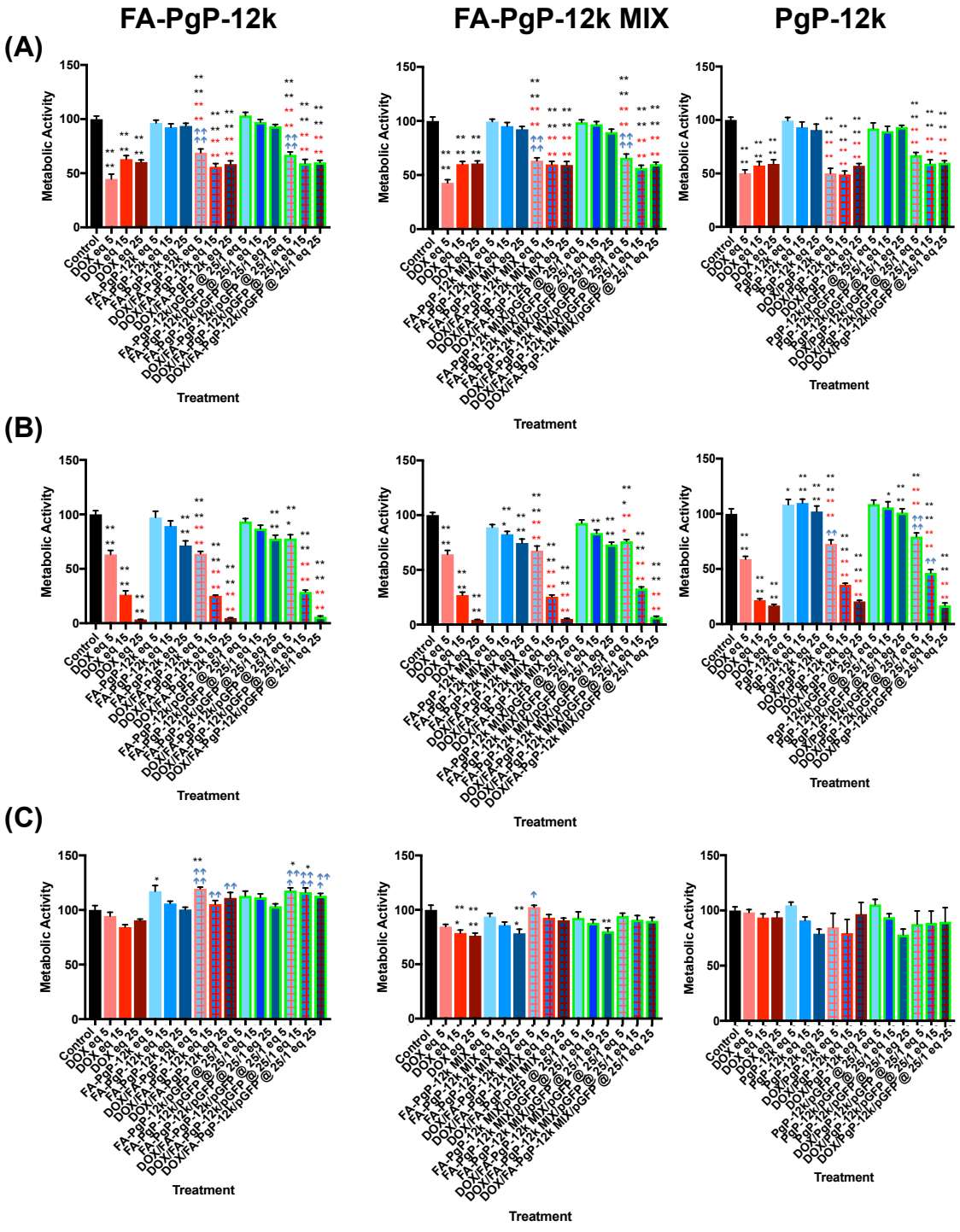

Figure 5.13: Cytotoxicity of Doxorubicin HCl, FA-PgP-12k and mixed micelles comprised of one part FA-PgP-12k to two parts PgP-12k by weight, FA-PgP-12k and mixed micelles comprised of one part FA-PgP to two parts PgP-12k by weight/pGFP

complexes, DXR (Figure 5.13 caption, continued) loaded FA-PgP and Doxorubicin loaded mixed micelles comprised of one part FA-PgP-12k to two parts PgP-12k by weight, Doxorubicin loaded FA-PgP-12k and Doxorubicin loaded mixed micelles comprised of one part FA-PgP-12k to two parts PgP-12k by weight/pGFP complexes in (A) MCF-7, (B) MDA-MB-435 Wild Type, and (C) MDA-MB-435 ADR cells (top row to bottom row respectively). Concentration of Doxorubicin HCl used was equivalent to amount of Doxorubicin used in DOX loaded PgP groups. PgP/pGFP complexes were formed at N/P 25/1 and both PgP alone and PgP/pGFP complexes were diluted down to concentration of PgP found in designated N/P equivalent. * P≤ 0.05, ** P≤0.01, *** P≤0.001, **** P≤0.0001 vs control, * P≤ 0.05, ** P≤0.01, *** P≤0.001, **** P≤0.0001 vs equivalent PgP or PgP/pGFP group, ↑P≤ 0.05, ↑↑ P≤0.01, ↑↑↑ P≤0.001, ↑↑↑↑ P≤0.0001 vs equivalent DOX HCl dose

Statistically significant cytotoxicity was induced by FA-PgP-12k in both forms at 25/1 equivalent dose and FA-Pgp-12k Mix groups at 15/1 and 25/1 equivalent doses in MDA-MB-435 Wild Type cells and 25/1 in MDA-MB-435 ADR cells. Interestingly, there was a statistically significant increase in metabolic activity in FA-PgP-12k at the equivalent PgP dose of a 5/1 transfection in MDA-MB-435 ADR cells. All DOX loaded groups were significantly cytotoxic relative to their unloaded counterparts except DOX/FA-PgP-12k/pGFP at 5/1 dose in MDA-MB-435 Wild Type and all DOX loaded groups tested in MDA-MB-435 ADR cells. All DOX/FA-PgP-12k groups and DOX/FA-PgP-12k Mix at 5/1 equivalent dosage in MDA-MB-435 ADR cells were found to induce an increase in overall metabolic activity over comparable DOX HCl groups. In MDA-MB-435 ADR increased cell viability is induced by FA-PgP-12k at 5/1 equivalent dose with similar elevated metabolic activity in DOX Loaded counterparts, this trend extends into DOX/FA-PgP-12k/pGFP at 10/1 equivalent dosage (Fig 5.13).

PgP-12k permutations were discussed in detail in chapter 3 but their graphs are shown here to illustrate the similarities in metabolic across dose and form between FA-PgP-12k,

FA-PgP-12k MIX, and PgP-12k groups, again further emphasizing the greater importance of dose over form in context of PgP.

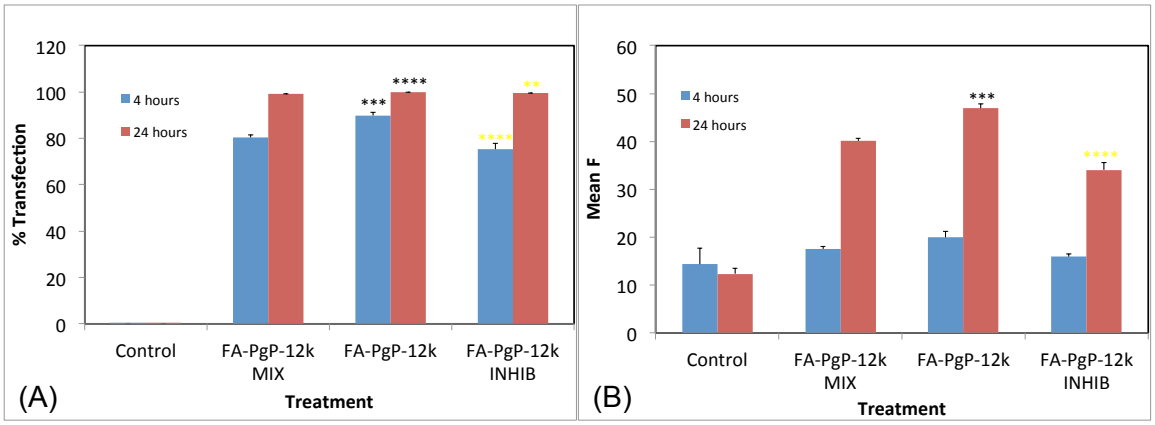

Figure 5.14: Cell uptake of siGLO/FA-PgP-12k and of one part FA-PgP-12k to two parts PgP-12k by weight (N/P: 25/1) complexes in MDA-MB-435 ADR cells 4 and 24 hours post transfection. Groups designated with "INHIB" were co incubated with (0.33 mg/mL free folate). (A)% uptake (B) mean fluorescence value (F). * P≤ 0.05, ** P≤0.01, *** P≤0.001, **** P≤0.0001 vs FA-PgP-12k MIX, P<0.01 * P≤ 0.05, ** P≤0.01, *** P≤0.001, **** P≤0.0001 vs FA-PgP-12k.

Although mitigation of transfection efficacy with free folate supports some degree of uptake pathway specificity, confirmation of reduction of uptake would further support this theory. In a siGLO uptake experiment in MDA-MB-435 ADR cells, FA-PgP-12k/siGLO polyplex uptake and mean fluorescence was higher than FA-PgP-12k MIX/siGLO polyplexes (Fig 5.14). Greater uptake noted in FA-PgP-12k over FA-PgP-12k MIX groups is interesting since elevated cytotoxicity and transfection efficacy is noted in FA-PgP-12k MIX groups. In the presence of free folate, FA-PgP-12k/siGLO polyplexes induces lower transfection and mean brightness, suggesting reduction of FA receptor related trafficking of folate functionalized PgP-12k is at least partially responsible for lower transgene expression, with other differences resulting in differences

in trafficking, endosomal escape, or nuclear localization. Since less FA-PgP-12k MIX/siGLO is shown to be taken up by cells than with FA-PgP-12k, the increase in transfection efficiency is likely due to more favorable outcomes in intracellular trafficking, endosomal escape, or nuclear localization, at least in MDA-MB-435 ADR cells. Further research is warranted but identification and relative positioning of critical factors is the first step in being able to compare DDV systems across contexts.

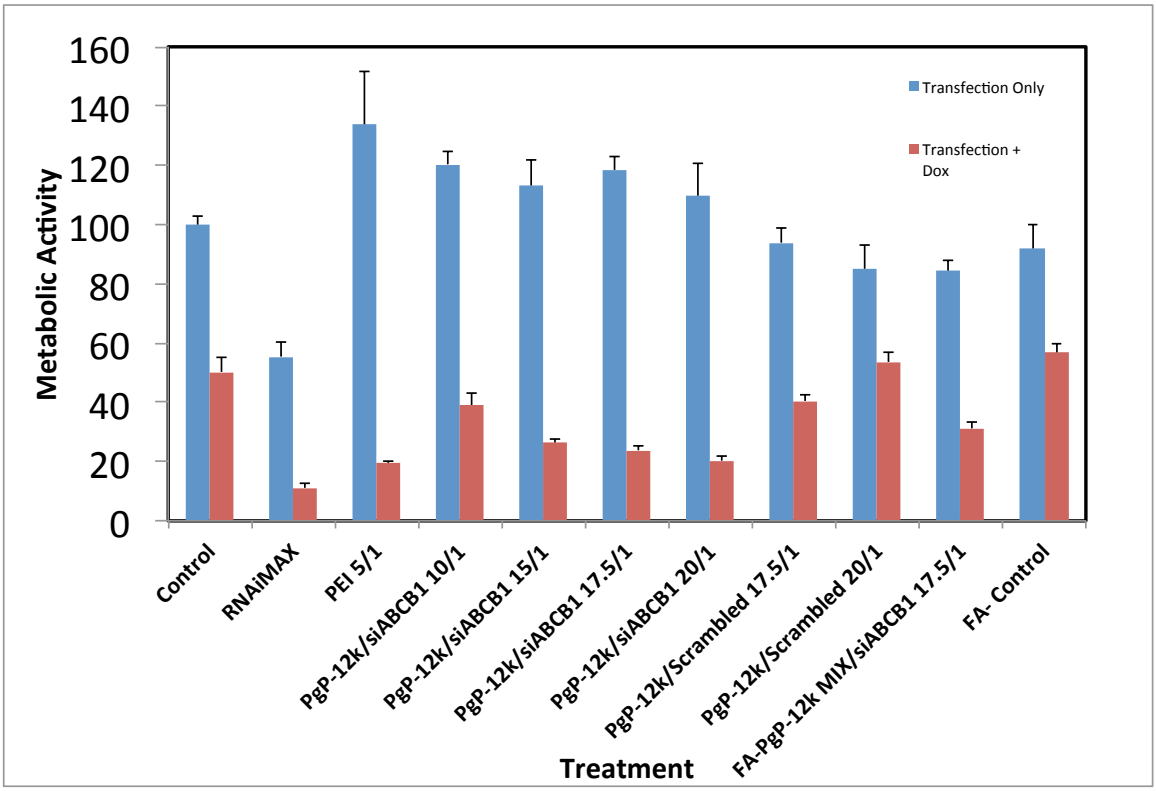

Figure 5.15: Metabolic activity in MDA-MB-435 ADR cells after knockdown with ABCB1 targeted or scrambled siRNA polyplexes. RNAiMAX, PEI, PgP-12k, or FA-PgP-12k/siRNA (N/P) polyplexes with and without 50 µg/mL DOX treatment.

The accepted practice of siRNA validation dictates that the delivery vector be confirmed to not effect off-target mRNA levels, as to mitigate unintended side effects. A siRNA

knockdown study was performed in which the cell viability of various N/P ratios of ABCB1 targeted or scrambled siRNA complexes (1 μg siRNA/48 well) in MDA-MB-435 (ADR) cells. Cells were transfected and 48 hours post transfection media containing 50 μg/mL Doxorubicin was added to specified group. At 96 hours, post transfection, % knockdown was assessed via RT-PCR while cell viability was assessed via MTT to compare differences in metabolic activity. Non-targeted PgP-12k groups effects altered endogenous GAPDH levels to an unwanted degree, invaliding RT-PCR quantification, however there were significant differences found between cell viabilities. In groups not dosed with Doxorubicin only RNAiMAX was found to be more cytotoxic than the no treatment control (Fig 5.15). Both PEI 5/1 and PgP-12k 10/1 groups induced cell viabilities over control in a significant fashion, potentially as a result of induced knockdown, general or MDR1 specific. All DOX dosed groups were found to be significantly different from the non-treated control ($p \leq 0.0001$) and all DOX treated groups were found to be statistically different than their non-treated counterparts, indicating significant cytotoxicity induced by DOX treatment ($p \leq 0.0001$). Compared to DOX treated control: RNAiMAX, PEI 5/1, PgP-12k 10/1, PgP-12k 15/1, and PgP-12k 20/1, ABCB1-targeted groups were all found to have significantly reduced metabolic activity ($p \leq 0.0001$, $p \leq 0.0001$, $p=0.0037$, $p=.0006$, and $p \leq 0.0001$ respectively). PgP-12k 10/1 and FA-PgP-12k MIX increased DOX related cytotoxicity but not in a significant fashion. Non-targeting PgP-12k at N/P 20/1 also did not induce DOX related cytotoxicity and was found have higher metabolic activity than the DOX dosed control. While RT-PCR studies were unable to indicate if ABCB1 knockdown in ABCB1 targeted groups

was specific or generic but increased cytotoxicity in ABCB1 groups relative to non-targeted group ($p \leq 0.0001$), does support at least some degree of therapeutic efficacy.

Altogether, this suggests that a variety of therapeutically relevant PgP target/gene/drug configurations are yet to be investigated. The development of PgP as a lyophilizable system will begin to address shelf life and production issues while maintaining the standard format, accomplished by DDV reconstitution and subsequent administration via intravenous injection. Development of this system will strike a balance between the realities of medicine today with the potential of the personalized treatments of tomorrow. This incorporation of genetic and targeting technologies in a product that in a familiar format to practitioners will ease the transition, adoption and incorporation of nanotherapeutics drug delivery vehicles into the clinical workspace.

It was unclear if inhibition with free FA resulted in decreased uptake along with decreased transfection so an experiment was performed to determine uptake; PgP-12k uptake did in fact increase with FA-moiety conjugation. Furthermore, there is decreased uptake with increased presence of competitive moiety (free folate) which corroborates decreased percentage transfected in FA blocked transfection experiments. These trends however, are contingent on reasonable presence of FA receptor alpha, which is present in higher levels in MCF-7 and MDA-MB-435 groups but in lower levels in MDA-MB-468 groups.

Conclusions

PgP-12k has illustrated the greatest versatility as a multifunctional drug delivery platform, out of tested PgP weights. High levels of transfection with low levels of cytotoxicity were observed in PgP-12k experiments. Adequate drug loading performance with the ability to undergo industry preferred 0.2 micron filter based purification was noted in PgP of all weights with DOX loading content being most closely related to PLGA content. With this in mind, lower transfection efficacies associated with PgP-25k and PgP-50k may be redeemed by higher levels of DOX loading per weight. Functionalization with FA in PgP-12k only marginally effects physicochemical properties including DOX loading compared to base PgP-12k while imbuing some folate receptor alpha receptor related specificity to DDV. Plasmid DNA completely binds with PgP-12k and FA-PgP-12k more strongly with less polymer compared to siRNA indicating that for siRNA applications, higher concentrations of PgP may need to be used. While loss of function induced by ABCB1 siRNA have shown to make drug resistant phenotypes more susceptible to chemotherapeutics and combined with target specificity represents a potential therapy, production of a therapeutic protein with pDNA transfection may be a better application of PgP. Further investigation into the transgene expression of individual cells will help quantify the potential of gain of function therapies as well as help better understand the dynamics behind in loss of function if that is the desired modality. Based on this pilot study, new combinations of therapeutically relevant nucleic acids and drugs with PgP warrant further investigation.

REFERENCES

1. Sun J, Luo C, Wang Y, He Z. The holistic 3M modality of drug delivery nanosystems for cancer therapy. *Nanoscale*. 2013;5(3):845-859. http://dx.doi.org/10.1039/C2NR32867D. doi: 10.1039/C2NR32867D.

2. Sayed A, Layne G, Abraham J, Mukdadi O. Nonlinear characterization of breast cancer using multi-compression 3D ultrasound elastography in vivo. *Ultrasonics*. 2013;53(5):979-991. doi: 10.1016/j.ultras.2013.01.005.

3. Hurvitz SA, Hu Y, O'Brien N, Finn RS. Current approaches and future directions in the treatment of HER2-positive breast cancer. *Cancer Treat Rev*. 2013;39(3):219-229. doi: 10.1016/j.ctrv.2012.04.008.

4. Gottesman MM, Fojo T, Bates SE. Multidrug resistance in cancer: Role of ATP-dependent transporters. *Nat Rev Cancer*. 2002;2(1):48-58. doi: 10.1038/nrc706.

5. Apostolou P, Toloudi M, Chatziioannou M, Ioannou E, Papasotiriou I. Cancer stem cells stemness transcription factors expression correlates with breast cancer disease stage. *Curr Stem Cell Res Ther*. 2012;7(6):415-419.

6. Yi S, Hao Y, Nan K, Fan T. Cancer stem cells niche: A target for novel cancer therapeutics. *Cancer Treat Rev*. 2013;39(3):290-296. doi: 10.1016/j.ctrv.2012.10.004.

7. Cuncins-Hearn A, Saunders C, Walsh D, et al. A systematic review of intraoperative radiotherapy in early breast cancer. *Breast Cancer Res Treat*. 2004;85(3):271-280. doi: 10.1023/B:BREA.0000025411.77758.1e.

8. Greenberg S, Stopeck A, Rugo HS. Systemic treatment of early breast cancer-A biological perspective. *J Surg Oncol*. 2011;103(6):619-626. doi: 10.1002/jso.21842.

9. Thomas H, Coley HM. Overcoming multidrug resistance in cancer: An update on the clinical strategy of inhibiting p-glycoprotein. *Cancer Control*. 2003;10(2):159-165.

10. WOODLE M. Sterically stabilized liposome therapeutics. *Adv Drug Deliv Rev*. 1995;16(2-3):249-265. doi: 10.1016/0169-409X(95)00028-6.

11. Stierle V, Laigle A, Jolles B. Modulation of MDR1 gene expression in multidrug resistant MCF7 cells by low concentrations of small interfering RNAs. *Biochem Pharmacol*. 2005;70(10):1424-1430. doi: 10.1016/j.bcp.2005.08.007.

12. Leonessa F, Clarke R. ATP binding cassette transporters and drug resistance in breast cancer. *Endocr Relat Cancer*. 2003;10(1):43-73.

13. Kim D, Lee ES, Oh KT, Gao ZG, Bae YH. Doxorubicin-loaded polymeric micelle overcomes multidrug resistance of cancer by double-targeting folate receptor and early endosomal pH. *Small*. 2008;4(11):2043-2050. doi: 10.1002/smll.200701275; 10.1002/smll.200701275.

14. Blagbrough IS, Zara C. Animal models for target diseases in gene therapy - using DNA and siRNA delivery strategies. *Pharm Res*. 2009;26(1):1-18. doi: 10.1007/s11095-008-9646-8.

15. Dong J, Fan P, Frizzell R. Quantitative analysis of the packaging capacity of recombinant adeno-associated virus. *Hum Gene Ther*. 1996;7(17):2101-2112. doi: 10.1089/hum.1996.7.17-2101.

16. Liu X, Sun C, Yang X, Wang J. Polymeric-micelle-based nanomedicine for siRNA delivery. *Particle & Particle Systems Characterization*. 2013;30(3):211-228. doi: 10.1002/ppsc.201200061.

17. Liu Y, Du F, Chen W, Yao M, Lv K, Fu P. Knockdown of dual specificity phosphatase 4 enhances the chemosensitivity of MCF-7 and MCF-7/ADR breast cancer cells to doxorubicin. *Exp Cell Res*. 2013;319(20):3140-3149. doi: http://dx.doi.org.libproxy.clemson.edu/10.1016/j.yexcr.2013.08.023.

18. Gary DJ, Puri N, Won Y. Polymer-based siRNA delivery: Perspectives on the fundamental and phenomenological distinctions from polymer-based DNA delivery. *J Controlled Release*. 2007;121(1-2):64-73. doi: 10.1016/j.jconrel.2007.05.021.

19. Cai X, Conley S, Naash M. Nanoparticle applications in ocular gene therapy. *Vision Res*. 2008;48(3):319-324. doi: 10.1016/j.visres.2007.07.012.

20. Mahmud A, Xiong XB, Aliabadi HM, Lavasanifar A. Polymeric micelles for drug targeting. *J Drug Target*. 2007;15(9):553-584. doi: 783599225 [pii].

21. Hanahan D, Weinberg RA. Hallmarks of cancer: The next generation. *Cell*. 2011;144(5):646-674. doi: 10.1016/j.cell.2011.02.013; 10.1016/j.cell.2011.02.013.

22. Jhaveri AM, Torchilin VP. Multifunctional polymeric micelles for delivery of drugs and siRNA. *Front Pharmacol*. 2014;5:77. doi: 10.3389/fphar.2014.00077.

23. Southall N, Dill K, Haymet A. A view of the hydrophobic effect. *J Phys Chem B*. 2002;106(3):521-533. doi: 10.1021/jp015514e.

24. Heinzelmann G, Figueiredo W, Girardi M. Micellar dynamics and water-water hydrogen-bonding from temperature-jump monte carlo simulations. *Chem Phys Lett*. 2012;550:83-87. doi: 10.1016/j.cplett.2012.09.011.

25. Zana R, Marques C, Johner A. Dynamics of micelles of the triblock copolymers poly(ethylene oxide)–poly(propylene oxide)–poly(ethylene oxide) in aqueous solution. *Adv Colloid Interface Sci*. 2006;123–126:345-351. doi: http://dx.doi.org/10.1016/j.cis.2006.05.011.

26. Nicolai T, Colombani O, Chassenieux C. Dynamic polymeric micelles versus frozen nanoparticles formed by block copolymers. *Soft Matter*. 2010;6(14):3111-3118. doi: 10.1039/b925666k.

27. de Moraes JNB, Figueiredo W. Temporal evolution of micellar aggregates in the temperature jump experiments. *Chem Phys Lett*. 2010;491(1-3):39-43. doi: 10.1016/j.cplett.2010.03.070.

28. Zheng M, Pavan GM, Neeb M, et al. Targeting the blind spot of polycationic nanocarrier-based siRNA delivery. *ACS Nano*. 2012;6(11):9447-9454. http://dx.doi.org/10.1021/nn301966r. doi: 10.1021/nn301966r.

29. Hillen F, Griffioen AW. Tumour vascularization: Sprouting angiogenesis and beyond. *Cancer Metastasis Rev*. 2007;26(3-4):489-502. doi: 10.1007/s10555-007-9094-7.

30. Mahmud A, Xiong XB, Aliabadi HM, Lavasanifar A. Polymeric micelles for drug targeting. *J Drug Target*. 2007;15(9):553-584. doi: 10.1080/10611860701538586.

31. Greish K. Enhanced permeability and retention of macromolecular drugs in solid tumors: A royal gate for targeted anticancer nanomedicines. *J Drug Target*. 2007;15(7-8):457-464. doi: 10.1080/10611860701539584.

32. Nichols JW, Bae YH. Odyssey of a cancer nanoparticle: From injection site to site of action. *Nano Today*. 2012;7(6):606-618. doi: 10.1016/j.nantod.2012.10.010.

33. Owens D, Peppas N. Opsonization, biodistribution, and pharmacokinetics of polymeric nanoparticles. *Int J Pharm*. 2006;307(1):93-102. doi: 10.1016/j.ijpharm.2005.10.010.

34. Kircheis R, Wightman L, Wagner E. Design and gene delivery activity of modified polyethylenimines. *Adv Drug Deliv Rev*. 2001;53(3):341-358. doi: 10.1016/S0169-409X(01)00202-2.

35. Szachowicz-Petelska B, Figaszewski Z, Lewandowski W. Mechanisms of transport across cell membranes of complexes contained in antitumour drugs. *Int J Pharm*. 2001;222(2):169-182. doi: 10.1016/S0378-5173(01)00713-X.

36. Hsu CYM, Uludag H. Nucleic-acid based gene therapeutics: Delivery challenges and modular design of nonviral gene carriers and expression cassettes to overcome intracellular barriers for sustained targeted expression. *J Drug Target*. 2012;20(4):301-328. doi: 10.3109/1061186X.2012.655247.

37. Nicolas J, Mura S, Brambilla D, Mackiewicz N, Couvreur P. Design, functionalization strategies and biomedical applications of targeted biodegradable/biocompatible polymer-based nanocarriers for drug delivery. *Chem Soc Rev*. 2013;42(3):1147-1235. doi: 10.1039/c2cs35265f; 10.1039/c2cs35265f.

38. Sahay G, Alakhova DY, Kabanov AV. Endocytosis of nanomedicines. *J Controlled Release*. 2010;145(3):182-195. doi: 10.1016/j.jconrel.2010.01.036.

39. Meneksedag-Erol D, Sun C, Tang T, Uludag H. Molecular dynamics simulations of polyplexes and lipoplexes employed in gene delivery. *Fundam Biomed Technol*. 2014;7:277-311. doi: 10.1007/978-94-017-8896-0_15.

40. Zhang C, Gao S, Jiang W, et al. Targeted minicircle DNA delivery using folate-poly(ethylene glycol)-polyethylenimine as non-viral carrier. *Biomaterials*. 2010;31(23):6075-6086. doi: 10.1016/j.biomaterials.2010.04.042; 10.1016/j.biomaterials.2010.04.042.

41. Richard I, Thibault M, De Crescenzo G, Buschmann MD, Lavertu M. Ionization behavior of chitosan and chitosan-DNA polyplexes indicate that chitosan has a similar capability to induce a proton-sponge effect as PEI. *Biomacromolecules*. 2013;14(6):1732-1740. doi: 10.1021/bm4000713; 10.1021/bm4000713.

42. Benjaminsen RV, Mattebjerg MA, Henriksen JR, Moghimi SM, Andresen TL. The possible "proton sponge" effect of polyethylenimine (PEI) does not include change in lysosomal pH. *Mol Ther*. 2013;21(1):149-157. doi: 10.1038/mt.2012.185.

43. Bertschinger M, Backliwal G, Schertenleib A, Jordan M, Hacker DL, Wurm FM. Disassembly of polyethylenimine-DNA particles in vitro: Implications for polyethylenimine-mediated DNA delivery. *J Controlled Release*. 2006;116(1):96-104. doi: 10.1016/j.jconrel.2006.09.006.

44. Wong SY, Pelet JM, Putnam D. Polymer systems for gene delivery-past, present, and future. *Prog Polym Sci*. 2007;32(8-9):799-837. doi: 10.1016/j.progpolymsci.2007.05.007.

45. Bhattacharjee S. DLS and zeta potential - what they are and what they are not? *J Controlled Release*. 2016;235:337-351. doi: 10.1016/j.jconrel.2016.06.017.

46. Kataoka K, Harada A, Nagasaki Y. Block copolymer micelles for drug delivery: Design, characterization and biological significance. *Adv Drug Deliv Rev*. 2012;64:37-48. doi: 10.1016/j.addr.2012.09.013.

47. Kedar U, Phutane P, Shidhaye S, Kadam V. Advances in polymeric micelles for drug delivery and tumor targeting. *Nanomedicine: Nanotechnology, Biology and Medicine*. 2010;6(6):714-729. doi: http://dx.doi.org.libproxy.clemson.edu/10.1016/j.nano.2010.05.005.

48. Menard S, Pupa SM, Campiglio M, Tagliabue E. Biologic and therapeutic role of HER2 in cancer. *Oncogene*. 2003;22(42):6570-6578. doi: 10.1038/sj.onc.1206779.

49. Mohd Sharial MS, Crown J, Hennessy BT. Overcoming resistance and restoring sensitivity to HER2-targeted therapies in breast cancer. *Ann Oncol*. 2012;23(12):3007-3016. doi: 10.1093/annonc/mds200; 10.1093/annonc/mds200.

50. Carlsson J, Nordgren H, Sjostrom J, et al. HER2 expression in breast cancer primary tumours and corresponding metastases. original data and literature review. *Br J Cancer*. 2004;90(12):2344-2348. doi: 10.1038/sj.bjc.6601881.

51. Di Cosimo S, Baselga J. Targeted therapies in breast cancer: Where are we now? *Eur J Cancer*. 2008;44(18):2781-2790. doi: 10.1016/j.ejca.2008.09.026.

52. Hicks DG, Kulkarni S. HER2+ breast cancer: Review of biologic relevance and optimal use of diagnostic tools. *Am J Clin Pathol*. 2008;129(2):263-273. doi: 10.1309/99AE032R9FM8WND1; 10.1309/99AE032R9FM8WND1.

53. Lee ALZ, Wang Y, Cheng HY, Pervaiz S, Yang YY. The co-delivery of paclitaxel and herceptin using cationic micellar nanoparticles. *Biomaterials*. 2009;30(5):919-927. doi: 10.1016/j.biomaterials.2008.10.062.

54. Chen T, Cheng T, Chen C, et al. Targeted herceptin-dextran iron oxide nanoparticles for noninvasive imaging of HER2/neu receptors using MRI. *J Biol Inorg Chem*. 2009;14(2):253-260. doi: 10.1007/s00775-008-0445-9.

55. Damiano JS, Wasserman E. Molecular pathways: Blockade of the PRLR signaling pathway as a novel antihormonal approach for the treatment of breast and prostate cancer. *Clin Cancer Res*. 2013;19(7):1644-1650. doi: 10.1158/1078-0432.CCR-12-0138; 10.1158/1078-0432.CCR-12-0138.

56. Llovera M, Pichard C, Bernichtein S, et al. Human prolactin (hPRL) antagonists inhibit hPRL-activated signaling pathways involved in breast cancer cell proliferation. *Oncogene*. 2000;19(41):4695-4705. doi: 10.1038/sj.onc.1203846.

57. Tomblyn S, Springs AE, Langenheim JF, Chen WY. Combination therapy using three novel prolactin receptor antagonist-based fusion proteins effectively inhibits tumor recurrence and metastasis in HER2/neu transgenic mice. *Int J Oncol*. 2009;34(4):1139-1146.

58. Morrison B, Schmidt C, Lakhani S, Reynolds B, Lopez JA. Breast cancer stem cells: Implications for therapy of breast cancer. *Breast Cancer Research*. 2008;10(4):210. http://breast-cancer-research.com/content/10/4/210.

59. Goffin V, Hoang DT, Bogorad RL, Nevalainen MT. Prolactin regulation of the prostate gland: A female player in a male game. *Nature Reviews Urology*. 2011;8(11):597-607. http://dx.doi.org/10.1038/nrurol.2011.143. doi: 10.1038/nrurol.2011.143.

60. Chen WY, Lee EH, inventors; Simkin M, assignee. METHOD FOR SENSITIZING CELLS TO CANCER THERAPY. patent WO/2011/097268. 11.08.2011, 2011.

61. Lu Y, Low PS. Immunotherapy of folate receptor-expressing tumors: Review of recent advances and future prospects. *J Control Release*. 2003;91(1-2):17-29.

62. Lu Y, Sega E, Leamon CP, Low PS. Folate receptor-targeted immunotherapy of cancer: Mechanism and therapeutic potential. *Adv Drug Deliv Rev*. 2004;56(8):1161-1176. http://www.sciencedirect.com/science/article/pii/S0169409X04000195. doi: http://dx.doi.org/10.1016/j.addr.2004.01.009.

63. Meier R, Henning TD, Boddington S, et al. Breast cancers: MR imaging of folate-receptor expression with the folate-specific nanoparticle P1133. *Radiology*. 2010;255(2):527-535. doi: 10.1148/radiol.10090050; 10.1148/radiol.10090050.

64. Bosch A, Eroles P, Zaragoza R, Vina JR, Lluch A. Triple-negative breast cancer: Molecular features, pathogenesis, treatment and current lines of research. *Cancer Treat Rev*. 2010;36(3):206-215. doi: 10.1016/j.ctrv.2009.12.002.

65. Oâ€™Shannessy D,J., Somers EB, Maltzman J, Smale R, Fu Y. Folate receptor alpha (FRA) expression in breast cancer: Identification of a new molecular subtype and association with triple negative disease. *SpringerPlus*. 2012;1:22. http://www.ncbi.nlm.nih.gov/pmc/articles/PMC3725886/. doi: 10.1186/2193-1801-1-22.

66. Zhang Z, Wang J, Tacha DE, et al. Folate receptor alpha associated with triple-negative breast cancer and poor prognosis. *Arch Pathol Lab Med*. 2014;138(7):890-895. doi: 10.5858/arpa.2013-0309-OA [doi].

67. Leamon CP, Reddy JA. Folate-targeted chemotherapy. *Adv Drug Deliv Rev*. 2004;56(8):1127-1141. doi: 10.1016/j.addr.2004.01.008.

68. Neve RM, Chin K, Fridlyand J, et al. A collection of breast cancer cell lines for the study of functionally distinct cancer subtypes. *Cancer Cell*. 2006;10:515-527.

69. Jhaveri MS, Rait AS, Chung KN, Trepel JB, Chang EH. Antisense oligonucleotides targeted to the human alpha folate receptor inhibit breast cancer cell growth and sensitize the cells to doxorubicin treatment. *Mol Cancer Ther*. 2004;3(12):1505-1512.

70. Chavez KJ, Garimella SV, Lipkowitz S. Triple negative breast cancer cell lines: One tool in the search for better treatment of triple negative breast cancer. *Breast disease*. 2010;32(1-2):35-48. http://www.ncbi.nlm.nih.gov/pmc/articles/PMC3532890/. doi: 10.3233/BD-2010-0307.

71. Mahmud A, Xiong X, Aliabadi HM, Lavasanifar A. Polymeric micelles for drug targeting. *J Drug Target*. 2007;15(9):553-584. doi: 10.1080/10611860701538586.

72. Kim D, Gao ZG, Lee ES, Bae YH. In vivo evaluation of doxorubicin-loaded polymeric micelles targeting folate receptors and early endosomal pH in drug-resistant ovarian cancer. *Mol Pharm*. 2009;6(5):1353-1362. doi: 10.1021/mp900021q.

73. Cho H, Lai TC, Tomoda K, Kwon GS. Polymeric micelles for multi-drug delivery in cancer. *AAPS PharmSciTech*. 2015;16(1):10-20. doi: 10.1208/s12249-014-0251-3.

74. Jhaveri AM, Torchilin VP. Multifunctional polymeric micelles for delivery of drugs and siRNA. *Front Pharmacol*. 2014;5:77. doi: 10.3389/fphar.2014.00077.

75. Mishra D, Kang HC, Bae YH. Reconstitutable charged polymeric (PLGA)2-b-PEI micelles for gene therapeutics delivery. *Biomaterials*. 2011;32(15):3845-3854. doi: http://dx.doi.org.libproxy.clemson.edu/10.1016/j.biomaterials.2011.01.077.

76. Mishra D, Kang HC, Cho H, Bae YH. Dexamethasone-loaded reconstitutable charged polymeric (PLGA)(n)-b-bPEI micelles for enhanced nuclear delivery of gene therapeutics. *Macromol Biosci*. 2014;14(6):831-841. doi: 10.1002/mabi.201300432.

77. Gwak S, Nice J, Zhang J, et al. Cationic, amphiphilic copolymer micelles as nucleic acid carriers for enhanced transfection in rat spinal cord. *Acta Biomaterialia*. . doi: http://dx.doi.org/10.1016/j.actbio.2016.02.013.

78. Mishra D, Kang HC, Cho H, Bae YH. Dexamethasone-loaded reconstitutable charged polymeric (PLGA)(n)-b-bPEI micelles for enhanced nuclear delivery of gene therapeutics. *Macromol Biosci*. 2014;14(6):831-841. doi: 10.1002/mabi.201300432.

79. Tacar O, Sriamornsak P, Dass CR. Doxorubicin: An update on anticancer molecular action, toxicity and novel drug delivery systems. *J Pharm Pharmacol*. 2013;65(2):157-170. doi: 10.1111/j.2042-7158.2012.01567.x.

80. Subedi RK, Kang KW, Choi H. Preparation and characterization of solid lipid nanoparticles loaded with doxorubicin. *Eur J Pharm Sci*. 2009;37(3-4):508-513. doi: 10.1016/j.ejps.2009.04.008.

81. He Yueying, Zhang Yan, Gu Chunhua, Dai Weifeng, Lang Meidong. Micellar carrier based on methoxy poly(ethylene glycol)-block-poly(epsilon-caprolactone) block copolymers bearing ketone groups on the polyester block for doxorubicin delivery. *J Mater Sci -Mater Med*. 2010;21(2):567-574. doi: 10.1007/s10856-009-3887-x.

82. Barenholz Y(. Doxil (R) - the first FDA-approved nano-drug: Lessons learned. *J Controlled Release*. 2012;160(2):117-134. doi: 10.1016/j.jconrel.2012.03.020.

83. Motlagh NSH, Parvin P, Ghasemi F, Atyabi F. Fluorescence properties of several chemotherapy drugs: Doxorubicin, paclitaxel and bleomycin. *Biomed Opt Express*. 2016;7(6):2400-2406. doi: 10.1364/BOE.7.002400.

84. Nicholson JK. Global systems biology, personalized medicine and molecular epidemiology. *Molecular Systems Biology*. 2006;2:52-52. http://www.ncbi.nlm.nih.gov/pmc/articles/PMC1682018/. doi: 10.1038/msb4100095.

85. Makadia HK, Siegel SJ. Poly lactic-co-glycolic acid (PLGA) as biodegradable controlled drug delivery carrier. *Polymers*. 2011;3(3):1377-1397. doi: 10.3390/polym3031377.

86. Bahadur KCR, Landry B, Aliabadi HM, Lavasanifar A, Uludag H. Lipid substitution on low molecular weight (0.6-2.0 kDa) polyethylenimine leads to a higher zeta potential of plasmid DNA and enhances transgene expression. *Acta Biomater*. 2011;7(5):2209-2217. doi: 10.1016/j.actbio.2011.01.027.

87. Dinh A, Pangarkar C, Theofanous T, Mitragotri S. Understanding intracellular transport processes pertinent to synthetic gene delivery via stochastic simulations and sensitivity analyses. *Biophys J*. 2006;92(3):831-846. http://www.ncbi.nlm.nih.gov/pmc/articles/PMC1779970/. doi: 10.1529/biophysj.106.095521.

88. Yanan Y. Revisiting complexation between DNA and polyethylenimine: The effect of uncomplexed chains free in the solution mixture on gene transfection. In: Yanan Y, ed. *How free cationic polymer chains promote gene transfection.* Heidelberg: Springer International Publishing; 2013:29-48. http://dx.doi.org/10.1007/978-3-319-00336-8_2. 10.1007/978-3-319-00336-8_2.

89. Zhao Q, Chen J, Lv T, et al. N/P ratio significantly influences the transfection efficiency and cytotoxicity of a polyethylenimine/chitosan/DNA complex. *Biol Pharm Bull*. 2009;32(4):706-710.

90. Meneksedag-Erol D, Bahadur RKC, Tang T, Uludag H. A delicate balance when substituting a small hydrophobe onto low molecular weight polyethylenimine to improve its nucleic acid delivery efficiency. *ACS Appl Mater Interfaces*. 2015;7(44):24822-24832. doi: 10.1021/acsami.5b07929.

91. Aliabadi HM, Landry B, Sun C, Tang T, Uludag H. Supramolecular assemblies in functional siRNA delivery: Where do we stand? *Biomaterials*. 2012;33(8):2546-2569. doi: 10.1016/j.biomaterials.2011.11.079.

92. Kim SH, Jeong JH, Mok H, Lee SH, Kim SW, Park TG. Folate receptor targeted delivery of polyelectrolyte complex micelles prepared from ODN-PEG-folate conjugate and cationic lipids. *Biotechnol Prog*. 2007;23(1):232-237. doi: 10.1021/bp060243g.

93. Yoo HS, Park TG. Folate receptor targeted biodegradable polymeric doxorubicin micelles. *J Controlled Release*. 2004;96(2):273-283. doi: http://dx.doi.org.libproxy.clemson.edu/10.1016/j.jconrel.2004.02.003.

94. Liu X, Sun C, Yang X, Wang J. Polymeric-micelle-based nanomedicine for siRNA delivery. *Part Part Syst Charact*. 2013;30(3):211-228.

95. Wagner E. Functional polymer conjugates for medicinal nucleic acid delivery. In: Kunugi S, Yamaoka T, eds. Vol 247. Springer Berlin Heidelberg; 2012:1-29. http://dx.doi.org/10.1007/12_2011_148. 10.1007/12_2011_148.

96. Scholz C, Wagner E. Therapeutic plasmid DNA versus siRNA delivery: Common and different tasks for synthetic carriers. *J Controlled Release*. 2012;161(2):554-565. doi: http://dx.doi.org.libproxy.clemson.edu/10.1016/j.jconrel.2011.11.014.

97. Brannon-Peppas L, Blanchette JO. Nanoparticle and targeted systems for cancer therapy. *Adv Drug Deliv Rev*. 2012;64, Supplement(0):206-212. doi: http://dx.doi.org/10.1016/j.addr.2012.09.033.

98. Yuan H, Miao J, Du Y, You J, Hu F, Zeng S. Cellular uptake of solid lipid nanoparticles and cytotoxicity of encapsulated paclitaxel in A549 cancer cells. *Int J Pharm*. 2008;348(1–2):137-145. doi: http://dx.doi.org.libproxy.clemson.edu/10.1016/j.ijpharm.2007.07.012.

99. Lee ES, Na K, Bae YH. Doxorubicin loaded pH-sensitive polymeric micelles for reversal of resistant MCF-7 tumor. *J Controlled Release*. 2005;103(2):405-418. doi: http://dx.doi.org/10.1016/j.jconrel.2004.12.018.

100. Lungwitz U, Breunig M, Blunk T, Göpferich A. Polyethylenimine-based non-viral gene delivery systems. *European Journal of Pharmaceutics and Biopharmaceutics*. 2005;60(2):247-266. doi: http://dx.doi.org/10.1016/j.ejpb.2004.11.011.

101. Meneksedag-Erol D, Tang T, Uudag H. Probing the effect of miRNA on siRNA-PEI polyplexes. *J Phys Chem B*. 2015;119(17):5475-5486. doi: 10.1021/acs.jpcb.jb00415.

102. Kang HC, Samsonova O, Bae YH. Trafficking microenvironmental pHs of polycationic gene vectors in drug-sensitive and multidrug-resistant MCF7 breast cancer cells. *Biomaterials*. 2010;31(11):3071-3078. doi: http://dx.doi.org/10.1016/j.biomaterials.2010.01.001.

103. Aravindan L, Bicknell KA, Brooks G, Khutoryanskiy VV, Williams AC. Effect of acyl chain length on transfection efficiency and toxicity of polyethylenimine. *Int J Pharm*. 2009;378(1–2):201-210. doi: http://dx.doi.org/10.1016/j.ijpharm.2009.05.052.

104. Delgado D, Gascón AR, del Pozo-Rodríguez A, et al. Dextran–protamine–solid lipid nanoparticles as a non-viral vector for gene therapy: In vitro characterization and in vivo transfection after intravenous administration to mice. *Int J Pharm*. 2012;425(1–2):35-43. doi: http://dx.doi.org/10.1016/j.ijpharm.2011.12.052.

105. Yang Z, Sahay G, Sriadibhatla S, Kabanov AV. Amphiphilic block copolymers enhance cellular uptake and nuclear entry of polyplex-delivered DNA. *Bioconjug Chem*. 2008;19(10):1987-1994. http://www.ncbi.nlm.nih.gov/pmc/articles/PMC2574534/. doi: 10.1021/bc800144a.

106. Batrakova E, Li S, Vinogradov S, Alakhov V, Miller D, Kabanov A. Mechanism of pluronic effect on P-glycoprotein efflux system in blood-brain barrier: Contributions of energy depletion and membrane fluidization. *J Pharmacol Exp Ther*. 2001;299(2):483-493.

107. Allen C, Maysinger D, Eisenberg A. Nano-engineering block copolymer aggregates for drug delivery. *Colloid Surf B-Biointerfaces*. 1999;16(1-4):3-27. doi: 10.1016/S0927-7765(99)00058-2.

108. Lu J, Owen SC, Shoichet MS. Stability of self-assembled polymeric micelles in serum. *Macromolecules*. 2011;44(15):6002-6008. http://pubs.acs.org/doi/abs/10.1021/ma200675w. doi: 10.1021/ma200675w.

109. Meneksedag-Erol D, Tang T, Uludag H. Molecular modeling of polynucleotide complexes. *Biomaterials*. 2014;35(25):7068-7076. doi: 10.1016/j.biomaterials.2014.04.103.

110. Kang HC, Samsonova O, Kang S, Bae YH. The effect of environmental pH on polymeric transfection efficiency. *Biomaterials*. 2012;33(5):1651-1662. doi: http://dx.doi.org/10.1016/j.biomaterials.2011.11.006.

111. Thapa B, Plianwong S, Bahadur RKC, Rutherford B, Uludag H. Small hydrophobe substitution on polyethylenimine for plasmid DNA delivery: Optimal substitution is critical for effective delivery. *Acta Biomater*. 2016;33:213-224. doi: 10.1016/j.actbio.2016.01.025.

112. Fitzsimmons REB, Uludag H. Specific effects of PEGylation on gene delivery efficacy of polyethylenimine: Interplay between PEG substitution and N/P ratio. *Acta Biomater*. 2012;8(11):3941-3955. doi: 10.1016/j.actbio.2012.07.015.

113. Parmar MB, Ballesteros BEA, Fu T, et al. Multiple siRNA delivery against cell cycle and anti-apoptosis proteins using lipid-substituted polyethylenimine in triple-negative breast cancer and nonmalignant cells. *J Biomed Mater Res Part A*. 2016;104(12):3031-3044. doi: 10.1002/jbm.a.35846.

114. Mishra D, Kang HC, Bae YH. Reconstitutable charged polymeric (PLGA)2-b-PEI micelles for gene therapeutics delivery. *Biomaterials*. 2011;32(15):3845-3854. doi: http://dx.doi.org.libproxy.clemson.edu/10.1016/j.biomaterials.2011.01.077.

115. Makadia HK, Siegel SJ. Poly lactic-co-glycolic acid (PLGA) as biodegradable controlled drug delivery carrier. *Polymers*. 2011;3(3):1377-1397. http://www.ncbi.nlm.nih.gov/pmc/articles/PMC3347861/. doi: 10.3390/polym3031377.

116. Encyclopaedia Britannica Online. Proteins of the blood serum. http://www.britannica.com/EBchecked/topic/479680/protein. Updated 2014.

117. Hwa Kim S, Hoon Jeong J, Chul Cho K, Wan Kim S, Gwan Park T. Target-specific gene silencing by siRNA plasmid DNA complexed with folate-modified poly(ethylenimine). *J Control Release*. 2005;104(1):223-232. doi: 10.1016/j.jconrel.2005.02.006.

118. Yang X, Deng W, Fu L, et al. Folate-functionalized polymeric micelles for tumor targeted delivery of a potent multidrug-resistance modulator FG020326. *J Biomed Mater Res A*. 2008;86(1):48-60. doi: 10.1002/jbm.a.31537 [doi].

119. Cheng Z, Al Zaki A, Hui JZ, Muzykantov VR, Tsourkas A. Multifunctional nanoparticles: Cost versus benefit of adding targeting and imaging capabilities. *Science*. 2012;338(6109):903-910. doi: 10.1126/science.1226338.